Title
Smart EV Energy Management System to Support Grid Services

Author
Wang, Bin

Publication Date
2016

Peer reviewed|Thesis/dissertation

University of California

Los Angeles

Smart EV Energy Management System to Support Grid Services

A dissertation submitted in partial satisfaction of the

requirements for the degree Doctor of Philosophy

in Mechanical Engineering

by

Bin Wang

2016

ABSTRACT OF THE DISSERTATION

Smart EV Energy Management System to Support Grid Services

by

Bin Wang

Doctor of Philosophy in Mechanical Engineering

University of California, Los Angeles, 2016

Professor Rajit Gadh, Chair

Under smart grid scenarios, the advanced sensing and metering technologies have been applied to the legacy power grid to improve the system observability and the real-time situational awareness. Meanwhile, there is increasing amount of distributed energy resources (DERs), such as renewable generations, electric vehicles (EVs) and battery energy storage system (BESS), etc., being integrated into the power system. However, the integration of EVs, which can be modeled as controllable mobile energy devices, brings both challenges and opportunities to the grid planning and energy management, due to the intermittency of renewable generation, uncertainties of EV driver behaviors, etc. This dissertation aims to solve the real-time EV energy management problem in order to improve the overall grid efficiency, reliability and economics, using online and predictive optimization strategies.

Most of the previous research on EV energy management strategies and algorithms are based on simplified models with unrealistic assumptions that the EV charging behaviors are perfectly known or following known distributions, such as the arriving time, leaving time and energy consumption values, etc. These approaches fail to obtain the optimal solutions in real-time because

of the system uncertainties. Moreover, there is lack of data-driven strategy that performs online and predictive scheduling for EV charging behaviors under microgrid scenarios. Therefore, we develop an online predictive EV scheduling framework, considering uncertainties of renewable generation, building load and EV driver behaviors, etc., based on real-world data. A kernel-based estimator is developed to predict the charging session parameters in real-time with improved estimation accuracy. The efficacy of various optimization strategies that are supported by this framework, including valley-filling, cost reduction, event-based control, etc., has been demonstrated.

In addition, the existing simulation-based approaches do not consider a variety of practical concerns of implementing such a smart EV energy management system, including the driver preferences, communication protocols, data models, and customized integration of existing standards to provide grid services. Therefore, this dissertation also solves these issues by designing and implementing a scalable system architecture to capture the user preferences, enable multi-layer communication and control, and finally improve the system reliability and interoperability.

This dissertation of Bin Wang is approved.

Jonathan Hopkins

Douglas S. Parker

Tsu-Chin Tsao

Rajit Gadh, Committee Chair

University of California, Los Angeles

2016

To my lovely wife, Wang Shu,

and my dear parents.

Acknowledgement

To Dr.Rajit Gadh, many thanks to his continuous support, encouragement and guidance on my research interests. This dissertation could not have been finished without the experiences and suggestions from him. It has been a quite an enjoyable and fruitful research experience at Smart Grid Energy Research Center (SMERC) at UCLA.

To my committee, Dr. Jonathan B. Hopkins, Dr. D. Stott Parker, and Dr.Tsu-Chin Tsao, for offering me great comments and suggestions on the subjects I have been working on.

I would like to thank my colleagues at UCLA SMERC: Dr. Chi-Cheng Chu, who is the project principal investigator and Mr.Charlie Qiu, who is the senior software engineer, for their discussion and collaborations. Thanks to the fellow Ph.D students at SMERC: Yubo Wang, Hamidreza Nazaripouya, and Yingqi Xiong for their significant advice and contributions to the research work; Tianyang Zhang, Behnam Khaki, Zhiyuan Cao and Yuwei Chung for their collaborations on the EV integration project. Thanks to Dr.Boyang Hu, Dr.Wenbo Shi, Dr.Rui Huang for their valuable experiences and suggestions on research directions. Special thanks to Dr.Hemanshu Pota for his technical guidance during my Ph.D study.

Thanks to LADWP, from whom I received the financial support for my Ph.D study.

To my wife, Wang Shu, and my dear parents, whose love supports me all the way towards my degree.

TABLE OF CONTENTS

LIST OF FIGURES

LIST OF TABLES

VITA

2008 - 2012 Bachelor of Engineering (Vehicle Engineering), Jilin University, Changchun, Jilin, China.

PUBLICATION

Bin Wang, Yubo Wang, Hamidreza Nazaripouya, Charlie Qiu, Chi-cheng Chu, and Rajit Gadh, "Predictive Scheduling Framework for Electric Vehicles with Uncertainties of User Behaviors," *IEEE Internet Things J.*, submitted, Jan. 2016.

Yingqi Xiong, Bin Wang, Chi-cheng Chu, and Rajit Gadh, "Extending IEC61850 with Smart EV Charging", accepted, *2016 IEEE ISGT Asia*, Nov. 2016.

Yubo Wang, Bin Wang, Chi-cheng Chu, Himanshu R. Pota, and Rajit Gadh, "Energy management for a commercial building microgrid with stationary and mobile battery storage," *Energy Build.*, vol. 116, pp. 141–150, Mar. 2016.

Bin Wang, Yubo Wang, Charlie Qiu, Chi-cheng Chu, and Rajit Gadh, "Event-based electric vehicle scheduling considering random user behaviors," in *2015 IEEE International Conference on Smart Grid Communications (SmartGridComm)*, 2015, pp. 313–318.

Bin Wang, Rui Huang, Yubo Wang, Hamidreza Nazaripouya, Charlie Qiu, Chi-cheng Chu, and Rajit Gadh, "Predictive scheduling for Electric Vehicles considering uncertainty of load and user behaviors," in *2016 IEEE/PES Transmission and Distribution Conference and Exposition (T&D)*, 2016, pp. 1–5.

Yubo Wang, Bin Wang, Rui Huang, Chi-cheng Chu, Himanshu R. Pota, and R. Gadh, "Two-tier prediction of solar power generation with limited sensing resource," in *2016 IEEE/PES Transmission and Distribution Conference and Exposition (T&D)*, 2016, pp. 1–5.

Hamidreza Nazaripouya, Bin Wang, Yubo Wang, Peter Chu, Himanshu R. Pota, and Rajit Gadh, "Univariate time series prediction of solar power using a hybrid wavelet-ARMA-NARX prediction method," in *2016 IEEE/PES Transmission and Distribution Conference and Exposition (T&D)*, 2016, pp. 1–5.

Yubo Wang, Bin Wang, Tianyang Zhang, Hamidreza Nazaripouya, Chi-cheng Chu, and Rajit Gadh, "Optimal energy management for Microgrid with stationary and mobile storages," in *2016 IEEE/PES Transmission and Distribution Conference and Exposition (T&D)*, 2016, pp. 1–5.

Bin Wang, Boyang Hu, Charlie Qiu, Peter Chu, and Rajit Gadh, "EV charging algorithm implementation with user price preference," in *Innovative Smart Grid Technologies Conference (ISGT), 2015 IEEE Power Energy Society*, 2015, pp. 1–5.

PATENT

Rajit Gadh, Bin Wang, Li Qiu, Tianyang Zhang, Ching-yen Chung, Chi-cheng Chu, "Multi-layer Electric Vehicle Energy Management System with Customized Data Models" – UC-2016-957

Chapter 1 Introduction

In this chapter, we briefly introduce the research background, including the technologies of smart grid, demand response (DR), EVs and the existing EV energy scheduling strategies, based on which the research challenges and the contributions of this dissertation are summarized. The dissertation outline is given at the end.

1.1 Background technologies

1.1.1 Smart Grid

Due to the urgency from the public and government to reduce air pollution caused by burning the fossil fuels, a variety of innovative Smart Grid (SG) technologies have been proposed to upgrade the legacy electric grid. According to [1], a general definition for SG is provided as a digitally enabled electric grid that gathers, distributes, and acts on information about the behavior of all components in order to improve the efficiency, reliability, and sustainability of electricity services. Advanced communication technologies [2][3][4] and control strategies [5] are critical to fulfill the complex energy management tasks, such as load control via demand response (DR) [6], ancillary services in wholesale market [7], etc. Accordingly, coordination of a myriad of grid components can be achieved under SG scenarios with shared information. Referred as Demand Side Management (DSM) [8], multiple types of loads can be managed by intelligent energy management strategies, considering a set of different factors, not only from the demand side, but also the generation side, such as the properties of on-site solar generation, etc. In addition, Micro-grid [9] is introduced as the local smaller electric grid that can run in either grid-connected mode

or islanded mode, using its local generation and renewable resources. By employing communication technologies to support advanced control strategies in multiple levels, the whole electric grid, including generation, transmission, distribution systems, can be upgraded to a higher level of reliability, efficiency, security and economy.

As possible alternatives for fossil fuels, distributed energy resources (DERs), including solar Photovoltaic generation, wind generation, and Battery Energy Storage System (BESS) and Electric Vehicles (EVs), etc., are being integrated into the legacy grid [10], [11]. Each newly added component has its distinct properties. For instance, output measures of renewable generation, such as solar and wind energy, cannot be predicted with 100% accuracy in extremely short time periods [12], [13]. EVs can be regarded as mobile energy storage devices, however, the mobility is largely dependent on the drivers' travel behaviors, which can be described by driver traveling preferences, *i.e.* start charging time, stop charging time, energy consumption values [14], [15], etc. Thus, to properly control the DERs, it is required to understand their stochasticity. Taking into account the uncertainties of renewable generations, load fluctuations and the customer preferences, the above-mentioned issues of DERs bring challenges to managing the electric grid in real-time.

1.1.2 Demand Response and Standards

With the purpose to improve overall grid reliability and efficiency, DR is a demand-side management program offer by utility companies to change the normal power consumption patterns during critical system conditions or periods of high market energy costs. [16]. The utility company or a microgrid coordinator is facing with a decision making problem of when and how to control load on the demand side at different time scales, i.e. long-term planning activities to schedule the bulk power purchases, local generation resources, etc., and the real-time energy management actions, such as demand response to curtail the electricity load. Enabled by the Advanced Metering

Infrastructure (AMI) and time-varying rates, DR is projected as a quantifiable, reliable resource for regional planning purposes with potential to improve the overall system cost performances [16]. Existing DR programs [7] offered by Regional Transmission Organizer (RTOs)/Independent Service Operators (ISOs) and load serving entities (LSEs), such as California ISO (CAISO), New York ISO (NYISO), and PJM, etc., across in the U.S., include Emergency Demand Response Program (EDRP), Day-Ahead Demand Response Program (DADRP), Demand-Side Ancillary Service Program (DSASP), Real-Time Demand Response (RDR) Program, Participating Load Program (PLP), etc. In term of time scale, EDRP and RDR are operated in real-time, while DSASP, PLP and DADRP are operated day-ahead or hours-ahead fashion. In addition, it is required for some DR programs, such as DSASP and PLP, to aggregate a number of small loads, which can be either residential [6], [17], [18] or commercial [19], [20], to participate in the wholesale energy market, by providing ancillary/regulation services or load curtailment. Corresponding communication protocols[21]–[23], such as OpenADR 2.0 (a), (b) and Smart Energy Profile (SEP) 2.0, are developed to improve information-sharing and interoperability. IEC 61850 can be modified and extended to partially support load management [14]. Based on the aforementioned DR frameworks, more complex and intelligent load management strategies can be designed and implemented.

1.1.3 Electric Vehicles, EVSE Standards and Protocols

Electric Vehicles (EVs) are gaining popularity among consumers in the market according to sales statistics in [24], [25]. Thus, there exists increasing demand to deploy electric vehicle supply equipment (EVSE) to accommodate Electric Vehicles (EVs). Since EVSE permits EVs to interact with the electric grid, proper communication and data transfer protocols have been developed to support complex grid integrations. The most up-to-date charging protocols and their corresponding

maximum power values are summarized in Table 1-1. For instance, IEC 61850 as a distribution automation standard has been used for data and information exchange models, including EVs and Plug-in Electric Vehicles (PEVs) [26]. The energy management strategies developed in this dissertation are mainly focused on Level II charging devices based on SAE J1772.

Table 1-1 EV/PEV charging standards and protocols

Charging Station Type	**Power**	**Protocol/Standard**
AC Level I	1.4 kW@12 amps	SAE J1772/SAE J2847/ISO 15118
AC Level II	3.3 kW@15 amps 6.6 kW@30 amps	SAE J1772/ SAE J2847/ISO 15118
DC Fast Charging	25-50 kW@100 amps	CHAdeMO & SAE Combo/ SAE J2847/ISO 15118

1.1.4 EV Energy Management Strategies

As the penetration of EVs grows larger, uncoordinated charging behaviors will create new load peaks in the aggregated load curve, leading to a myriad of issues, such as power quality degradation [27], [28] and operational cost increase [29]. According to hardware capabilities, a variety of previous researchers have proposed algorithms that consider the Vehicle-to-Grid (V2G) options, i.e. sending the power back to the grid to provide services, while the rest solely model the EV charging problem. In [11], [30]–[32], V2G strategies are developed considering the automatic load sharing among vehicles, DR integrations, stochastic EV driver behaviors, etc. However, due to the lack of commercialization and large-scale real-world implementation of V2G technologies, the validity of these approaches remain un-verified. Therefore, within the scope of this dissertation, we focus primarily on the EV charging problems. Based on the paradigm of optimization algorithms, the existing energy management strategies for EV charging problem can be further

categorized by: centralized strategies and distributed ones. Centralized strategies formulate the scheduling problem as one single optimization problem, e.g. algorithms in [29], [32]–[34], which is solved sequentially by a central solver. On the contrary, distributed approaches, e.g. algorithms in [35], [36], divide the single large optimization problem into multiple sub-problems with smaller size to parallelize the optimization, which improves the computation efficiency and preserves the customer privacy. [35]–[37] have defined the load from EV charging as deferrable load, which can be shifted to a different time window without compromising user's schedule requirements. EV charging load has also been considered in demand response researches [38], [39], where the problem is formulated as a convex optimization problem with the objective to minimize the overall operational cost. Time-varying electricity price signals are utilized for controlling the EV energy scheduling in order to achieve cost optimal solutions[39]–[44], i.e. optimize the charging schedules according to the time-varying electricity prices, reducing the energy bills for participating users. However, the simulation-based work assumes that the battery Status of Charge (SOC) values and charging session parameters, i.e. the arrival and departure time, energy demand, etc., are perfectly known once vehicles are plugged, which is not realistic in practical implementations. These methods cannot be applied directly to the EVSEs with multiple power sources and outlets in our study since the constraints on different outlets are not explicitly formulated.

To handle uncertainties in the scheduling system, including renewable generations, base load and charging demand, scheduling algorithms based on Model Predictive Control (MPC) [36], [37], Markov Decision Process (MDP) and Queue Theory (QT) [45], [46], Monte Carlo simulations [34], have been proposed. To estimate the aggregated EV charging load, and EV driver behaviors, approaches based on k-Nearest Neighbors(KNN), Lazy-learning Algorithm and Pattern Sequence-based Algorithm (PSA) [47], Auto-Regressive Integrated Moving Average (ARIMA) [44],

existing distribution in [41], [48], such as Gaussian or Poisson distributions, are developed. These prediction and estimation methods assume that there are underlying stochastic models, such as Gaussian or Poisson distribution for EV charging behaviors, which is sometimes not realistic, as shown by the data collected on the UCLA campus. However, the practical implementation needs real-time parameter estimations for each charging session instead of aggregated load predictions.

1.2 Challenges and Contributions

The work by previous researches has not fully addressed the challenges to integrate PEVs into smart grid scenarios in a both user-friendly and grid-friendly way. The existing challenges are summarized in the following aspects:

First, none of the previous research/projects provides a comprehensive solution and practical validation for an EV charging system based on real-world implementations. Analysis and conclusion based on pure simulations suffer from over-simplification of models and negligence of practical issues in real-world implementations. For instance, a number of previous works assume that it is possible to obtain the battery status of charge (SoC) values for any vehicles and use them directly in their simulations, which is not realistic due to the proprietary standards among vehicle manufacturers. In addition, there is no existing EV energy management framework to consider user preferences, e.g. mobile applications that allow users to explicitly specify their requirements.

The second drawback of most simulation work is that it assumes the parameters for each charging session, including start charging time, stop charging time, leave time and the energy consumption values, are static. That is to say, before implementing the energy management strategies for PEVs, their exact demand and availabilities are perfectly known or known to follow specific distributions,

which is also unrealistic. Due to this drawback, it is difficult to accomplish real-time operations for electric vehicles (EVs) with dynamic charging behaviors.

Thirdly, most of the previous research does not jointly model the system uncertainties, including renewable generation, EV driver behaviors, and real-time build power consumption within the micro-grid scenarios. And there is lack of data-driven frameworks based on real-world data.

This dissertation aims to solve the above-mentioned issues of existing research projects. We have developed and implemented a real-world smart EV energy management system on the UCLA campus with both server and client applications, based on which energy consumption statistics are collected for users in campus. The contributions of this dissertations can be summarized:

First of all, we developed a predictive EV scheduling framework that performs on-line EV energy scheduling tasks, considering random user behaviors, uncertainties of building load and the solar Photovoltaics generation, etc., based on data from real-world implementations. It reduces load variation and operational cost while maintaining an energy delivery rate at a high level.

Second, a kernel-based estimator is developed to predict the charging session parameters in real-time, including the stay duration and energy consumption values, with improved estimation accuracy.

Finally, this dissertation presents and discusses a scalable implementation of real-world EV energy management system with multi-layer communication and control architecture. User preferences on travel schedules, energy prices, real-time DR signals from ISO/third party are considered to improve overall system efficiency, reliability and interoperability.

1.3 Dissertation Structure

In Chapter 2, we develop a predictive energy management framework with a kernel-based parameter estimator and a receding-horizon control strategy that takes current system states and estimated variables into account and predictively computes the optimal EV energy schedules. This chapter is adapted from the manuscript [49]. Unlike most previous research, our approach considers dynamic user participations in the smart EV charging problem with different user behaviors, i.e. the scheduling of EV charging behaviors is an on-line optimization process, which supports real-time and dynamic plug-in/off activities. Specifically, our kernel-based estimator is developed to adaptively predict the session parameters, including values of stay duration and energy consumption, based on the personalized historical charging records. The smoothing effect of the Gaussian kernel is demonstrated with improved estimation accuracy compared to the mean estimator developed in [15], and the unit energy cost is reduced across the samples.

An event-based control strategy with the integration of IEC 61850 standard is discussed in Chapter 3 based on the scheduling framework developed in Chapter 2. We develop an event-based control paradigm, where the data retrieval and computation are only initiated by the pre-defined events, which represent the critical change of the system states. The simulation results indicate that event-based strategies can effectively reduce the number of unnecessary computations while maintaining the energy delivery rate and unit energy cost at an acceptable level. Besides, data models from IEC 61850 protocol are developed to standardize the communications of our smart EV charging system, which improves system interoperability.

Chapter 4 discusses energy management strategies with the objectives of flattening the total system load, including EV power consumption, renewable solar generation, building load, etc., under a micro-grid scenario. Similarly, dynamic EV charging behaviors are considered and the EV batteries are modelled as controllable devices to serve the overall optimization objectives, while

the optimization tries to satisfy the energy consumption and travel schedule constraints for each participating EV. Compared to previous research, this formulation incorporates the real-world EV charging data with more dynamic properties. The overall power fluctuation for the micro-grid has been reduced up to 40% on the test days. This chapter is based on the publication [14].

In Chapter 5, a price-based charging strategy and implementation architecture [44] are discussed. Considering the EV users' price preferences and account priority, the proposed strategies with implementation are able to dynamically allocate energy to different EVs connected to the same EVSE, developed by UCLA SMERC. Retail energy prices are generated locally based on the price signals from the wholesale energy market and the predicted EV energy demand on the UCLA campus. An architecture including mobile application, scheduling services on the server side and communication networks are presented with details. Finally, the experiment results and the analysis are provided in Chapter 5.

In Chapter 6, we introduce the real-world implementation of a smart EV energy management system with both client-side and server-side applications, which are capable of performing scalable energy management for a number of EVs and supporting various grid-side operational events, such as demand response (DR). Practical concerns and the technical details of the proposed system are provided.

Chapter 7 concludes this dissertation with the summary of approaches, findings and contributions. Future research work is discussed with potential improvements for the existing methods and system.

Chapter 2 Predictive EV Energy Scheduling Framework

The randomness of user behaviors plays a significant role in Electric Vehicle (EV) scheduling problems, especially when the power supply for Electric Vehicle Supply Equipment (EVSE) is limited. Existing EV scheduling methods do not consider this limitation and assume charging session parameters, such as stay duration and energy demand values, are perfectly known, which is not realistic in practice. In this chapter, based on real-world implementations of networked EVSEs on UCLA campus, we developed a predictive scheduling framework, including a predictive control paradigm and a kernel-based session parameter estimator to perform the real-time energy management strategies for EVs. Specifically, the scheduling service periodically computes for cost-efficient solutions, considering the predicted session parameters, by the adaptive kernel-based estimator with improved estimation accuracies. We also consider the power-sharing strategy of existing EVSEs and formulate the virtual load constraint to handle the future EV arrivals with unexpected energy demand. To validate the proposed framework, 20-fold cross validation is performed on the historical dataset of charging behaviors. The simulation results demonstrate that average unit energy cost per kWh can be reduced by 29.42% with the proposed scheduling framework and 66.71% by further integrating solar generation with the given capacity, after the initial infrastructure investment. The effectiveness of kernel-based estimator, virtual load constraint and event-based control scheme are also discussed in detail.

2.1 Introduction

Electric Vehicles (EVs) and Plug-in Hybrid Electric Vehicles(PHEVs) are gaining more popularity in the auto-market in recent years according to the statistics published in [24], [25]. Due to the pressure from the public to reduce air pollution, 1.5 million zero emission vehicles (ZEV) will be put on roads in California by 2025, which requires the EVSEs to support 1 million ZEV by 2020 [50]. As the penetration of EVs grows larger, uncoordinated charging behaviors will create new load peaks in the aggregated load curve, leading to a myriad of issues, such as power quality degradation [27], [28] and operational cost increase [29]. Furthermore, there are uncertainties (e.g. start time, stay duration and energy demand, etc.) within the scheduling problem for EV charging behaviors, which cannot be completely solved by deterministic problem formulations. However, coordinating numerous EV charging behaviors in real-time is a challenging task due to the following reasons: 1) lack of sharing strategy to accommodate more EVs per EVSE; 2) lack of stochastic model to handle uncertainties of EV users' behaviors, including arriving time, leaving time and energy demand; 3) lack of predictive scheduling framework, that adaptively computes for cost optimal energy allocations, considering both current and future system states.

Previous researchers have developed numerous approaches to solve the aforementioned challenges. However, to the best of authors' knowledge, none of them provides a comprehensive solution and practical validation based on the real-world implementations. [36], [37], [35] have defined the load from EV charging as deferrable load, which can be shifted to a different time window without compromising user's schedule requirements. EV charging load has also been considered in demand response researches [38], [39], where the problem is formulated as a convex optimization problem with the objective to minimize the overall operational cost. In addition, valley filling and load following strategies[35] are also supported in the formulation. However, the simulation-based work assumes the battery Status of Charge (SOC) values and charging session parameters, i.e. the

arrival and departure time, energy demand, etc., are perfectly known once vehicles are plugged, which is not realistic in practical implementations. Time-varying electricity price signals are utilized for controlling the EV energy scheduling in order to achieve cost optimal solutions[39]–[44]. The validity of using Time-of-Use (TOU) prices for EV scheduling is discussed in [39], [41], [42], [11]. Maximum revenue model is defined in [43], where both regulation price and electricity price for curtailing EV charging load are defined. A social optimal pricing scheme is developed in [40] between utility and load aggregator, which is applied to a number of fleet vehicles. Vehicle-to-Grid and Vehicle-to-Building services[11], [31] are considered in EV scheduling problem. A framework for smart energy management is proposed in [51], considering time-varying load properties and user participation, etc.

To handle uncertainties in the scheduling system, including renewable generations, base load and charging demand, scheduling algorithms based on Model Predictive Control (MPC), are proposed in [36], [37], where virtual load is modelled for future EV energy demands. Markov Decision Process (MDP) and Queue Theory (QT) are utilized to handle stochastic EV arrival rate and intermittency of renewable generation in [45], [46]. [34] models EV load, time schedules and energy prices with Monte Carlo method. These methods cannot be applied directly to the EVSEs with multiple power sources and outlets in our study since the constraints on different outlets are not explicitly formulated. To estimate the aggregated EV charging load, [47] evaluates multiple methods on EV charging load predictions on each EVSE, including k-Nearest Neighbors(KNN), Lazy-learning Algorithm and Pattern Sequence-based Algorithm (PSA). [44] utilizes Auto-Regressive Integrated Moving Average (ARIMA) to predict aggregated EV load on UCLA campus for the next week. Estimation methods in [41], [48] assume that there are underlying stochastic models, such as Gaussian or Poisson distribution for EV charging behaviors, which is

sometimes not realistic, especially for the data collected on UCLA campus. However, the practical implementation needs real-time parameter estimations for each charging session instead of aggregated load predictions.

This chapter focuses on an implementable solution that considers uncertainties of user behaviors, time-varying energy prices, renewable generation integration and other practical concerns, such as the power source limitation and power sharing strategies. We first introduce a practical system architecture for data collection in detail, based on which we show the exploratory analysis for EV charging behavioral data by associating session parameters, such as start time, stay duration and energy consumption, etc., with specific users. The EV scheduling problem is formulated as a predictive convex optimization problem, which achieves a cost-efficient solution while maintaining high level of energy delivery rate with uncertainties of user behaviors. An online predictive control paradigm is developed, which adaptively estimates charging session parameters using kernel-based methods. Specifically, Gaussian kernel is utilized to model the joint probability density distributions based on the qualified historical records, which reduces the estimation deviations for both values of stay duration (h) and energy consumption (kWh). To handle future vehicle arrivals with unknown energy demand, we also model a virtual load constraint with proper relaxation strategies to reduce the level of deferability for EV load by limiting power supply for future time intervals. The effects of virtual load constraint on energy delivery rate and average unit energy cost are also studied. Finally, to minimize the number of estimations and controls, we extend the proposed Predictive Energy Scheduling Algorithm (PESA) by developing an event-based trigger scheme in Event-based Cost-optimal Scheduling Algorithm (ECSA), where re-computation is only initiated by pre-defined events. The real-world data for EV charging behaviors,

which is collected from UCLA test bed for 15 months, is randomly partitioned into training and test datasets to further evaluate the overall system performance.

Compared to the preliminary work in [52], the following new contributions are added: 1) More comprehensive description and analysis for the predictive framework are provided, including the details of scheduling services and exploratory analysis for EV charging behaviors, etc. 2) Kernel-based method is proposed to adaptively estimate parameters in charging sessions by constructing joint probability density distribution for the qualified data points with improved estimation accuracy. 3) Virtual load constraint is added to handle the unexpected EV energy demand by adjusting the deferability level of EV load. Its effects on operational cost and energy delivery rate are analyzed using experiment results; 4) 20-fold cross validation is utilized as the evaluation method for our proposed scheduling framework. Total charging records are randomly divided into 20 partitions, each of which is used as test set, and the remaining 19 partitions are used as training sets.

2.2 System Architecture

The proposed scheduling system includes three main components, *i.e.* EVSE, control center on server side and mobile application on user side, which are shown in Figure 2-1. The networked EVSEs are controllable by remote commands from Internet, which can be either from the mobile applications or from scheduling services running on the server. Charging requests from EV users are transmitted from the mobile applications to EV control center, which maintains an active interface that accepts the real-time requests via HTTP secured messages. After a verification process, the requests are stored in a database system and meanwhile directed to corresponding EVSEs. In addition, the control center also maintains active scheduling services based on the real-

time monitoring data retrieved by the data collector. Various scheduling algorithms with different objectives and constraints can be supported by this architecture that is built on top of the complex communication network within UCLA campus, involving multiple communication protocols, such as Zigbee, 3G, Wifi and Ethernet, etc. In addition, this architecture also supports event-based control strategies, with customized triggers from both server side and user side.

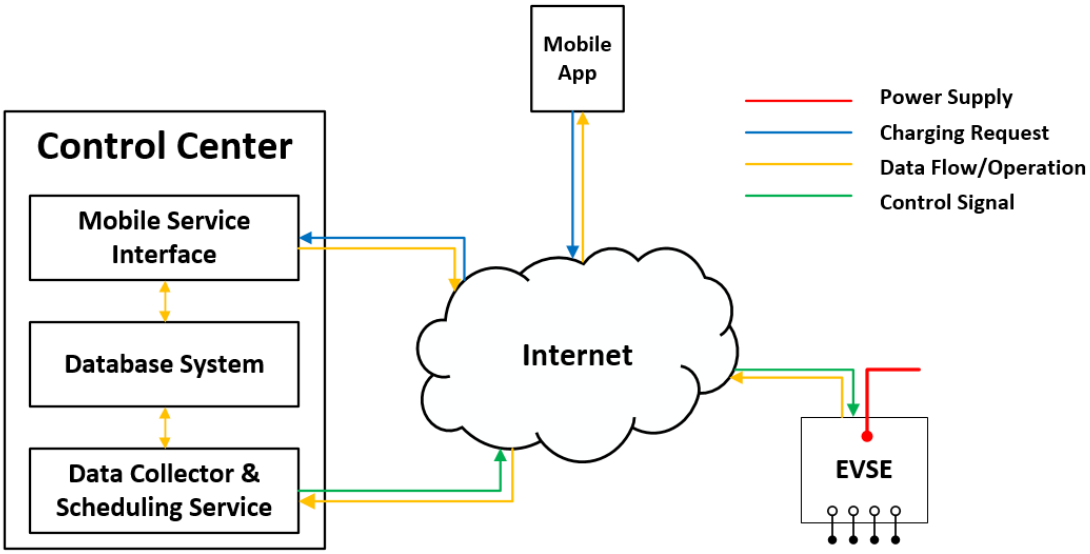

Figure 2-1 System overview

The hardware modeled in this chapter is the level II EVSE developed by UCLA Smart Grid Energy Research Center (SMERC) [53], [54], which has power sharing capability, *i.e.* split the power supply from single source to multiple charging outlets within the preset range. The charging duty-cycle for each outlet, defined by SAE J1772, is linearly correlated with the charging current allocated for this outlet. In our implementation, 50% duty-cycle denotes *30A* and 10% duty-cycle denotes *6A*. The firmware in our EVSEs provides explicit interfaces to modify the duty-cycles in order to adjust the power consumption for specific outlet.

2.3 Predictive Scheduling Framework

In this section, we will discuss the predictive scheduling framework, which includes two main components: the parameter estimator and predictive scheduling paradigm inspired by model predictive control (MPC).

2.3.1 Kernel-based Estimation for Session Parameters

2.3.1.1 Tuple Construction for Session Parameters

In order to simplify the process of behavioral data modeling, a 5-tuple is created for each charging session:

$$s \triangleq (u, t_s, t_f, t_l, e)$$

where u is the unique identifier (index) for each user in our system; t_s and t_f denote start time and finish time, respectively; t_l is the leave time for each charging session; e denotes energy consumption. Note that t_l is usually later than t_f since some vehicles get fully charged before being un-plugged by users. Stay duration d can be obtained by $d = t_l - t_s$ for each session. This sequence is illustrated in

Figure 2-2, where t_0 is the initial time for each day.

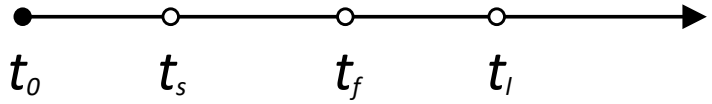

Figure 2-2 Charging session time parameters

- *Start Time*: t_s, represents the time when vehicle arrives at certain EVSE and submits a charging request.
- *Finish Time*: t_f, denotes the time when this charging session is terminated due to low charging current, which might be caused by fully charged battery or disconnected vehicle.

- *Leave Time:* t_l, is the time when the user unplugs her vehicle and leaves charging infrastructure directly.
- *Charging Power*: $r_n = \{r_{t_s}, r_{t_s+\Delta t}, r_{t_s+2\cdot\Delta t}, \dots, r_{t_f}\}$ is an array of power consumption rate at each time interval between t_s and t_f. Δt is time interval at which data collector service and scheduling service is working.
- Energy Consumption for vehicle n: E_n, denotes the energy consumed within each charging session. E_n can be computed as:

$$E_n = e_{tf} - e_{ts} \tag{2.1}$$

where e_{tf} and e_{ts} are accumulated energy consumption value read from meter at session start time and finish time, respectively.

Note that $t_f \leq t_l$ holds by the definition, which is obvious when vehicle is fully charged before departure. If vehicle leaves unexpectedly before battery is full, the charging session will be terminated by scheduling algorithm automatically and $t_f = t_l$ in this case. Another important parameter, stay duration d_n can be obtained by $t_l - t_s$. In later section, r_t will be the decision variable in our problem formulation.

Session parameters are significant for scheduling algorithms to determine optimal solutions. Once a charging session is initiated by a specific user, the estimated stay duration and energy consumption values are needed for the scheduling service to compute for energy allocation schedules. Thus, the purpose of estimation algorithm is to obtain the estimated values of stay duration $\hat{d}$ and energy consumption $\hat{e}$, given the start time t_s, user's index u and historical records.

2.3.1.2 Exploratory Data Analysis

Exploratory data analysis is performed for each user to exploit the distributions of session parameters and latent relations between them, *i.e.* start time vs. stay duration and stay duration vs. energy consumption.

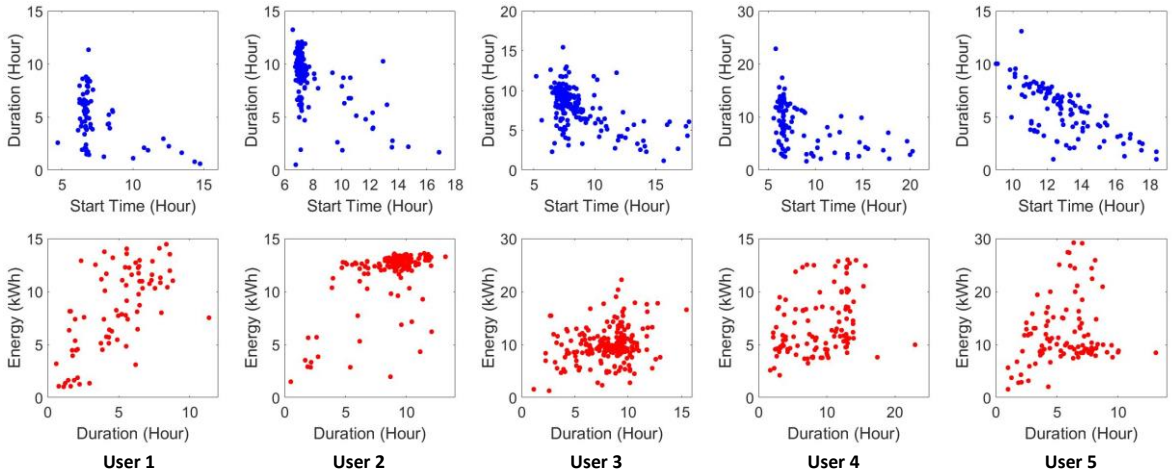

Figure 2-3 Typical user behaviors

The charts in Figure 2-3 show session parameters for typical users in our system. From the plots of start time vs. stay duration (upper level), one can tell that users tend to have a relatively stable start time in the morning, such as user 1, 2 and 4. However, the plots also show a few deviations of start time, *i.e.* the tails, indicating that users may plug in their vehicles later than usual. The tail effect is different among varied users. For instance, tail effect of user 3 is much heavier than that of user 1. Another observation is that in the tail part of the plots, the later users plug in their vehicles, the shorter their stay durations will be. This makes sense since most EV drivers in university campus tend to have fixed departure time. On the other hand, the duration vs. energy plots(lower level) cannot show apparent relations between users' energy consumption and their stay durations even though for user 1 and user 5, one can find that the longer user stay plugged the more energy will be consumed. However, as the duration grows larger, the variance of energy consumption values also increases. For user 2, 3 and 4, no obvious pattern can be identified from the plots.

These plots are only 5 samples from more than 100 users in our system, whose parameter distributions are far more diverse. Therefore, it is difficult to develop a comprehensive parametric model to describe the behavioral data for all users, which leads us to develop nonparametric model-free method.

2.3.1.3 Kernel Density Estimator

Nonparametric estimation method, such as kernel density estimation, does not require explicit parametric model to fit the data. Discrete kernel estimator with tutorial is discussed in [55]. Given the parameters already known (*e.g.* start time t_s or estimated stay duration $\hat{d}$), the objective here is to estimate the unknown session parameters (*e.g.* stay duration d and energy consumption e) with kernel methods. As discussed above, there exists latent relationship between session parameters, shown by plots in Figure 2-3, so that a bi-variate kernel density estimator is formulated. One can obtain the joint probability distribution of start time vs. stay duration or stay duration vs. energy consumption, respectively. Suppose $p(x, y)$ is joint probability for one of aforementioned chart, point estimation of random variable X, *i.e.* $\hat{x}$, can be calculated by the marginalization operation in equation (2.2):

$$\hat{x} = E[X] = \int_X x \cdot p(x)dx = \int_X x \cdot \int_Y p(x, y)dy \cdot dx \tag{2.2}$$

As an example, to estimate stay duration d for a specific user, joint distribution of start time t_s vs. duration d is utilized and univariate distribution for d is calculated by:

$$p(d) = \int_{t_S} p(t_S, d)dt_S = \int_{\underline{t_s}}^{\overline{t_s}} p(t_S, d)dt_S \tag{2.3}$$

where $\overline{t_s}$ is the upper bound of start time, denoted by $\overline{t_s} = t_s + \Delta t$. Δt is a tunable parameter, denoting the tolerance bandwidth for start time selections. Similarly, lower bound start time is

$\underline{t_s} = t_s - \Delta t$. The assumption for this modeling is the latent dependence of stay duration on start time and the consistency of users' behaviors, i.e. user's future behaviors resemble her historical charging records. Thus, the similar sessions with start time falling within the tolerance range of the start time t_s for current session are used as the base dataset to construct the kernelized joint distribution. For instance, if start time for current charging session is 8:00 AM and the tolerance interval is set to 1 hour, then historical sessions for current user with start time between 7:00 AM and 9:00 AM will be extracted. Thus, the following constraints have to be satisfied for each qualified tuple s in qualified tuple set S:

$$\overline{t_s} \geq s.t_s \geq \underline{t_s} \tag{2.4}$$

$$s.d \geq t - s.t_s \tag{2.5}$$

$$s.e \geq e_t^c \tag{2.6}$$

$$s.u = u \tag{2.7}$$

where $s.t_s$ denotes the start time t_s of tuple s; t is the current time when the estimation function is called and the e_t^c is energy already consumed by the time t. u denotes the user index for current user. These additional constraints serve to refine the selection of historical sessions. Similarly, energy consumption value can also be estimated by the distribution of stay duration vs. energy consumption, given estimated duration $\hat{d}$ and tolerance bandwidth Δt. However, as charging session proceeds, the qualified dataset extracted from historical records by equation (2.4) - (2.7) is quite different, which leads to the diversity of the joint distributions. The joint probability can be obtained as follows:

$$p_{KDE}(x) = \frac{1}{N}\sum_{i=1}^{N} K(x, B) \tag{2.8}$$

where B denotes the base dataset extracted for modeling and N is the total number of data points in B. Thus, $B \triangleq \{b_1, b_2, \cdots, b_N\}$ and each data point has D dimensions, i.e. $b \in \mathbb{R}^D$. For instance, $D = 2$ if we model a bi-variate distribution, such as start time vs. stay duration. $K(x, B)$ is the kernel function that is used to model the weight of each data point x. We use Gaussian kernel for a continuous probability density, *i.e.*:

$$K(x, B) = \frac{1}{\prod_{j=1}^{D} h_j} \cdot \prod_{j=1}^{D} K_j\left(\frac{x - b_i}{h_j}\right) \tag{2.9}$$

where h_j is the bandwidth for *j-th* dimension of the data point; K_j is the kernel function for *j-th* dimension with the following form, where g is a random variable:

$$K_j(g) = (2\pi)^{-\frac{1}{2}} \cdot e^{-\frac{1}{2}g^2} \tag{2.10}$$

This modeling process, i.e. (2.8) - (2.10), is performed every loop when the estimation is needed. As an illustrative example, sample probability distributions for a user are displayed in Figure 2-4 and Figure 2-5. The peak of joint probability distribution represents the region with highest probability, i.e. the highest density of qualified data points.

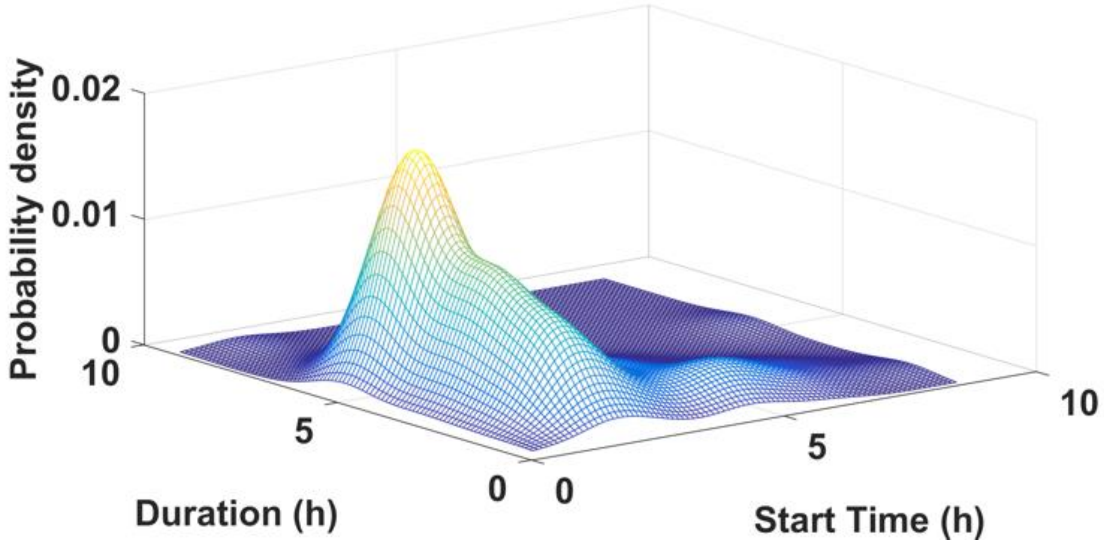

Figure 2-4 Joint probability for start time and stay duration

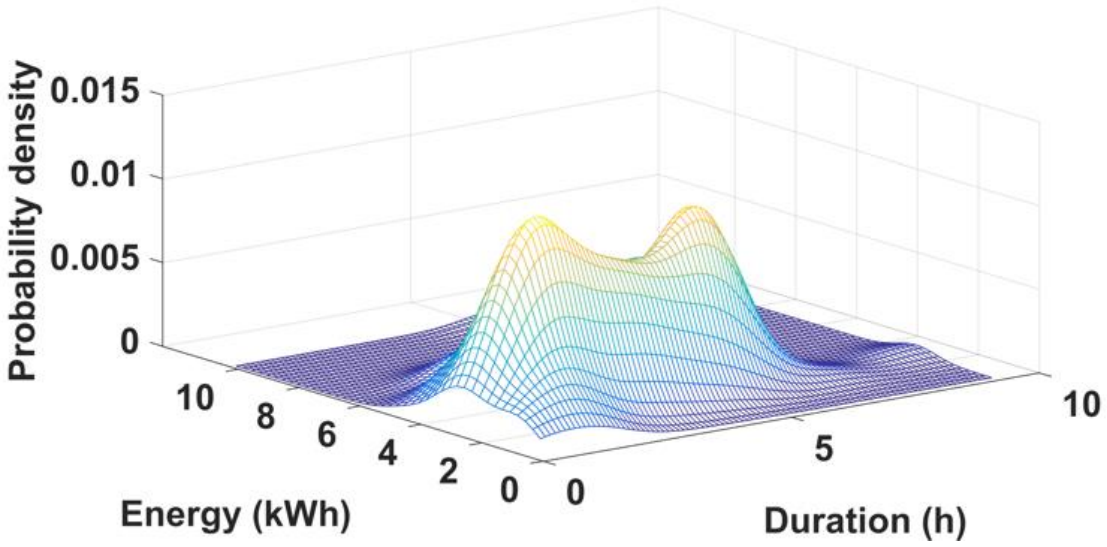

Figure 2-5 Joint probability for stay duration and energy consumption

Following the above steps, session parameters can be estimated adaptively. The complete steps for parameter estimation are summarized in Algorithm 1. Note that, there will be less qualified tuples as the charging session proceeds. Specifically, a new user may also have less similar historical records. In this case, we grant priority to these users by updating the estimated energy demand and stay durations in each loop with preset values. For example, estimation algorithm may assume the

energy demand is about 2 kWh for a new user within the next half an hour. In cases where the estimated stay duration $\hat{d}$ is smaller than modified current value by time t, which is denoted by $t - s.t_s + \Delta d$, the *max* operation is added to prevent the early terminations of certain charging sessions with less estimation accuracy, which may further lead to lower energy delivery rate. Accordingly, the modified estimated leave time is always later than the current time t. Similar operations are made for the estimated energy consumption $\hat{e}$, so that the charging sessions will not be terminated pre-maturely. Note that the estimation is computed every time if the scheduling optimization service is set to run periodically at a fixed time interval. However, under the event-based control paradigm, where computation is only triggered by pre-defined events, a considerable number of computations can be reduced, which we will discuss in later sections.

Algorithm 1: Kernel-based Parameter Estimator

Input*:* current session ***s***, current time ***t***

Output*:* $\hat{e}$, $\hat{d}$

Extract historical tuples with the constraints (2.4) - (2.7);

If number of tuples found > threshold number

Calculate Gaussian kernel by (2.8) - (2.10);

Calculate estimated $\hat{d}$ and $\hat{e}$ by (2.2) and (2.3);

$\hat{e} \leftarrow max\{\hat{e}, e_t^c + \Delta e\}$;

$\hat{d} \leftarrow max\{\hat{d}, t - s.t_s + \Delta d\}$;

Else

$\hat{e} \leftarrow e + \Delta e$

$\hat{d} \leftarrow d + \Delta d$

End

2.3.2 Mean Estimator

A simplified estimator was developed and described in [15],which is based on averaging the session parameters of the qualified sessions, specified by equation (2.4) - (2.7). For the comparison purpose, the performance of the mean estimator is also discussed as a benchmark for the proposed kernel-based estimator.

In mean estimator, equation (2.11) - (2.12) are replaced with the following:

$$\hat{e} = \frac{1}{M} \cdot \sum_{i \in M} S[i].e \tag{2.11}$$

$$\hat{d} = \frac{1}{M} \cdot \sum_{i \in M} S[i].t_l - S[i].t_s \tag{2.12}$$

where S is the set of qualified charging session tuples and the M is the number of the qualified tuples. In this formulation, all data points are measured with equal importance without considering the smoothing effects of the kernel methods. The experiment results from the kernel-based estimator and the mean estimator are discussed in later sections.

2.3.3 Problem Formulation

2.3.3.1 EVSE Model

Since the EVSE in this chapter can be equipped with multiple power sources and certain outlets may share the same power source, one more constraint is added to ensure that total power drawn from each power source cannot exceed its upper limit. In addition, power consumption rate at each outlet cannot exceed the maximum value for that power source:

$$0 \leq r_n^k(t) \leq r_k^{max} \cdot \eta, \qquad \forall t \in [t_n^s, t_n^s + \hat{d}_n] \tag{2.13}$$

where the charging rate at time t for vehicle n connected to power source k, is defined as $r_n^k(t)$. r_k^{max} denotes the limitation of power source k and η is the safety coefficient for each power source. t_n^s is the start time for vehicle n. Let $k \triangleq \{1,2,\dots,K\}$ denote the order of power source number in one EVSE. For each power source k in the EVSE, we have:

$$0 \leq \sum_{n \in N_k} r_n^k(t) \leq r_k^{max} \cdot \eta, \qquad \forall t \in [t_n^s, t_n^s + \hat{d}_n] \tag{2.14}$$

where N_k denotes active charging sessions for power source k.

2.3.3.2 Battery Model

As discussed above, each charging session for user n can be described by the aforementioned parameters defined in the tuple $s_n \triangleq (u_n, t_n^s, t_n^f, t_n^l, e_n)$. Thus, the ideal scenario is that scheduling algorithm allocates more energy than expected, i.e. $e_n > \hat{e}_n$, and meanwhile below the battery capacity e_B, before user's leave time t_n^l, which is represented by $t_n^s + \hat{d}_n$. The actual energy consumption e_n increases as the charging process goes on.

$$e_n(t) = e_n(t - \Delta t) + r_n(t) \cdot \Delta t, \ \ \forall t \in [t_n^s, t_n^s + \hat{d}_n] \tag{2.15}$$

$$e_B \geq e_n\left(t_n^s + \hat{d}_n\right) \geq \hat{e}_n \tag{2.16}$$

2.3.3.3 Virtual Load Constraint

Since the hardware we are modeling has the power sharing circuit design, it means that the charging schedules for vehicles connected to the same power source will be interrelated with each other. Another concern with the EV scheduling problem with random user behavior is that the scheduling process is not quite robust if the power supply is limited. In other words, the pre-computed schedules may be not valid if unexpected additional energy demands are requested by

new coming users for the same power source. For instance, if the scheduling algorithm arranges the energy consumptions in several hours later without considering the future new demand, it is highly possible that the limited power source fails to deliver enough energy to satisfy the unexpected charging demand because the total power consumption violates the power capacity constraints.

We propose a method based on virtual load constraint to solve this issue, by adding constraints on power supply for a future time window. Intuitively, if the future power supply is further limited and the scheduling algorithm has to arrange earlier time intervals for vehicle charging. Thus, the deferability level of EV load is reduced and more energy consumption will be shifted forward to avoid infeasible solutions. The detailed mathematical formulation is in equation (2.17):

$$\sum_{\tau=t+\Delta H}^{\tau=T} \sum_{n \in N_k} r_n^k(\tau) < \lambda \cdot \sum_{\tau=t+\Delta H}^{\tau=T} r_k^{max}, \forall \tau \in [t+\Delta H, T] \tag{2.17}$$

This constraint is to limit the total power consumption for a specific EVSE by virtual load constraint coefficient λ. Note this limit is only valid for the time range from $t + \Delta H$ to the end time T. $\lambda = 1$ is equivalent to remove this constraint and $\lambda = 0$ is actually only allowing power consumption from time t to $t + \Delta H$. Thus, for different scenarios, λ value and ΔH should be tuned to achieve better overall scheduling performance. The effects of λ parameter are discussed in later section.

2.3.3.4 Introduction to Model Predictive Control (MPC)

Model predictive control is an optimal control strategy based on numerical optimizations. From its origin as a computational technique for improving control performance in applications within the process and petrochemical industries, predictive control has become arguably the most

widespread advanced control methodology currently in use in industry [56]. Typically, MPC has three functioning components:

- Predictor based on system model;
- Online optimization tool;
- Receding horizon control implementation.

The simplified process for executing a typical MPC strategy, which is shown in Figure 2-6 is as follows:

- The future system states $\hat{x}_k, \hat{x}_{k+1}, \cdots, \hat{x}_{k+N-1}$ are predicted based on the system model;
- Using the predicted inputs and system states, an online optimization problem is formulated and solved with a numerical optimization solver; The output is inputs $u_k, u_{k+1}, \cdots, u_{k+N-1}$;
- Only the first element of the optimized control signals are implemented. Meanwhile, the prediction and optimization steps are repeated as the time step reaches the end of the time horizon.

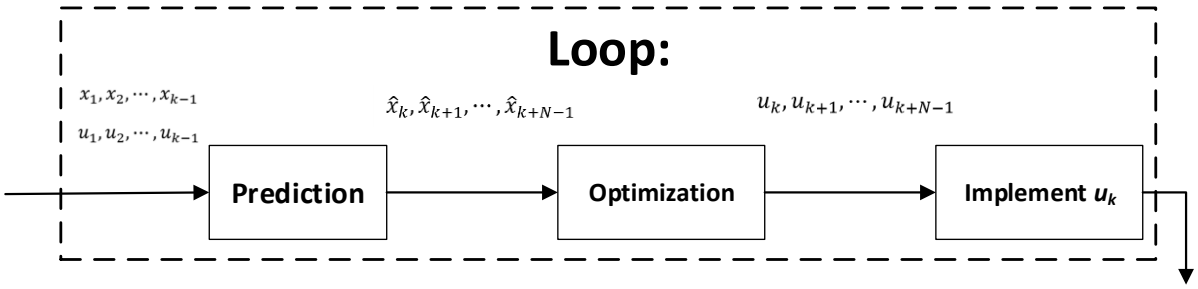

Figure 2-6 Paradigm of model predictive control

2.3.3.5 Receding Horizon Control

We formulate EV charging scheduling problem as a predictive control problem, which can be applied to a variety of objectives, as long as the problem can be formulated as a convex optimization problem.

In our case, the input variables to the system are the current and historical states, e.g. the energy consumption values by each connected vehicle, the solar generation value before current, etc. Based on these most up-to-date system variables, a predictor is developed to estimate the system input variables in the following time series. For instance, the kernel-based session parameter estimator discussed in previous sections will be used to obtain estimations of user behaviors. Similarly, the predictors for other variables can also be applied in this framework, e.g. solar generation predictor, building load predictor, etc. An online optimization solver has the capability to combine the current system states and the estimated future variables as an optimization problem with the objective to minimize the overall system cost (dependent on definition of system cost, e.g. overall operational cost, or total system load variance, etc.), while complying with the constraints of each variable. In the case study of this chapter, we select the total operational cost for the remaining time intervals as the optimization objective, which is formulated as convex problem and computed using an open-source solver. At each time interval, the algorithm hosted by scheduling service will call optimization program to compute an optimal EV charging schedule for the remaining time intervals, considering the estimated session parameters and energy consumption values for all active charging sessions. With only the first element in the list of output variables is implemented to control the EV charging behaviors. More importantly, the process, including prediction, optimization, is repeated every time interval, which could be set to different values, until the current time step reaches the end of the scheduling horizon.

The optimization objective is formulated as follows:

$$\min_{r_n^k(\tau),\tau\in[t,\mathrm{T}]} \sum_{\tau=t}^{\tau=T} P(\tau)\cdot max(\sum_{k\in K}\sum_{n\in N_k} r_n^k(\tau) - PV(\tau)),0) \tag{2.18}$$

$s.t.$ (2.13) - (2.17)

Algorithm 2: Predictive EV Scheduling Algorithm(PESA)

Generate price data;

Retrieve forecast solar data;

$\tau = t_0$;

Do

For each power source $k \in K$:

Terminate charging sessions whose leave time $t_l \leq \tau$;

For each vehicle $n \in N_k$:

Estimate stay duration $\hat{d}_n$ and energy consumption $\hat{e}_n$ for vehicle n, according to **Algorithm 1**;

End

Solve problem (2.18) ,subject to (2.13) - (2.17);

If solution infeasible:

Relax constraint (2.17), and set $\eta = 1$ in equation (2.13) and (2.14);

End

For each vehicle $n \in N_k$:

Implement $r_n^k(\tau)$;

End

End

$\tau = \tau + \Delta t$;

While $\tau \leq T$

The solar generation integration, EV power consumption as deferrable load, will be shifted to the time interval with abundant solar generations. On the other hand, when solar generations cannot support the total EV charging load, algorithm will choose the time range with lower energy prices for EV charging. τ denotes to the current time when the scheduling algorithm is called and T is the maximum time step for the scheduling horizon. $PV(\tau)$ denotes the forecast solar generation at time τ from the installed panels. $P(\tau)$ is the electricity price at time τ. The max operation actually models the integration of solar generation by comparing the total charging load with the solar output value for each future time interval. Inspired by the model predictive control paradigm, the optimal energy consumption schedules for all the remaining time intervals are computed, however, only the first element, $r_n^k(t)$, is implemented to control EVSE. As the scheduling proceeds, the scheduling horizon recedes to the maximum time step T, indicated by the name receding horizon control. The complete charging control algorithm is summarized in the following Algorithm 2.

Note that this control paradigm requires the scheduling service to be initiated every time step, which leads to the successive operations for data retrieval, parameter estimation and optimization. In cases when the computing resources are limited or quality of communication network is not reliable, failure to update charging schedules may happen. Therefore, to overcome this drawback, we propose an event-based scheduling paradigm that minimizes the number of charging session controls.

2.4 Results and discussion

2.4.1 Experiment setup

To evaluate the performance of our proposed scheduling framework, charging sessions of real-world users on the UCLA campus are utilized to set up the simulation experiments. The dataset

includes UCLA experiment data from August. 2013 to Mar. 2015. 20-fold cross validation, discussed in [57], section 5.3.3, is utilized to justify the performance of the proposed scheduling framework. Specifically, the total charging records of 588 days are randomly divided into 20 partitions, *i.e.* approximate 30 days in each partition, and the simulation will run for each partition as the test set, using the remaining 19 partitions as training datasets. The details of this method are shown in Figure 2-7. Training sets provide the historical records for all users as basis for session parameter estimation, while test set is used to evaluate the scheduling performances, in terms of energy delivery rate, cost performance, etc. The dataset properties are displayed in Table 2-1.

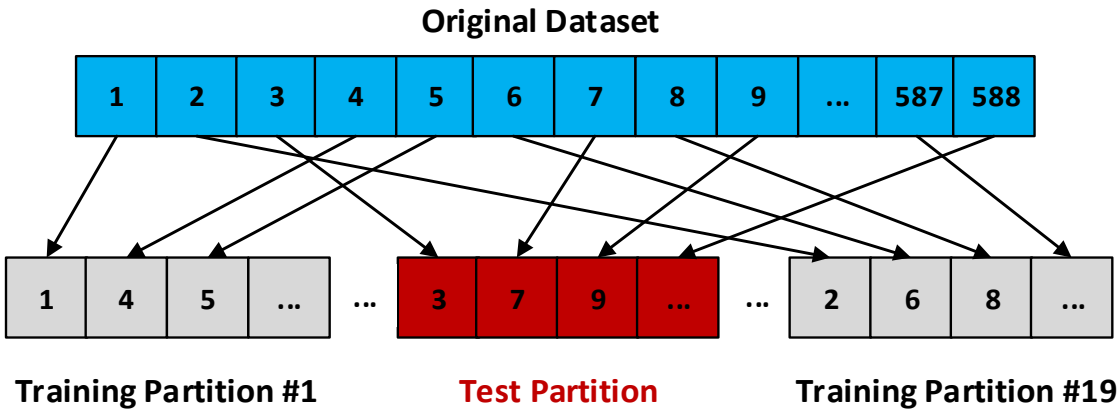

Figure 2-7 20-fold cross validation

Table 2-1 Dataset properties

	Training Set	Test Set
Number of Partitions	19	1
Number of Days	558	30
Number of Sessions	≈4400	≈200
Number of Users	79	79

TOU price list is generated based on the wholesale price signals from California Independent System Operator (CAISO) [58]. The original prices are modified with additional values for certain hours during the day to simulate the retail electricity prices in distribution networks, which are displayed in Figure 2-8.

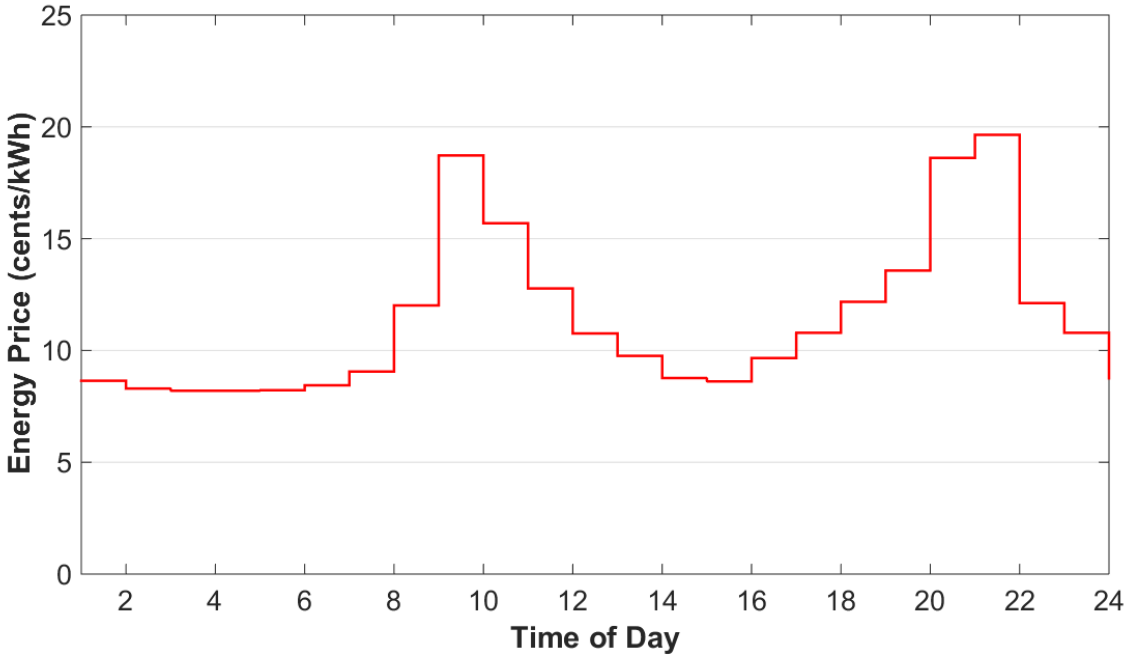

Figure 2-8 Energy price used for simulation

The solar generation data we used in simulation is from solar integration project [10], [59] on the UCLA campus. We assume that each EVSE is equipped with 10 solar panels. Since the focus of this scheduling framework is on the uncertainty of user behaviors, details of solar prediction algorithm are not within the scope of this dissertation. We simply apply the smoothed solar curve as our forecast solar generation data, which is shown in Figure 2-9.

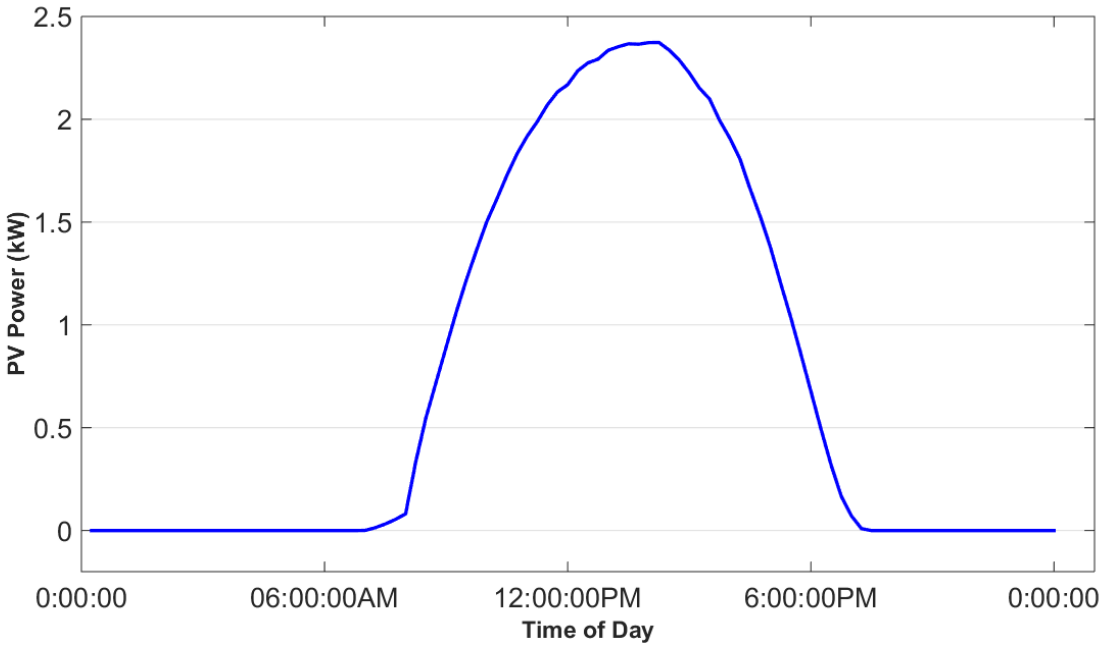

Figure 2-9 Sample solar generation data

Table 2-2 Charging records on 17th, Marth, 2015

No.	User Index	Start Time	Duration (h)	Energy Demand (kWh)
1	CE1*	06:10:12	9.33	8.561
2	F42*	06:42:33	2.02	4.468
3	BFE*	07:07:44	6.87	12.207
4	155*	07:17:24	9.92	9.185
5	9CA*	14:08:58	7.3	6.154
6	8D5*	15:30:23	4.2	11.11
7	2E7*	18:31:56	1.05	5.722

Note that the time interval Δt for scheduling algorithm is set to 15 min. For each dimension, bandwidth h in kernel based estimator, i.e. equation (2.9), is set to $1.06\sigma \cdot N^{-\frac{1}{5}}$ according to [55], where σ is standard deviation of the values in that dimension. Adjustable values in session parameter estimator, i.e. Δd and Δe in Algorithm 2, are set to 0.5 hour and 2 kWh, respectively. For virtual load constraint in equation (2.17), horizontal length ΔH is set to 3 hours. The EVSE picked for simulation has 2 power sources and each one has the maximum output 6.6 kW. The

safety coefficient η in equation (2.13) and (2.14) is set to 0.7. The virtual load constraint λ is set to 0.3. The package in [60] is employed to solve the schedule optimization problem.

2.4.2 Cost Saving and Load Shifting Effects

Since the primary objective of the scheduling framework is to optimize the overall cost performance for providing charging services and satisfy the charging demand from EV users, we randomly pick one day for the single day simulation, with the following records shown in Table 2-2.

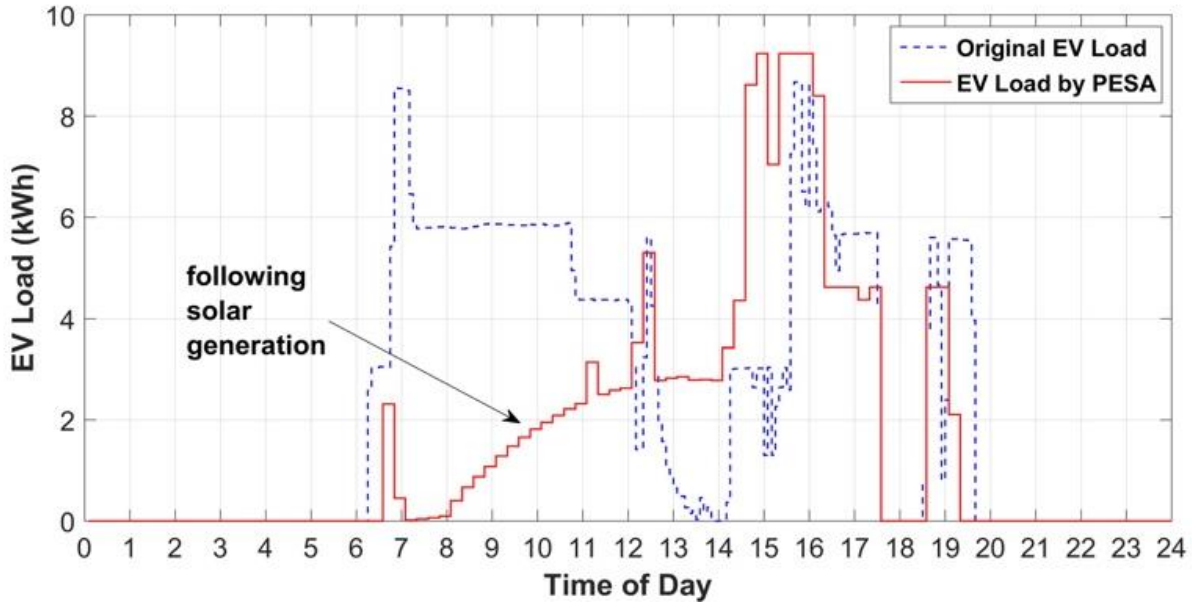

Figure 2-10 EV Load Scheduling Results ($\lambda = 1$)

The scheduling results from the original ESSA and our proposed PESA (virtual load constraint $\lambda = 1$) are shown in Figure 2-10.The blue dot curve denotes the original EV load created by the charging sessions in Table 2-2, while the red curve is the new EV power consumption schedule generated by PESA. From the figure, one can see that a large portion of the load is shifted from early morning to early afternoon when there is abundant solar generation and the energy prices are lower, which can be found in Figure 2-8 and Figure 2-9. Another interesting phenomena is the

solar generation following effects of this algorithm. Since the local solar generation can be utilized as alternative power source instead of purchasing electricity from grid, the allocation of EV charging energy tends to follow the curve of solar generation, as is shown in Figure 2-10. Thus, due to the load shifting effects, the total energy cost by PESA has been reduced.

However, it should be noted that the total delivered energy by the new PESA algorithm is not as much as the originally delivered energy, *i.e.* the area under the red curve is less than that under blue dot one. A close investigation reveals that this issue is caused by the uncertainty of session parameter estimation. In other words, there exist certain users in this EVSE who leave earlier than their estimated leave time so that not enough energy is allocated to their EVs. In the single day test, the energy delivered by PESA is 51.6 kWh, which is 10.12% less than the original value. On the other hand, the average unit energy cost (¢/kWh) is originally 11.23 ¢/kWh without optimization and solar integration, and it is then reduced to 5.72 ¢/kWh by PESA.

Thus, we define another criteria to evaluate the robustness of the scheduling framework over all the test samples in each partition, *i.e.* Average Schedule Error Rate (ASER), whose mathematical form is:

$$ASER = \frac{1}{M} \cdot \sum_{m=1}^{M} \left\{ \frac{1}{N_m} \cdot \sum_{i=1}^{N_m} \frac{e_i^m - min(e_i^{m,c}, e_i^m)}{e_i^m} \right\} \cdot 100\% \qquad (2.19)$$

where e_i^m is the actual energy consumption from ESSA for *i-th* charging session on *m-th* test day of a particular partition in training sets. $e_i^{m,c}$ is the corresponding energy consumption from PESA. N_m here denotes the number of charging sessions in *m-th* test day. M is the total number of test days in *m-th* partition. Smaller ASER value represents a more robust solution with higher EV energy delivery rate, while the larger one indicates higher probability of failures to provide enough

energy to EVs due to their uncertain charging behaviors. For a particular charging session, it is possible for the system to provide either more or less energy, *i.e.* $e_i^{m,c}$, than actual consumption value e_i^m, however, only the cases where $e_i^{m,c} < e_i^m$, are defined as schedule errors, which should be avoided or minimized.

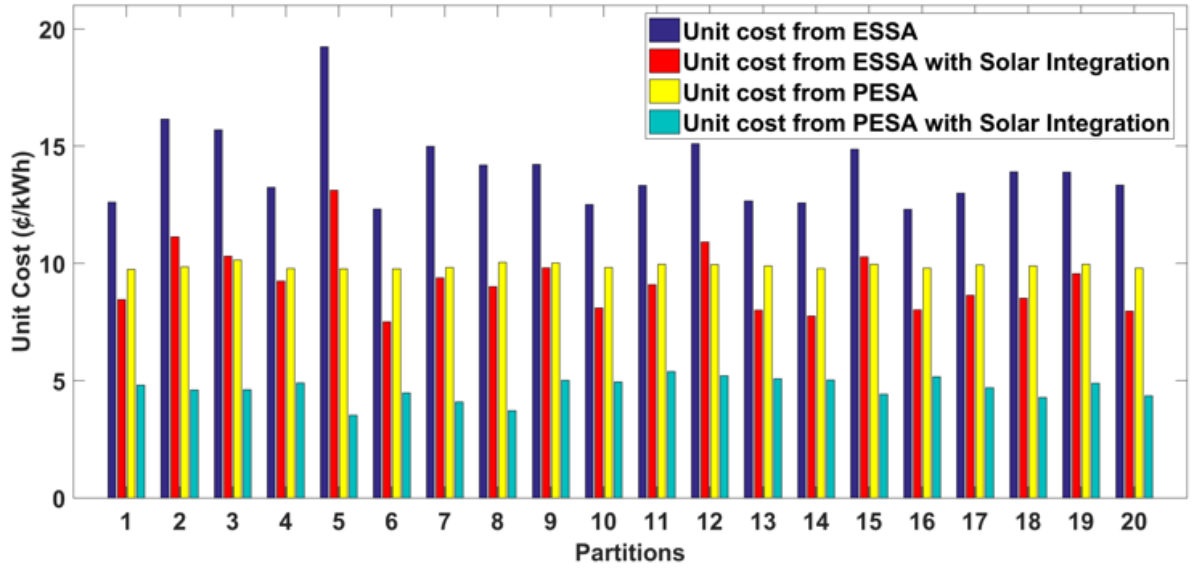

Figure 2-11 Average unit energy cost on partitions

To validate overall performance, the average unit energy cost and ASER values across all test partitions are computed and shown in Figure 2-11 and

Figure 2-12, respectively. The scheduling results demonstrate that the PESA is more effective in cost optimization compared to the original ESSA. With the solar integration and time-varying energy prices, PESA will adaptively minimize the total operational cost by searching for the optimal time ranges and charging power for each vehicle. The average reduction of unit energy cost across all partitions reaches 29.42% (blue vs. yellow bars) and it can be further improved to 66.71% (blue vs. green bars) by integrating renewable generations with EVSEs. PESA can also outperform ESSA when both are with solar integration (green vs. red bars). In our experiment, the

maximum solar output is around 3 kW so the cost saving performance can be further optimized by increasing the capacity of solar integration, especially when the energy demand is high on the test days. Besides, the ASER values for all partitions are also computed to evaluate the energy delivery rate. The maximum ASER value, in

Figure 2-12 is approximately 12%, indicating that the energy delivery rates are acceptable across all test samples. Note that, ASER values can be improved by tuning the virtual load constraint (λ), which is discussed in later sections.

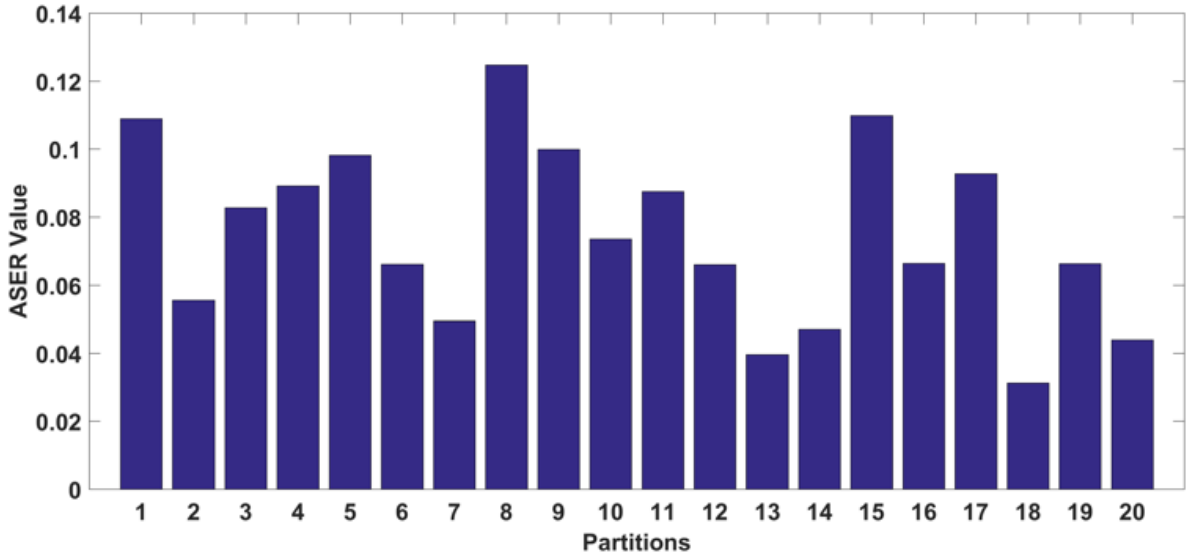

Figure 2-12 ASER values for partitions

2.4.3 Impact of Solar Infrastructure Investment

Considering the initial investment on the solar Photovoltaics (PV) infrastructure, including fees of installation and maintenance, etc., the overall operational costs by one EVSE with and without solar installation, are visualized in Figure 2-13, respectively, by plotting the accumulated values of energy consumption and operational cost by PESA and ESSA. According to [61], the solar installation and maintenance cost in California in 2015 Q1 is roughly 2.14 $/W, and lifetime of

service is longer than 30 years. Therefore, it is estimated that after 82000 kWh energy delivery (approximate 6.6 years), the proposed EVSE with solar integration will provide more benefits than the traditional solution. As the cost of solar panel drops, the time it takes to reach the cost match point in Figure 2-13 is becoming shorter.

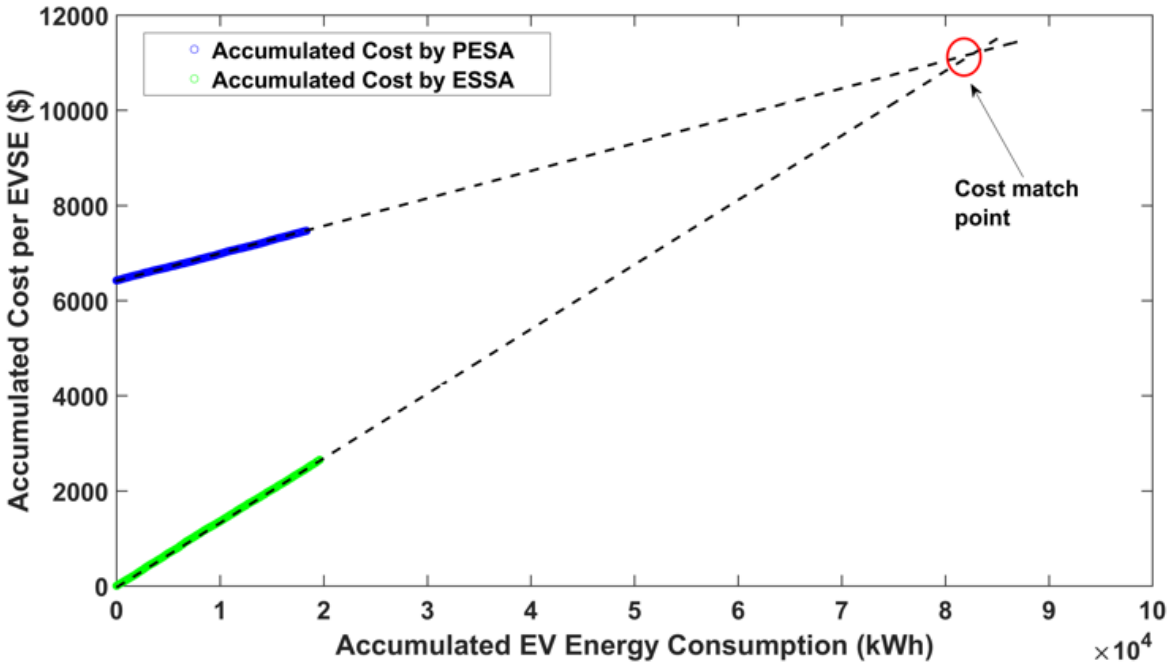

Figure 2-13 Accumulated energy consumption and cost

2.4.4 Effects of Virtual Load Constraint

Since the energy delivery deviations are caused by users' early departures which cannot be estimated with 100% accuracy, here we demonstrate the effects of virtual load factor on improving the ASER values.

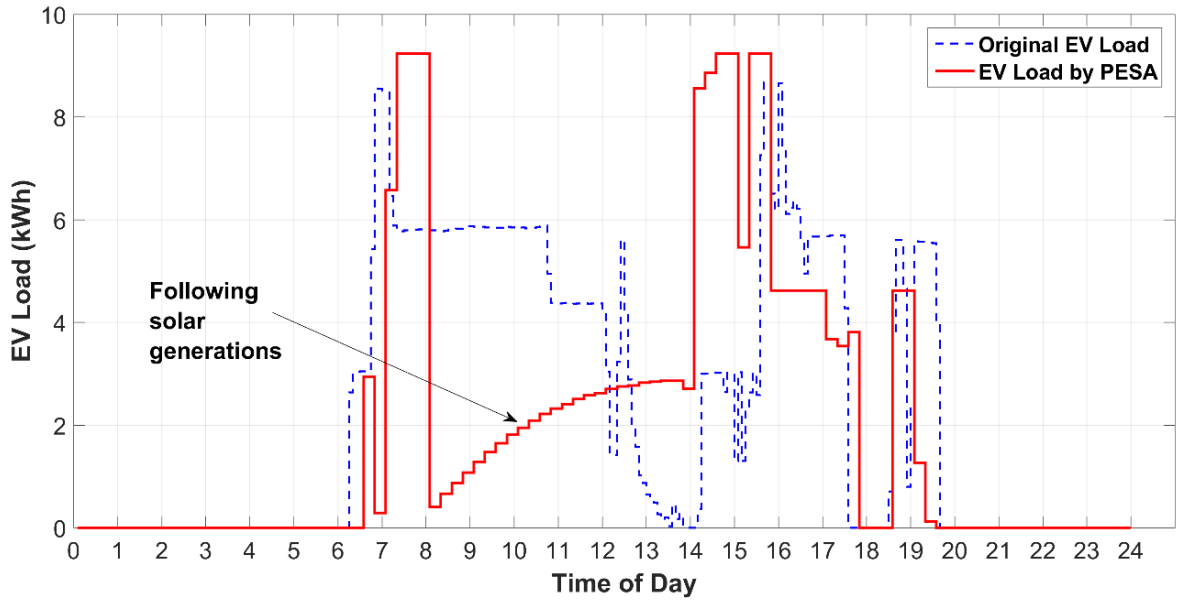

Figure 2-14 EV load scheduling results (λ=0.3)

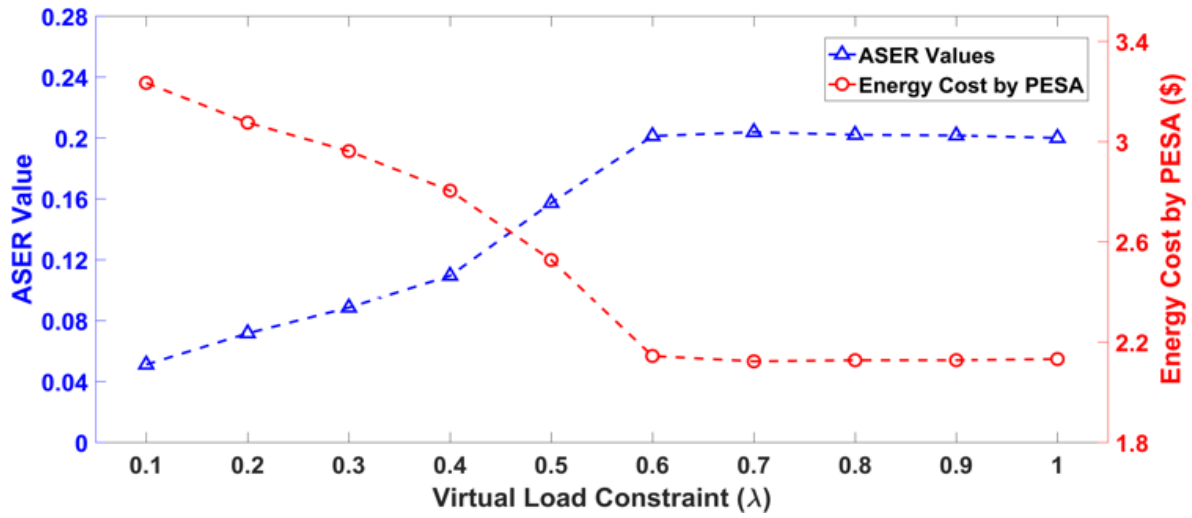

Figure 2-15 Virtual load constraint factor effect

First, single-day experiment is performed to demonstrate the load shifting effect of the virtual load constraint. By setting $\lambda = 0.3$, we explicitly throttle the power supply for each EVSE with multiple vehicles connected, so that less energy should be provided after ΔH intervals. Accordingly, the it is projected that portion of the charging energy, which should consumed in later time intervals, are actually consumed in earlier time intervals. Real-world charging records in Mar. 17th, 2015, are

utilized for the simulation, which is shown in Figure 2-14. Compared to the results shown in Figure 2-10 where load constraint factor is set to 1, new EV load curve is slightly different, i.e. there is a portion of the charging load shifted to the time range between 06:30 AM and 08:00 AM in the morning. The ratio of the shifted energy consumption from the original time intervals to new time intervals is monotonically related to the value of virtual load constraint λ. That is to say, the as the constraint λ goes tighter, more energy consumption from EVs will be shifted forward to time range with higher energy prices or less solar generation (6:30 AM – 8:00 AM in the case shown in Figure 2-14). Meanwhile, due to this load shifting effect, it is also projected that the ASER value should be improved because the system becomes less vulnerable to the unexpected vehicle departures, since load from EVs is less deferrable.

Intuitively, constraints on the future power supply renders the algorithm to allocate more energy as soon as possible in order to avoid infeasible schedules, *i.e.* the power source cannot provide enough energy to match the total demands from active charging sessions after ΔH. For one test day, the ASER value and the total operational cost are computed with different λ values and the results are shown in Figure 2-15. As the value of constraint factor λ goes smaller, tighter restrictions after ΔH are applied on power sources, the algorithm tends to shift as much EV energy consumption as possible to time intervals before time $t + \Delta H$, so that energy delivery rate is improved even though users may leave unexpectedly earlier. However, as more energy is consumed in earlier non-preferable time ranges with higher prices or less solar generation, which is forced by virtual load constraints, the solution becomes less optimal. Thus, the total energy cost increases as λ goes smaller. Due to the uncertainties of user behaviors, this is a trade-off one has to consider. For example, in scenarios where requirements on schedule error rates are restrict, a

smaller λ is minimize the ASER value down to 5%, however, it will not achieve the best overall cost.

2.4.5 Estimation Accuracy

In preliminary work [52], a simpler estimator was utilized to estimate session parameters, including stay duration and energy consumption. The original solution is a simple mean estimator, which calculates the mean value across all qualified sessions extracted by (2.4) - (2.7). At each time interval when the scheduling algorithm is initiated, the estimated values from both the simple mean estimator and kernel-based estimator are recorded for performance assessment. Due to the variety of session parameters, the number of estimations for each charging session may be varied so that we define another metric, *i.e.* sample estimation deviation to evaluate the overall estimation accuracy.

$$Dev_m = \sqrt{\frac{1}{N_m} \cdot \sum_{i=1}^{N_m} \frac{1}{L_n} \cdot \sum_{l=1}^{L_n} (v_l^i - v_T^i)^2} \tag{2.20}$$

where L_n is the total number of estimations that belongs to *i-th* charging session in the *m-th* partition. Note there must be at least one estimation for each charging session. N_m denotes the total number of charging sessions on partition m. v_l^i is the *l-th* estimated value of *i-th* session and v_T^i is the actual parameter, *i.e.* true values for stay duration or energy consumption.

According to equation (2.20), the estimation deviations for stay duration and energy consumption are both displayed in Figure 2-16. The performance of kernel-based estimator is better than the mean estimator for both stay duration and energy consumption, with smaller deviation values. The advantage of Gaussian kernel estimator is the smoothing effect across all the variable space, which does not require a specific model. The averaged estimation deviation for stay duration by kernel-

based estimator is 1.52 h, which is 26.05% less than that of mean estimator, while for energy consumption, the deviation value is reduced from 2.91 kWh to 2.50 kWh by 14.22%. The effectiveness of kernel-based estimator is demonstrated thereby.

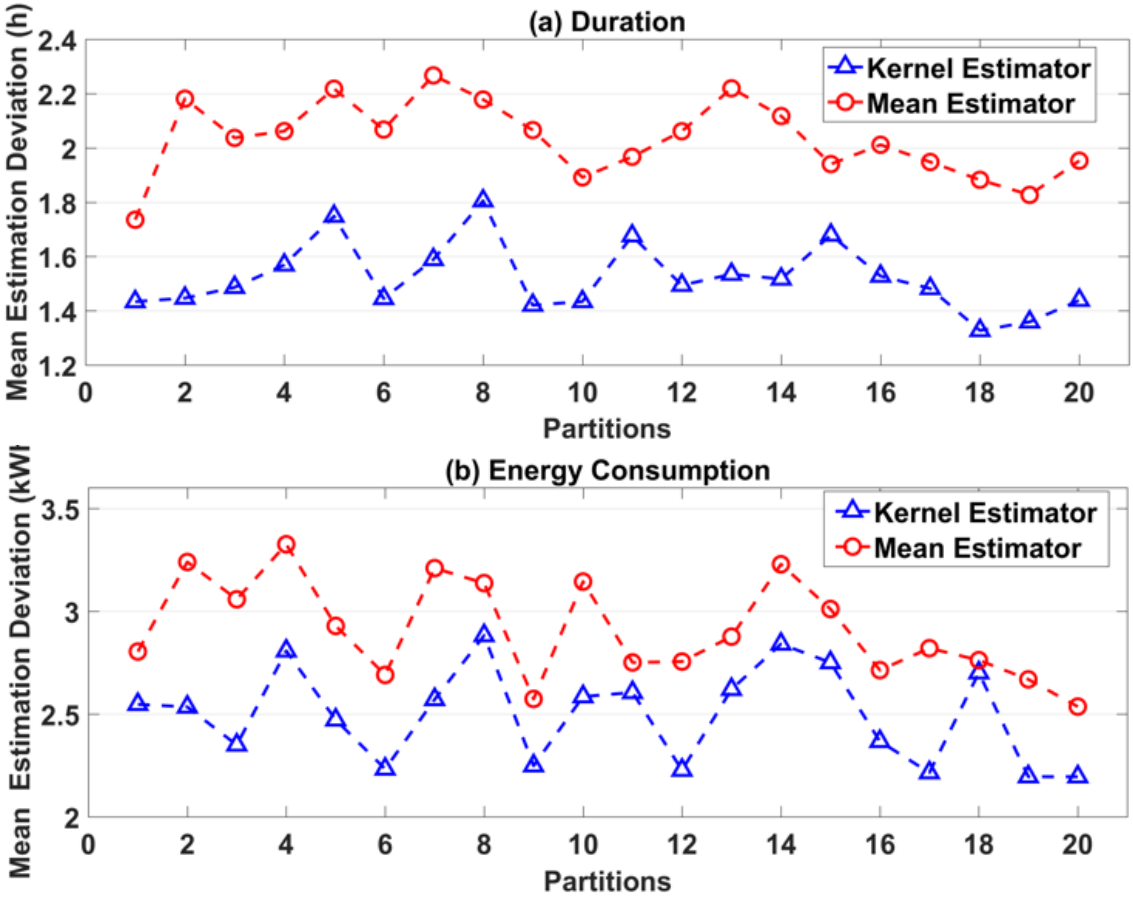

Figure 2-16 Estimation deviation

2.5 Summary

In this chapter, we propose a predictive scheduling framework which takes into account the uncertainties of EV user behaviors. Specifically, Gaussian kernel estimator is designed to dynamically estimate the charging session parameters with improved estimation accuracies. In addition, virtual load constraint is also formulated to handle the unexpected EV energy demand arriving in the near future. Real-world data on the UCLA campus is utilized for the cross validation

of the proposed framework to demonstrate the improved cost performance and EV energy delivery rate.

Chapter 3 Event-based EV Charging Strategy with Integration of IEC 61850

Coordinating charging behaviors of a number of EVs is a challenging task, which involves not only the deterministic schedule computing but also nondeterministic EV driver behaviors with random arrival time and energy demands. Chapter 2 introduces the predictive energy management framework, which is adaptable to a myriad of energy management strategies with varied optimization objective, however, it requires the system states and session parameters related to EVs to be updated every time interval, which is not efficient, and even not practical in real-world systems. In this chapter, an implementable event-based cost optimal scheduling algorithm (ECSA) is developed, which solves EV scheduling problem by dynamically estimating the stay duration and energy demand for each participating EV user. The steps to update the system states and to solve the optimization problem are only triggered by the pre-defined the events, which indicate a critical system state change. Datasets, including users' historical charging records and time series meter data collected from EVSEs on the UCLA campus, are utilized for feature extraction. In addition, IEC 61850 is integrated with the smart EV management program, which provides a standardized communication protocol and data model to improve the overall system interoperability. The proposed approaches are tested and validated by real EV charging schedules of users on the UCLA campus. The results from simulation experiment demonstrate that the proposed algorithm has a better performance in cost minimization and load shifting compared to

existing equal-sharing scheduling algorithm (ESSA). Meanwhile, we also compare ECSA to PESA in terms of different performance metrics.

3.1 Introduction

Numerous energy management strategies on EVs have been developed by previous researchers with different objectives and constraints, e.g. algorithms in [35], [36], [41], [48], [62]–[66]. However, few of them consider three practical issues in real-world implementations: 1) there exists delay and packet loss among the communication network; 2) frequent data retrieval and optimization, such as PESA described in Chapter 2, may exert great burden on the server, increasing the chance of server crash; 3) standardization of the data models with different variables, such as physical parameters of the power system, and the energy consumer related variables, etc.

Therefore, considering these issues, we develop an event-based cost-optimal scheduling algorithm (ECSA) based on the predictive energy management strategies from Chapter 2, with integration of IEC 61850 standard. Event-based control strategies are widely used as advanced control technologies that have been applied to a variety of applications, e.g. traffic flow optimization [67], software engineering with high communication load or high computational efficiency requirement [68] [69], [70], supply-chain management [71] and robotics [72], etc. Typically, event-based strategies improve the system efficiency by reducing the number of un-necessary computations, while still satisfying the system performance requirements. Specifically, if the system states and the predicted input values do not change very much, it is not necessary to re-initiate the optimization step. Case studies are provided to verify the performance of the proposed ECSA and the simulation results indicate that ECSA is effective in reducing system computation load while

maintaining the values of the system operational cost and energy delivery rate on an acceptable level.

In addition, we provide a method to integrate IEC 61850 into EV smart charging infrastructure with multiplexing capabilities [44], [73]–[75], by defining customized data models. The data transmitted between EVSE and the aggregated control center includes charging control commands, power metering data and user interactions, etc. IEC 61850 is integrated to standardize these data strings, making them immediately available to others devices. New features such as power sharing, current multiplexing and mobile app charging control is also integrated [44].

The contributions of this work can be summarized as:

- Event-based EV energy management strategy is developed with improved system efficiency, while maintaining acceptable system performance on cost and energy delivery rate;
- Standardize communication and data models involved in smart EV charging to improve the system interoperability and scalability;
- Extend IEC 61850 with new features, such as mobile applications, power source constraints, energy prices, etc;

3.2 Event Trigger Scheme

In most cases, the continuous estimation of session parameters does not have large variations, which means the schedules obtained previously are still valid under current conditions and the re-computation is not necessary. Under the proposed event-based control paradigm, the scheduling services will only be initiated when the pre-defined events are detected, instead of being computed every time interval. The pre-defined events should represent obvious deviations of system states.

Therefore, the do-while structure in Algorithm 2 needs to be updated with the event trigger structure based on the real-time monitoring of charging sessions, shown in Algorithm 3. The following events are defined.

***Event 1*:** New vehicle arrives with charging request;

***Event 2*:** Vehicle leaves from EVSEs or terminates charging;

***Event 3*:** Energy already consumed exceeds the estimated one, which is believed as an abnormal behavior and we infer that this user needs more energy than consumed;

***Event 4*:** Leave time exceeds the estimated one, which might indicate the extended stay duration for this user;

***Event 5*:** New estimated session parameters deviates the original estimations by a pre-defined value.

As shown in Figure 3-1, an Event Monitor is running periodically to check if the system has changed and only when such an event is detected, the scheduling algorithm developed in Chapter 2, will be invoked.

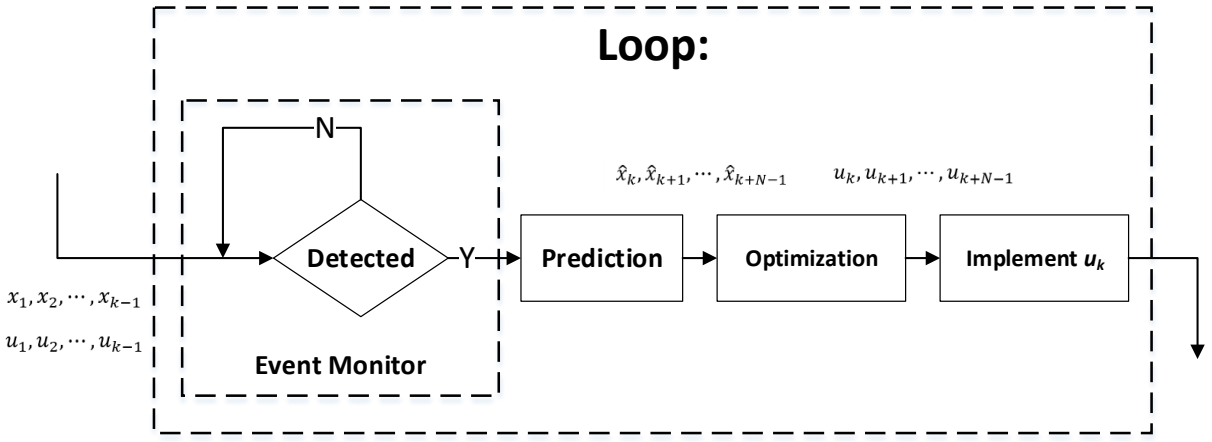

Figure 3-1 Event-based control paradigm

Algorithm 3: Event-based Cost-optimal Scheduling Algorithm(ECSA)

Generate price data;

Retrieve forecast solar data;

Event triggered:

For each power source $k \in K$:

Terminate charging sessions whose leave time $t_l \leq \tau$;

For each vehicle $n \in N_k$:

Estimate stay duration $\hat{d}_n$ and energy consumption $\hat{e}_n$ for vehicle n, according to **Algorithm 2**;

End

Solve problem (2.18) ,subject to (2.13) - (2.17);

If solution infeasible:

Relax constraint (2.17), and set $\eta = 1$ in equation (2.13) and (2.14);

End

For each vehicle $n \in N_k$:

Implement $r_n^k(\tau)$;

End

End

3.2.1 Experiment setup

Event-based EV scheduling paradigm is first introduced in [52], which is believed to reduce the number of controls and computer resources, while maintaining system performances. Event-based Cost-optimal Scheduling Algorithm (ECSA) is compared with Predictive Energy Scheduling Algorithm(PESA) and Equal-sharing Scheduling Algorithm (ESSA) in terms of ASER values and unit energy cost. The only difference between these two algorithms is that ECSA is initiated by the pre-defined events while PESA runs periodically at fixed time interval. Three sets of different experiments are performed to verify the proposed event-based EV charging control strategy: 1)

ESSA vs. ECSA on continuous 10 days; 2) ECSA vs. PESA on continuous 10 days; 3) ECSA vs. PESA by cross-validation. Real-world EV charging sessions on the UCLA campus are utilized to set up the simulation. The extracted charging sessions are ordered by the start time and labeled with power source number so that real charging events can be reproduced exactly. Δt, i.e. time interval for scheduling algorithm is set to *15* min. In the first 2 case studies, the virtual load constraint is set to 1, and in the third simulation, $\lambda = 0.3$.

3.2.2 Case Studies

3.2.2.1 Case 1: ECSA vs. ESSA on continuous 10 days

Figure 3-2 is the comparison of operational costs from 3 scheduling algorithms, ESSA, ESSA with solar integration and ECSA. Solar integration reduces the cost for both ESSA and ECSA. For ECSA, the cost decreases because of two reasons: 1) delayed energy consumption at the early stage of charging session 2) charging load shifted from regions with higher price and abundant solar energy, to regions with higher energy price and less solar energy. Suppose the energy consumptions are the same from ESSA and ECSA, there will still be larger portion of load in regions with lower price and ample solar energy, which can be observed from Figure 3-2. Thus, 1) is not dominant reason for cost reduction. The effectiveness of ECSA for cost minimization is demonstrated.

The other criteria is the deviation between actual energy consumption for each vehicle and that obtained from ECSA. A metric named Average Schedule Error Rate (ASER) is defined to represent this deviation:

$$ASER = \frac{1}{L} \cdot \sum_{i}^{L} \frac{e_i - e_{i,c}}{e_i} \cdot 100\% \tag{3.1}$$

where e_i is the actual energy consumption from ESSA for one charging session on a particular day. $e_{i,c}$ is the energy consumption from ECSA. L denotes the number of charging sessions on a particular test day. Smaller ASER value corresponds to less deviations. ASER values for the test days are generally acceptable considering the randomness of EV charging sessions. The energy consumption from ECSA, ESSA and ASER values are shown in Figure 3-3.

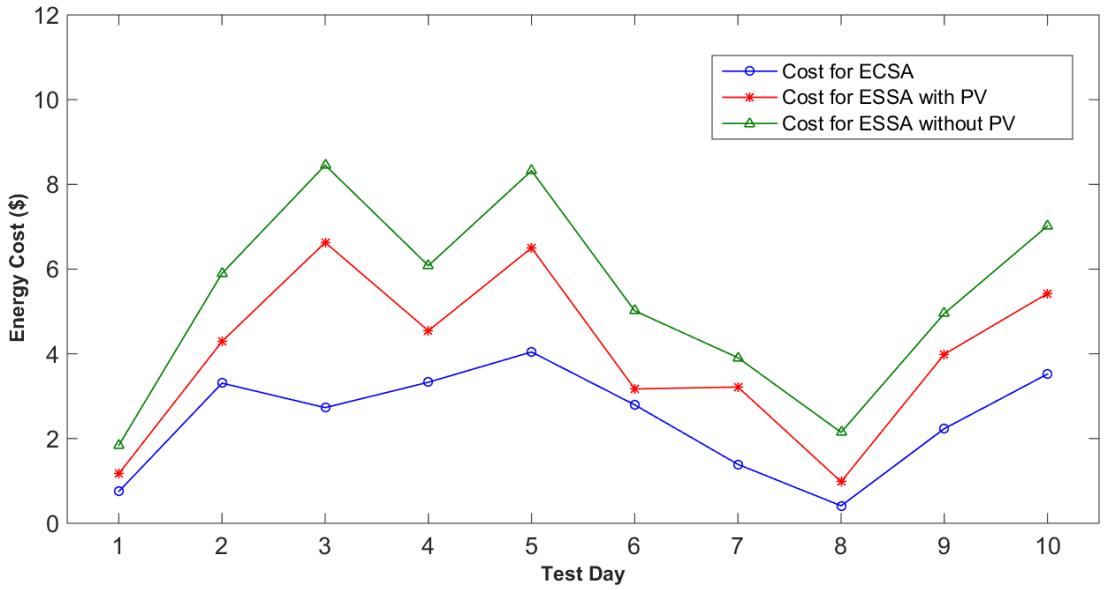

Figure 3-2 Operational cost from EV scheduling algorithms

To achieve smaller ASER values, scheduling algorithm needs to deliver as much energy as the ESSA does before each session ends. There exist trade-offs between cost minimization and error rate minimization. Being greedy for energy cannot guarantee optimal cost and vice versa. A possible modification to current ECSA is to increase the greediness for charging sessions that start not long ago and then perform optimal scheduling after energy consumption reaches certain level. Hereby, cost saving performance can be preserved while global *ASER* values can also be improved.

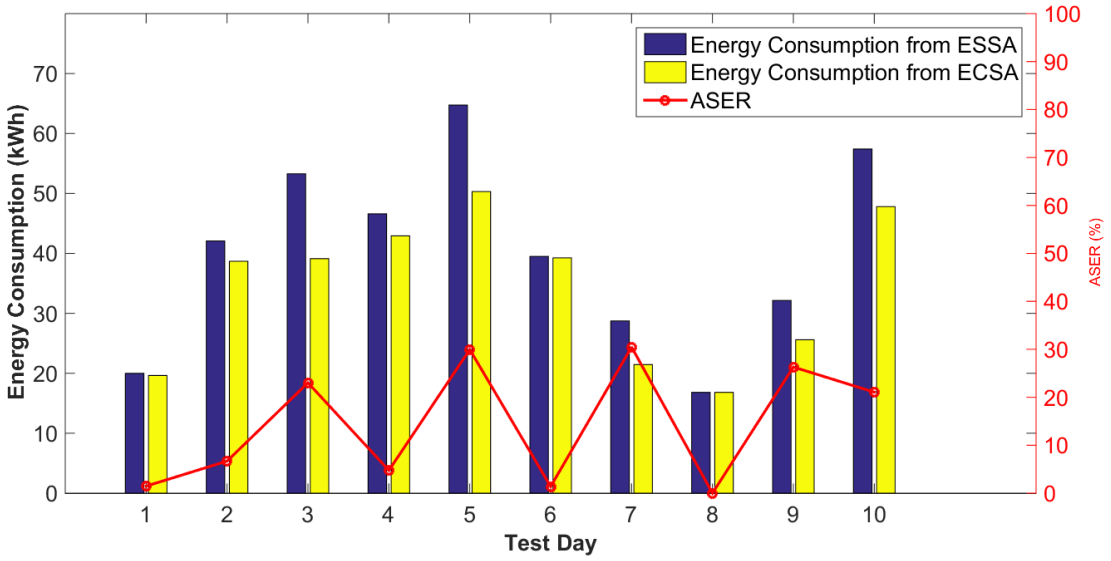

Figure 3-3 Energy consumption and error rate

3.2.2.2 Case 2: ECSA vs. PESA on continuous 10 days;

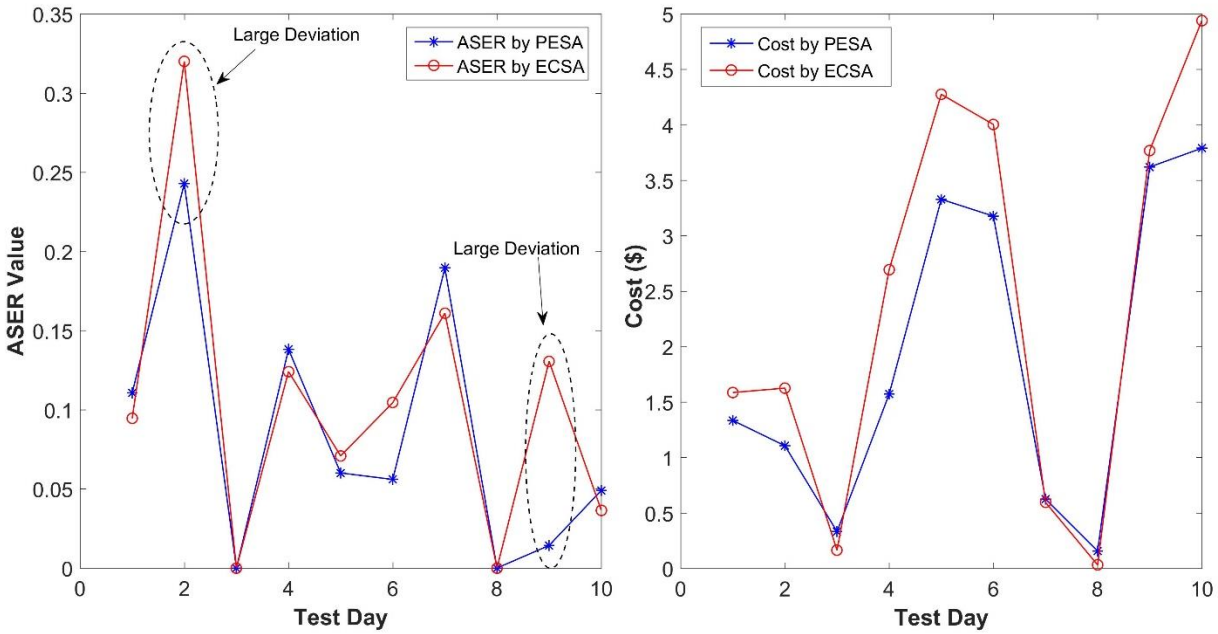

Figure 3-4 Scheduling results of PESA and ECSA for continuous 10 days

We randomly select a period of continuous 10 days to verify the performance of the proposed event-based strategy. With the dataset of the selected 10 days for a specific EVSE as the test dataset,

and the remaining data as the training dataset, overall operational cost and ASER values are displayed in Figure 3-4. In test day #2 and #9, there exist large deviations of ASER values between PESA and ECSA, which indicates less energy delivered to connected vehicles by ECSA. Without capturing the system dynamics, including the values of solar generations and the change of the estimated session parameters in every time interval, ECSA fails to allocate enough energy compared to PESA. The other phenomena is observed that the overall operational cost for ECSA is slightly higher than that of PESA on certain days, which is shown in the right diagram in Figure 3-4. One plausible explanation is that failure of ECSA to capture the most up-to-date system dynamics leads to the less optimal energy schedules from the optimization problem. For instance, if one of the vehicles in the morning stays longer than the previous estimated duration, meaning that it is possible to shift this amount of EV load backward with more solar generation and lower energy prices.

3.2.2.3 Case 3: ECSA vs. PESA by 20-fold cross-validation

The second case study is based on the 20-fold cross-validation on the whole dataset. The averaged ASER values and the unit energy cost (cent/kWh) are computed for each partition to study the averaged performance of ECSA compared to PESA. In the simulation, Δt is set to 15 minutes, the results are compared in Figure 3-5 and Figure 3-6. For all partitions, PESA has better ASER values, which indicates the better performance on energy delivery rate, than ECSA, which fails to capture the most up-to-date system states by skipping over certain time steps and assuming the previous estimations are still right. The average ASER values across all partitions for PESA and ECSA are 7.5% and 11.65%, respectively, shown in Figure 3-5. Interestingly, even though ECSA has a little worse ASER values, it has comparable average unit energy cost at 4.81 ¢/kWh, which is only ¢0.03 higher than that by PESA. Note that the maximum ASER value by ECSA is still less than 15%.

Therefore, ECSA can serve as a cost-efficient solution with acceptable performance, if the requirements on energy delivery rate are not too strict.

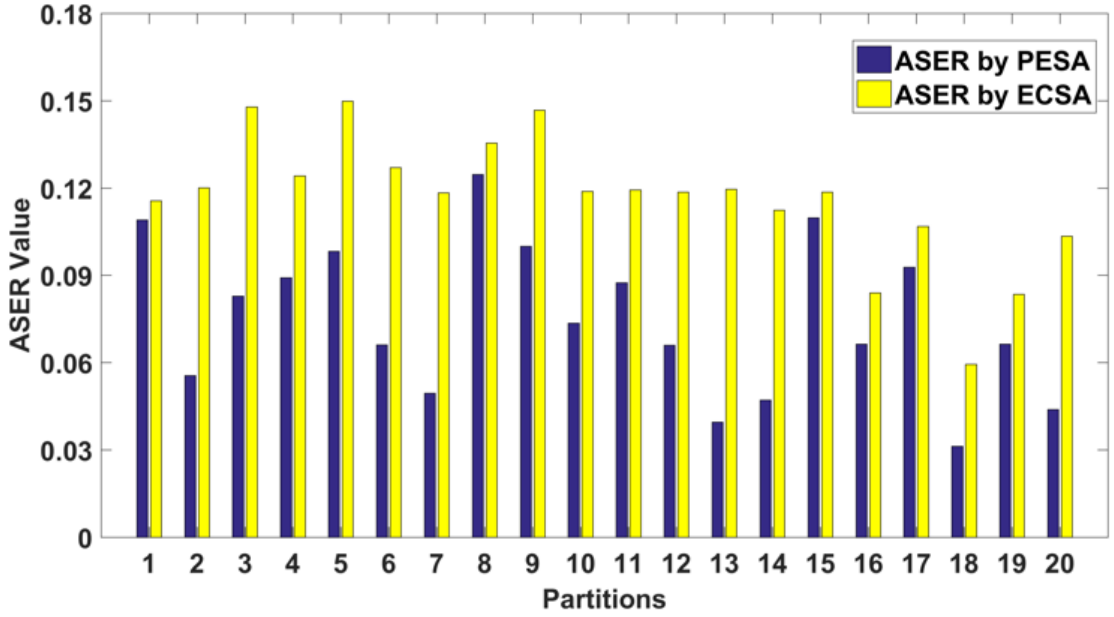

Figure 3-5 ASER values for PESA and ECSA

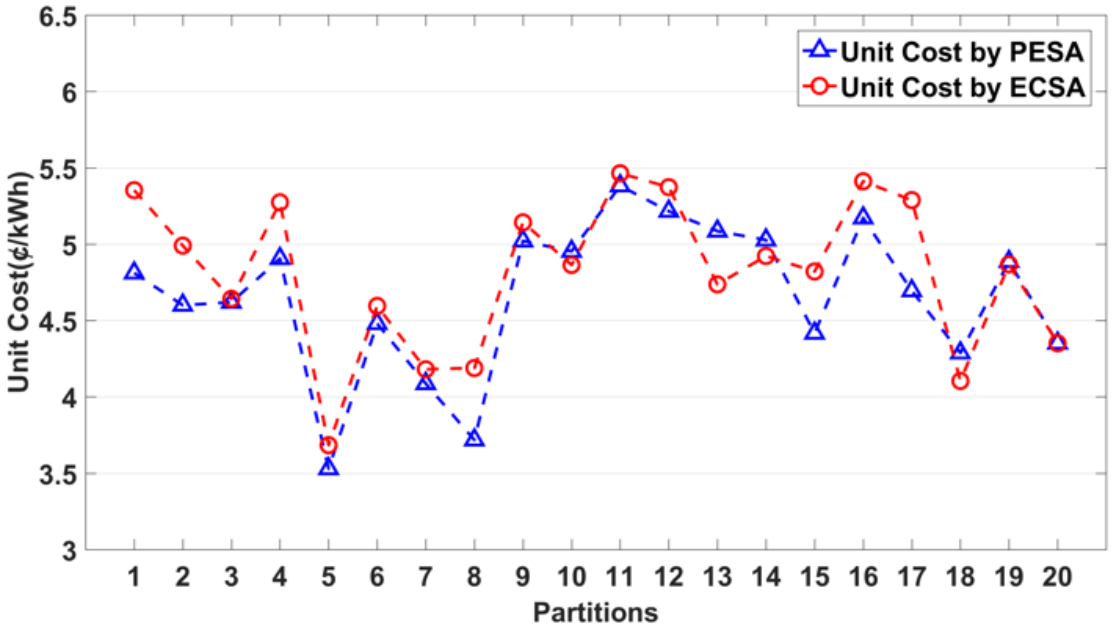

Figure 3-6 Unit cost for PESA and ECSA

3.3 IEC 61850 Integration with Smart Charging

3.3.1 Introduction to IEC 61850

Table 3-1 IEC 61850 Standard

Part #	Title
IEC 61850-1	Introduction of Overview
IEC 61850-2	Glossary of Terms
IEC 61850-3	General Requirement
IEC 61850-4	System and Project Management
IEC 61850-5	Communication Requirements
IEC 61850-6	Substation Configuration Language
IEC 61850-7-2	Abstract Communication Service Interface (ACSI)
IEC 61850-7-3	Common Data Classes
IEC 61850-7-420	Logical Nodes in DER system
IEC 61850-8	Mapping to MMS and ISO/IEC
IEC 61850-9	Mapping to Sample Values
IEC 61850-90-8	Logical Nodes in EV system
IEC 61850-10	Conformance Testing

IEC 61850 is an international standard for Ethernet-based communication in substations[76], founded by the International Electro-technical Commission's (IEC) Technical Committee 57 (TC57). IEC 61850 is gaining its popularity in smart grid design and implementation due to its advantage to reduce the configuration and maintenance cost by its nature of object-oriented data models. There are 10 major parts in current IEC 61850 standard, defining the different aspects of substation communication [77], [78], which are shown in Table 3-1.

3.3.2 IEC 61850 Integration

IEC 61850 interface is integrated into smart charging infrastructure to standardize the data and communication. The data model of IEC 61850 is customized to carry data to describe charging behaviors and mobile applications, which extends the current content of the standard. Figure 3-7 shows the integration architecture.

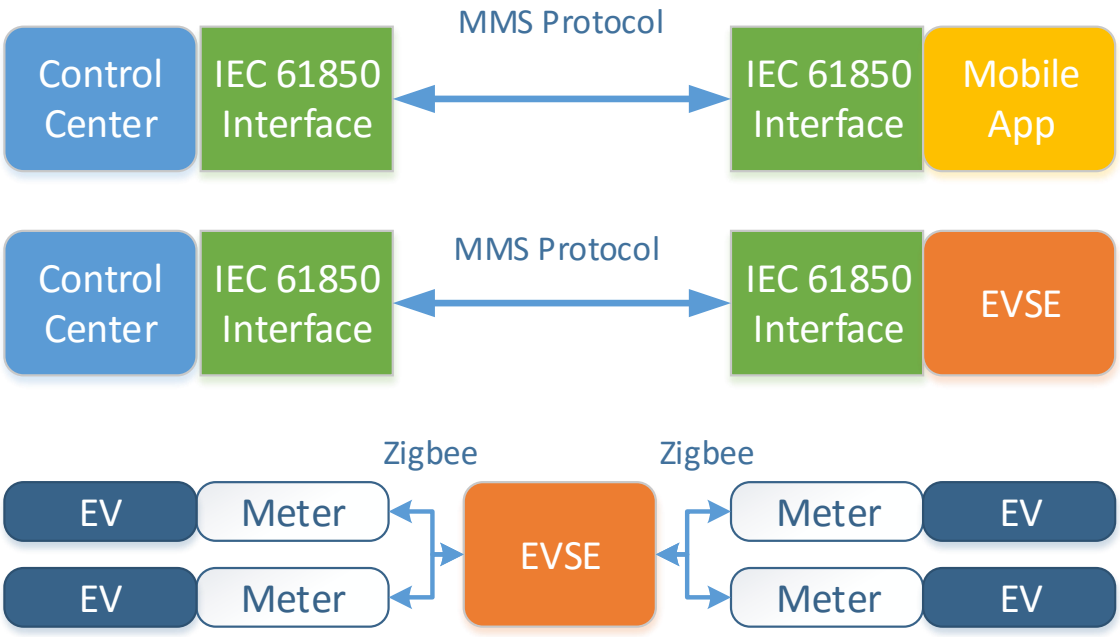

Figure 3-7 Smart charging infrastructure with IEC 61850 interface

As shown in Figure 3-7, all the communications between the mobile app, control center and EVSE are standardized by IEC 61850 interface and communicating using MMS protocol which is specified by IEC 61850-5. Inside EVSE, local communication between smart meter and EVSE is using Zigbee, and Powerline Communication (PLC) via control pilot line connection is implemented between EVSE and the EVs.

3.3.3 IEC 61850 Modeling

The procedure to integrate IEC 61850 data model and standardized communications with the smart charging infrastructure are presented as follows:

- Summarize the information and charging session parameters exchanged among the smart charging system;
- Design the IEC 61850 Service framework to describe the components in the smart charging infrastructure
- Design IEC 61850 data set to map the charging parameters and data into the system framework
- Construct Substation Configuration Language (SCL) file based on the data models from (2) and (3);
- Develop web service to manipulate variables in SCL file, integrate the IEC 61850 system framework into existing control center program, serving as the communication interface
- IEC 61850 Service Framework Design

In the IEC 61850 service framework, the root of system is the physical device, which has an IP address that can be accessed by other smart devices in the network. A physical device is defined as an Intelligent Electronics Device (IED) by IEC 61850 in the smart grid network. In this chapter, we define each EVSE as an IED. An IED contains a number of logical devices (LD), which are the function blocks inside the IED. Each LD is a collection of logical nodes (LN) that implement particular functions. LNs carry the dataset to describe the IED status, charging data and session parameters, such as energy consumption, charging current, user ID, charging time, etc. This data is made immediately available to other IEC 61850 devices. Figure 3-8 shows the smart charging infrastructure described by the IEC 61850 service framework.

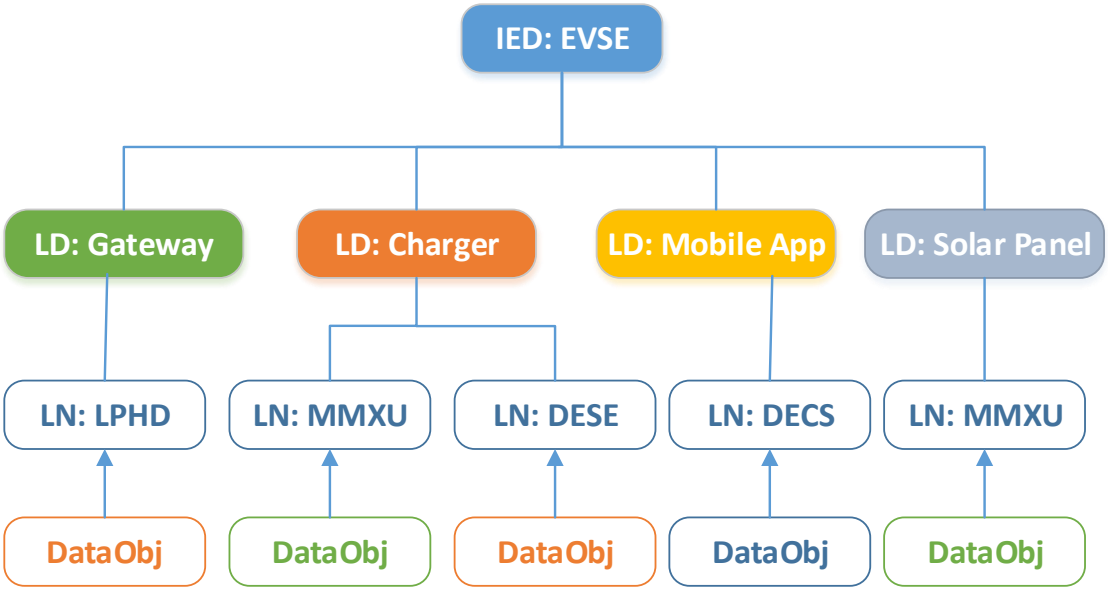

Figure 3-8 IEC 61850 framework for smart EV charging

There are one gateway, 4 EV chargers in each EVSE. Each charger is associated with one mobile app, *i.e.* one user can only use his mobile app to access data of the charger plugged in his EV. The data in each IED should be made available to all other IEDs in the network. Logical device gateway acts as an interface between the EVSE and outside network and not responsible for any data measuring and processing tasks. Logical device charger performs all interactions with EV, including authentication, charging control and monitoring. There are two logical nodes assigned to the charger, *i.e.* MMXU for data measuring and DESE for authentication and monitoring. Logical device mobile app is the user end charging control interface. User preference in the mobile should also be made accessible by IEDs, thus a DECS logical node is assigned to the mobile app to satisfy this need. Logical device solar panel provides real-time value of generated power to control center for the decision-making by charging scheduling algorithms. A logical node MMXU is assigned to this measurement unit.

3.3.4 Logical Node and Data Set Design

Several chapters of IEC 61850 are related to the logical node data set design. IEC 61850-7-2 is used for the design of data set, and it defines structure of data objects (DO) in the logical node. IEC 61850-7-3 is used to define the common data class (CDC) in the communication structure. IEC 61850-7-4 is used to select logical node classes and data classes. IEC 68150-90-8 is for logical node related to E-mobility, EV and EVSE. Data set of 4 different types of logical node in IED are shown in Table 3-2.

Table 3-2 LN: MMXU IN CHARGER

MMXU Class			
DO	DA	CDC	Explanation
Timestamp	stVal	INC	Charging session start time
PhV	mag	MV	Charging voltage
A	mag	MV	Charging current
Hz	mag	MV	Grid frequency
PF	mag	MV	Power factor
W	mag	MV	Charging active power
VA	mag	MV	Charging apparent power
TotWh	mag	MV	Total active power consumption

MMXU is a measurement type LN. MMXU logical node in the charger LD has 8 data objects. They represent the charging parameters in real-time including the charging voltage, current, power and total energy consumed, etc. Charging parameters are retrieved by the control center via gateway with a predefined time interval for smart charging algorithm analysis. Data object (DO) is the element in SCL file that contains the definition of data values in IEC 61850 format. Data attribute (DA) is the element inside a DO which defines the data type of a data object. DA can be status value (stVal), magnitude (mag), etc. Common data class (CDC) is properties of data object. CDC are mapped into concrete object definitions that are to be used for a particular protocol (*e.g.*

MMS) for communication. In Table 3-2, there are two CDC types, where INC stands for controllable integer status and MV stands for measured value.

Table 3-3 LN: DESE IN CHARGER

DESE Class			
DO	DA	CDC	Explanation
MeterStatus	stVal	INC	A flag shows meters on/off
RelayStatus	stVal	INC	A flag shows charger relay status
DutCycle	mag	MV	Current PWM duty cycle on CP
ID	stVal	INC	ID number of charger
Organization	stVal	INC	The organization EVSE belong to
AccessUsername	stVal	INC	Name of charger user
Availbility	stVal	INC	Charger is ready for charging
Offline	stVal	INC	Whether the charger is offline

Table 3-4 LN: DECS IN MOBILE APP

DECS Class			
DO	DA	CDC	Explanation
Price	stVal	INC	Real time energy price
Threshold	mag	MV	User price preference level
requireEnergy	stVal	INC	Indicate the user charging demand
EnergyRequired	mag	MV	The amount of energy needed
StartTime	stVal	MV	Charging start time
Duration	mag	MV	Whole charging session time span

Table 3-3 shows another logical node named DESE inside the charger logical device. DESE records user information and charger status. The data sets in DESE are obtained at the beginning of charging session except DutCycle, which contains the PWM duty cycle on the control pilot line

between EVSE and EV. The duty cycle determines charging current rate and may be changed during charging session by the control of smart charging algorithm.

Table 3-4 is the logical node data set in the mobile app logical device. These data are exchanged between the control center and user mobile app, representing user charging preference and demand. Table 3-5 is logical node in the solar panel, showing the photovoltaic power generated by solar panels connected with the smart charging infrastructure.

Table 3-5 LN: MMXU IN SOLAR PANEL

MMXU Class			
DO	DA	CDC	Explanation
PV	mag	MV	Power generated by solar panels

3.3.4.1 SCL File and Web Service

With all of these charging data and parameters mapped into IEC 61850 abstract data model, an SCL file is then written to carry the data. SCL file is used in IEC 61850 standardized communication between the controllable devices.

Before IEC 61850 integration, charging data and parameters are communicated in JSON and proprietary string formats between EVSE, control center and mobile apps. To integrate with IEC 61850 in the communication, a web service is developed to extract data from JSON files and strings, then map them into IEC 61850 SCL file data objects. The web service can also read data values in SCL file and map them back to JSON and string files. The web service serves as the interface to standardize the communication in the smart charging infrastructure.

The web service interface guarantees that all the charging related data inside the control center are in IEC 61850 format. With the integration of IEC 61850 by web service interface, all incoming

charging data to the control center are standardized into IEC 61850 SCL format, thus open to all other IEDs and smart grid applications in the network using IEC 61850 to read and manipulate, greatly improving the interoperability. All outgoing data are converted back to private protocols to be processed by particular local devices.

Figure 3-9 shows the visualization of integrated charging information with IEC 61850 data frame in SCL file. The information and data models are extracted during the simulation of real-world charging events. Left hand side of Figure 3-9 is the hierarchy architecture of IEC 61850 model, while some data object value extracted from hardware and meters are displayed on the right. Charging data and user preference are processed by the web service and stored in certain SCL data object. As shown in the figure, solar panel generation, charging power, real-time energy price, estimated remaining charging duration etc., which are critical parameters in ECSA, are mapped into the standardized IEC 61850 SCL data objects and ready to be used by the charging scheduling algorithm.

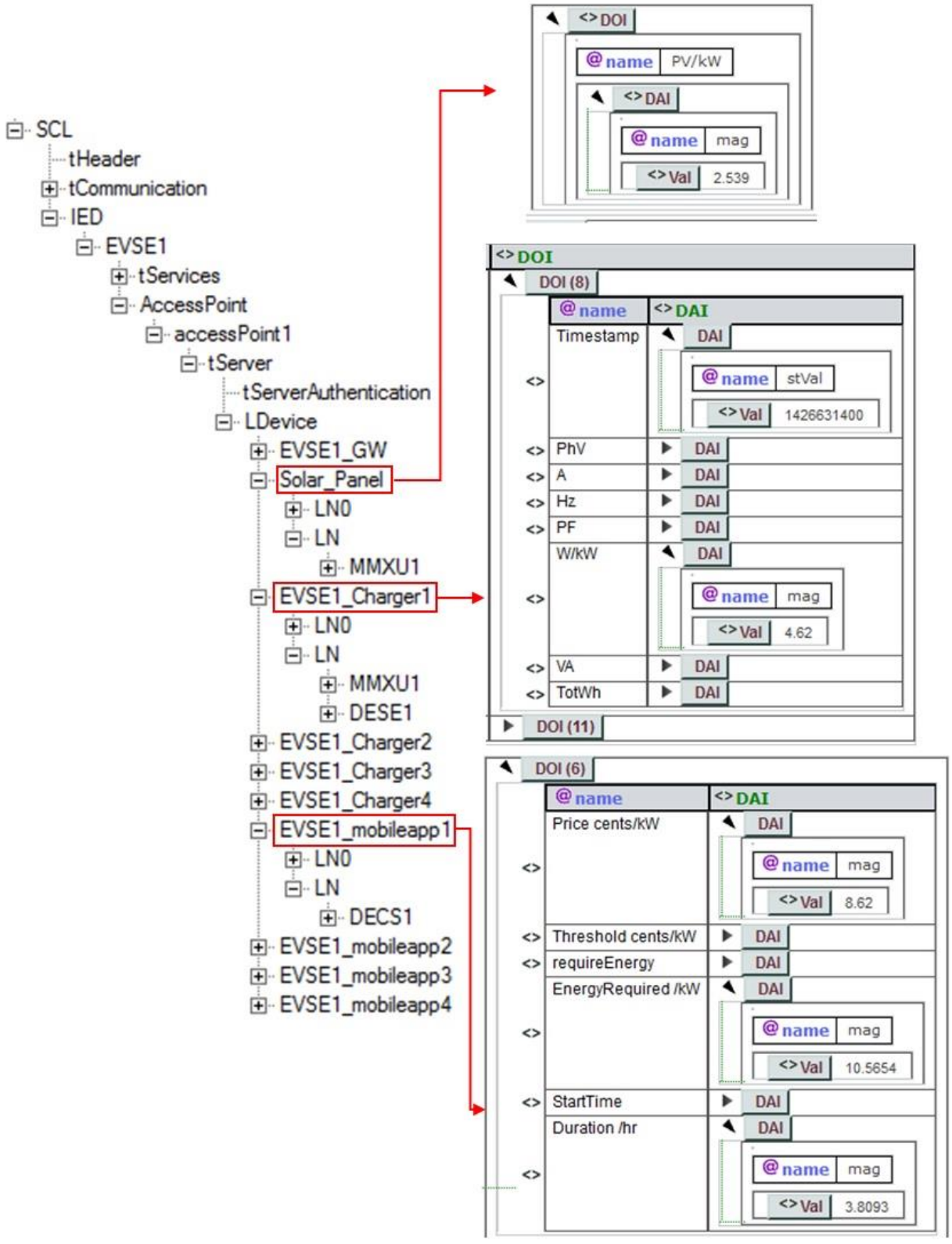

Figure 3-9 IEC 61850 SCL file visualization

3.4 Summary

In this chapter, event-based EV energy scheduling algorithm is developed based on predictive scheduling framework discussed in Chapter 2. ECSA has been demonstrated with the capability to reduce the number of unnecessary computations while maintaining a high level of energy delivery rate and system cost performance. With a variety of parameters, including the physical device status and the parameters in scheduling algorithms, IEC 61850 has been extended to implement such as smart EV charging system. With this IEC 61850 integration, the smart charging data and new features such as mobile app, current sharing are standardized into SCL configuration file, making them immediately available to any smart grid device and applications. Thus the works in this chapter not only extend the content of IEC 61850 in smart charging field but also greatly improve the scalability and interoperability of smart charging infrastructure.

Chapter 4 Load Flattening with Uncertainties

Un-coordinated Electric Vehicle (EV) charging can create unexpected load in local distribution grid, which may degrade the power quality and system reliability. As higher penetration of distributed energy resources (DERs), including EVs, renewable generation, battery energy storage system (BESS), etc. into the grid, grid services are needed to flatten the power/load fluctuation. The uncertainty of EV load, user behaviors and other types of DERs in the distribution system, is one of challenges that impedes optimal control for EV charging problem. Previous researches did not fully solve this problem due to lack of real-world EV charging data and proper stochastic model to describe the properties of DERs in a microgrid, including building load, solar generation and EV power consumption, etc. In this chapter, we extend the predictive EV energy management framework discussed in chapter 2, to support the scenarios in a microgrid scenarios. The scheduling objective is to reduce load variation caused by the system uncertainties, under the constraints of individual component. Current-multiplexing function in each Electric Vehicle Supply Equipment (EVSE) is considered and accordingly a virtual load is modeled to handle the uncertainties of future EV energy demands, which is different from the virtual load constraint defined in chapter 2. Additionally, IEC 61850 protocol is utilized to standardize the data models involved in this framework, which brings significance to more reliable and large-scale implementation to improve the interoperability. This system is validated by the real-world EV charging data collected on the UCLA campus and the experimental results indicate that our

proposed model not only reduces load variation up to 40% but also maintains a high level of robustness.

4.1 Introduction

Electric Vehicle and corresponding charging infrastructure have received much attention in recent years due to the lack of fossil fuel and pressure from government to reduce carbon emission. The initiative from California government, 1 million zero-emission EVs are expected to be on road by 2020[79]. Accordingly, there will be more Electric Vehicle Supply Equipments (EVSEs) to be installed as the penetration of EV increases in the foreseeable future. Un-coordinated Electric Vehicle charging can create unexpected load in local distribution grid, which may degrade the power quality and system reliability[80]. Many pioneer researches[15], [30], [73], [75], [81], [82] on advanced charging infrastructure, including both software and hardware that are developed to facilitate the acceptance of EVs. However, it is still a challenging task to regulate numerous EV charging behaviors in real-time due to the following reasons: 1) the randomness of EV user behaviors, such as arrival time, departure time and energy demand; 2) complexity of stochastic models that comprehensively describe the loads, renewables and EVs. Thus, more efforts should be made to design a real-time energy scheduling system that considers the above factors.

Previous researches have proposed several viable scheduling schemes for deferrable load control. An optimal distributed charging protocol is designed and implemented in simulations with a large number of EVs in [35]. Valley-filling and load-following strategies are proposed to provide grid-side regulations with deferrable EV load. However, these solutions assume static travel schedules for EV users without uncertainties, which is not true in reality. Price-based charging algorithm is designed and implemented with user preferences in [81]. Uncertainties of renewable generation

and EV load are considered in [36], [37], [48], [64]. [36] utilizes receding horizon scheduling techniques based on MPC to handle uncertainties of EV arrival and renewable generation periodically. In addition, in [36] a proof for optimality is provided given the Gaussian noise of baseload. However, the estimation for the short-term EV energy demand is derived from a simple assumption rather than from real-world EV energy consumption data, which undermines the problem formulation and the simulation results. The power consumptions for different EVSEs are also assumed to be un-correlated and no power sharing scheme exists. The EVSE [73] designed and manufactured by UCLA Smart Grid Energy Research Center (SMERC) has the capacity to allow multiple charging sessions at the same time by power-sharing and current-multiplexing circuit design. Event-based scheduling algorithms, considering random user behaviors are developed in [15]. Vehicle-to-Grid and Vehicle-to-Building services [30], [82] are developed for various EV energy consumption scenarios. Accordingly, smart EV charging algorithms are designed to support more complex functions that satisfy both EV energy demand and also provide grid-side services, such as load flattening and load following.

In this chapter, we proposed a new real-time EV charging scheduling algorithm inspired by MPC, which is designed and simulated in a micro-grid scenario, including building load, solar generation and EV load. A dynamic load estimation and a predictive optimization module are implemented to handle the uncertainties in system. The contributions of this chapter can be summarized as: 1) Current-multiplexing is considered in the problem formulation and accordingly a virtual load for each EVSE is modeled to simulate the uncertain short-term EV energy demand. 2) Dynamic estimation method based on K-nearest neighbor (KNN) are utilized for charging session parameters. 3) Online predictive optimization method based on MPC is formulated with the objective to flatten the system load in a microgrid scenario, considering the uncertainties of

building load and user behaviors; 4) IEC 61850 is utilized to standardize the information exchange by modeling the data involved in this algorithm, which gives practical meaning to more reliable and large-scale implementation.

4.2 System Overview

4.2.1 System Architecture

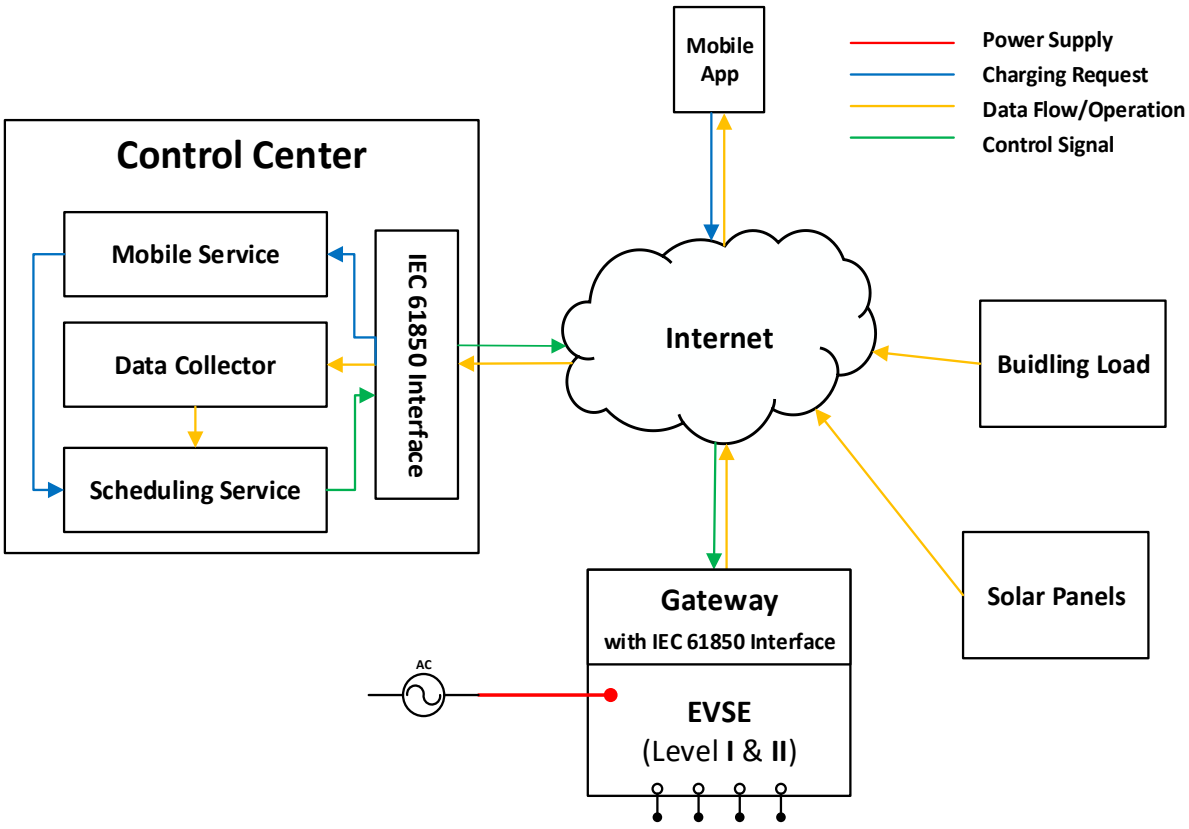

Figure 4-1 System overview

The proposed system architecture is illustrated in Figure 4-1. In general, the system has 5 main components, i.e. EVSE, building load, solar generation, client mobile application and a control center. Real-time energy consumption data with user index and device ID are retrieved and transmitted through advanced communication networks [74] constructed within UCLA campus,

and finally stored in a central database. EVSEs [81] are controllable by commands from scheduling service on server side or client mobile applications, via assigning different duty-cycles to different outlets that share the same power source from the grid. The mobile application can perform the remote control function for each EVSE in our system. Based on the real-time power data from all engaged buildings, solar generation sites, EVSEs and mobile charging requests, scheduling services are able to compute periodically for an optimal EV energy scheduling given dynamic estimation of short-term energy demand. The building load used here is from Cornell University Facilities Service[83] and the solar data is from UCLA Ackerman Union Solar Integration project [84]. To support reliable and large-scale implementation, IEC 61850 is implemented in EVSE gateways and the control center to encode/decode all the involved data and communication. This architecture has been tested by real EV users in UCLA and is friendly to more advanced charging algorithms.

4.2.2 IEC 61850 Protocol and Integration

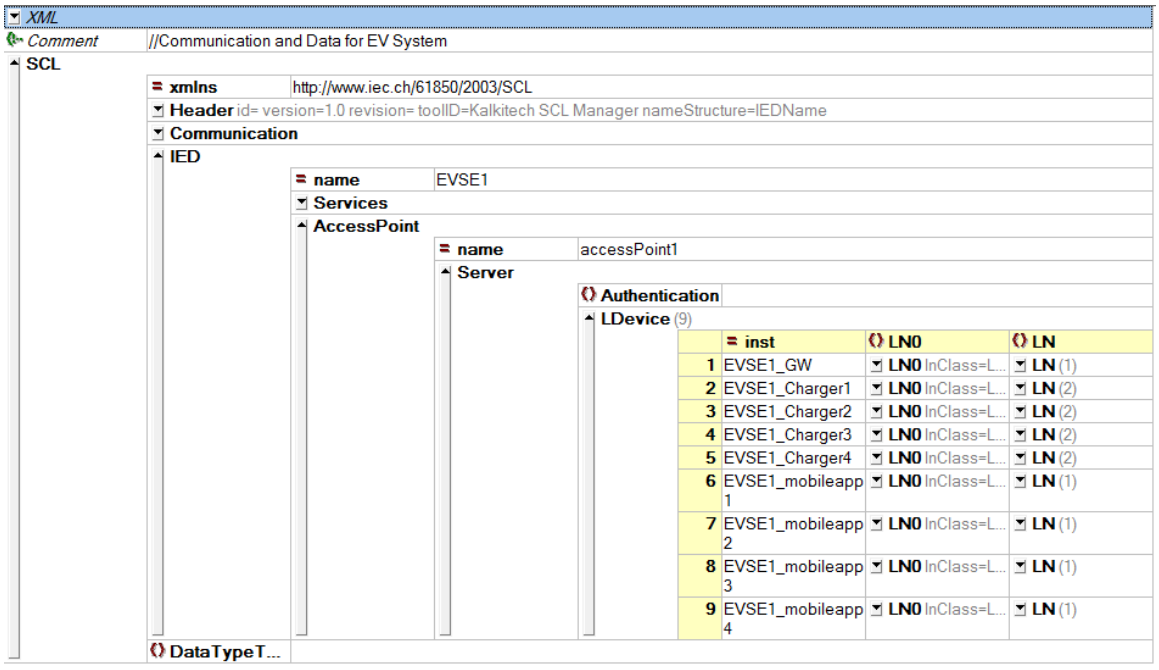

Figure 4-2 Communication and data modeling using IEC 61850

IEC 61850 is an international standard that provides a standardized framework that specifies the communication protocols, originally for power substation automation [85].The advantages include interoperability, free configuration and long-term stability [86]. A specialized IEC 61850 gateway is designed as communication interface for both control center and EVSE in our system. Data models, that include power information, EVSE status, charging requests and control signals, are all encoded as virtual components in xml-based messages to improve the system interoperability and reliability. Figure 4-2 is the schema view of communication and data modeling for EV system, based on IEC 61850 protocol.

4.3 Problem Formulation

4.3.1 Dynamic Parameter Estimation

The optimization method in this chapter is based on the framework discussed in Chapter 2, which is an online optimization method inspired by Model Predictive Control (MPC) and computes optimal schedules periodically in the future, however just realize the first element in the schedule results. The procedure continues in every step, taking the updated system states into consideration. The details of this framework can be found in Chapter 2. In our system, the optimization program needs to involve the estimations of leave time and energy consumption values for all the active charging sessions. Thus, proper estimation methods play a significant role in improving the system performance. The leave time and energy consumption values are estimated dynamically, using K-nearest neighbor (KNN) method.

4.3.1.1 Session Parameter Estimation

Each charging session, with a number of properties values, such as user index, device ID and start time, finish time, leave time and energy consumption, are stored as a record in database. We model each record associated with a charging session as a tuple:

$$s \coloneqq (u_n, t_s, t_f, t_l, e, d)$$

where u is the user index for this session, d is the EVSE ID or power source ID. t_s, t_f denotes the start time and finish time for the charging session, respectively; t_l is the leave time; e denotes the energy consumption. K-nearest neighbor (KNN) method is utilized to estimate e and t_f. In general, KNN calculates the weighted mean of neighbor values, which are among top k smallest distances with input value. In our case, the start time and stay duration in qualified sessions with top k smallest distances with current session value are extracted from database and averaged with weights.

$$dis_{i,j} = \left\| s_i.t_s - s_j.t_s \right\| \tag{4.1}$$

$$w_i = \frac{dis_{k+1,j} - dis_{n,j}}{dis_{k+1,j} - dis_{1,j}} \tag{4.2}$$

where $dis_{i,j}$ denotes the distance between session s_i and session s_j; $\mathrm{w_i}$ *denotes weight of the* ith *session* s_j.

$$\hat{e}_n = \frac{1}{k} \cdot \sum_{i=1}^{k} w_i \cdot (s_i.e) \tag{4.3}$$

$$\hat{t}_{n,f} = t_{n,s} + \frac{1}{k} \cdot \sum_{i=1}^{k} w_i \cdot (s_i.t_l - s_i.t_s) \tag{4.4}$$

where $\hat{e}_n$ and $\hat{t}_{n,f}$ are estimations of energy consumption and stay duration; k denotes the total number of qualified sessions.

4.3.1.2 Virtual Load Estimation

Since the hardware we are modeling has the power sharing and current multiplexing function, it means that the charging schedules for vehicles connected to the same power source will interact with each other. If taking uncertainties of future EV energy demands into consideration, the proposed system models an additional virtual EV load for each power source to account for the potential deviation. For each EVSE, historical data are extracted to construct the estimation of future EV load demand. Two steps are needed for dynamic virtual load estimation, i.e. total demand estimation and real-time update for remaining demand. Total demand after time t can be computed offline for all charging sessions in one specific EVSE:

$$D_t^k = \frac{1}{M} \cdot \sum_{i=1}^{i=M} s_i.e \tag{4.5}$$

where the qualified session s_i is subject to $s_i.t_s = t$ and $s_i.d = k$. Based on this methodology, we process the historical data for each EVSE on the UCLA campus and the remaining demand values are shown in Figure 4-3.

Real-time EV energy demand will be updated based on current active charging sessions in power source k and their estimated energy consumptions. The update for virtual load is illustrated in the following equation:

$$0 \le r_v^k(\tau) \le r_v^{max}.\eta, \qquad \forall \tau \in [t, t_{v,f}^k] \tag{4.6}$$

$$t_{v,f}^k = \max(s_i.t_f) \tag{4.7}$$

$$e_v^k = \max(0, D_t^k - D_{t_f}^k - \sum_{i \in N} s_i.e) \tag{4.8}$$

Taking the blue curve as an example, each data point D_t denotes the expected energy demand by EVs on this EVSE after time t. At the beginning of each day, the estimated value is 34 kWh and the value drops due to the new vehicles arrives with energy demand. Note that, 5:30 AM to 8:00 AM is the period with highest chance of new energy demand during the day. At each time step, the expected energy demand by future vehicles will be generated based on this curve using equation (3.6) and (3.7).

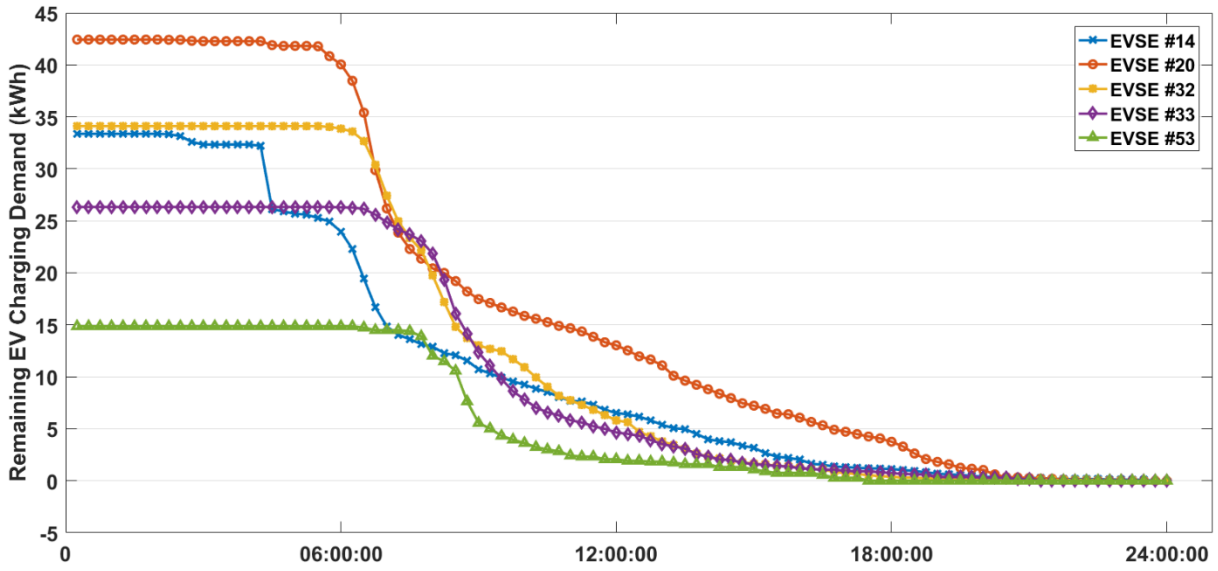

Figure 4-3 Remaining EV charging demand for different EVSEs

The virtual load charging rate $r_v^k(t)$ for power source$k$ is modeled as a regular EV load and will be input into the overall optimization problem. That is to say, there will be the 5-th charging station added to EVSE with original 4 charging stations, exclusively to simulate the future EV demand.

$$\sum_{\tau=t}^{t_{v,f}} r_v^k(\tau) = e_v^k \tag{4.9}$$

4.3.2 Load Modeling with Uncertainties

4.3.2.1 Building Load and Solar Generation

The power consumption for the building and solar power generation cannot be exactly known in advance and there exists little variation between different days. In this scheduling strategy, wiener filter and historical data are combined as a simple load predictor.

$$P_b(t) = P_b^e(t) + \overline{P_b(t)} \tag{4.10}$$

$$\overline{P_b(t)} = \overline{P_d(t)} - \overline{P_s(t)} \tag{4.11}$$

where $\overline{P_b(t)}$ denotes the average value of base load at the time t, which is the difference between average building power consumption value $\overline{P_d(t)}$ and the average solar generation value $\overline{P_s(t)}$. $\overline{P_d(t)}$ and $\overline{P_s(t)}$ can be simply obtained by averaging historical data for time t. The assumption for wiener filter is that the estimation error can be accumulated by previous steps and thus, real-time error calculation is performed by:

$$P_{b,t}^e = \sum_{i=1}^{i=T} \xi(i) \cdot f(t-i), \quad \forall t \in [1, T] \tag{4.12}$$

where $P_{b,t}^e$ is the error between real base load and predicted average baseload at time t. ξ is an identically distributed random variable with *zero* mean and variance σ^2. f is the impulse response of a causal filter, with following form:

$$f(t) = \begin{cases} 0, & t < 0 \\ a^{-t}, & t \geq 0 \end{cases} \tag{4.13}$$

Thus, the prediction error for current time t is only the summation of the previous estimation errors with different weights. Note that $f(0) = 1$.

4.3.2.2 EVSE Model

Due to the characteristics of our EVSE design, more than one vehicle can share the power source at the same time, which means each charging session has separate constraints. For each connected vehicle, we use $r_n = \{r_{t_s}, r_{t_s+\Delta t}, r_{t_s+2\cdot\Delta t}, \dots, r_{t_f}\}$ to denote the power consumption rates from session start time t_s to session finish time t_f. Δt is the time step we use in this chapter. The constraint for each charging session:

$$0 \le r_v^k(t) + r_n^k(t) \le r_k^{max}.\eta, \qquad \forall t \in [t_{n,s}, \hat{t}_{n,f}] \tag{4.14}$$

where $r_n^k(t)$ is the power consumption rate for vehicle n, which is connected to power souce k, at time t. r_k^{max} is the maximum power supply for power source k; η is the safety coefficient for this power source. $\hat{t}_{n,f}$ denotes the estimated finish time for vehicle n.

For each power source (EVSE), the same limitation of total power consumption also applies:

$$0 \le r_v^k(t) + \sum_{n \in N_k} r_n^k(t) \le r_k^{max}.\eta, \forall t \in [t_{n,s}, \hat{t}_{n,f}] \tag{4.15}$$

where N_k denotes the number of active charging sessions for power source k.

4.3.2.3 User Model

Each charging session in our system is labeled with a number of properties, such as user ID, session start time $t_{n,s}$, session finish time $t_{n,f}$, vehicle leave time $t_{n,l}$ and the session energy consumption e_n. At the beginning of each charging session, estimation algorithm will calculate the predicted energy consumption $\hat{e}_n$ and the real energy consumption should be larger than the predicted value, but less than battery capacity E_n:

$$\hat{e}_n \le e_n(t_{n,f}) \le E_n \tag{4.16}$$

As the time goes on, energy consumption is accumulated at each time interval:

$$e_n(t) = e_n(t - \Delta t) + r_n(t) \cdot \Delta t, \quad \forall t \in [t_{n,s}, \hat{t}_{n,f}] \tag{4.17}$$

4.3.2.4 Receding Horizon Control

Algorithm 4: Predictive EV Scheduling Algorithm (PESA)

Calculate baseload $\overline{P_{b,t}}$ by averaging historical data;

Estimate EV demand for each EVSE: D_t^k, using (4.1)(4.2)(4.5);

$t = 1$;

Do

Estimate $P_b(t)$ with error using (4.10)(4.11)(4.12);

For each vehicle $n \in N$:

Estimate leave time $\hat{t}_{n,f}$ and energy consumption $\hat{e}_n$ for vehicle n, using (4.3)(4.4);

End

Estimate virtual load parameters, using (4.1)(4.2), (4.6) - (4.9);

Solve problem (4.18) ,subject to (4.8)(4.9), (4.14) - (4.17);

For each vehicle $n \in N$

Implement $r_n(t)$

End

$t = t + 1$

While $t \leq T$

At each time interval, the scheduler on control center will call optimization program to compute for an optimal EV charging schedule, considering the estimated travel schedules and energy consumption values for all active charging sessions. To minimize the overall load fluctuations, the optimization problem, referring to [8], is modeled as:

Obj:

$$\min \sum_{\tau=t}^{\tau=T} (P_b(\tau) + \sum_{n \in N} r_n(\tau) - \frac{1}{T-t+1} \cdot (P_b(\tau) + \sum_{n \in N} r_n(\tau)))^2 \qquad (4.18)$$

$s.t.$ (4.8), (4.9), (4.14) - (4.17)

After the algorithm initiation, the base load that consists of building load and solar generation, and EV demand will be estimated. At each time interval, parameters for all active charging sessions in system will be extracted from database, and virtual load will be estimated to solve the optimization program. Only the first element in scheduling results $r_n(t)$ is used to control specific EVSE and then algorithm moves forward to next time interval. This procedure repeats until the end of the day. The whole algorithm is summarized in Algorithm 4.

4.4 Results and Discussion

In this section, results from PESA is discussed, based on comparisons with those algorithms without considering uncertainties. The overall load variation is utilized as metric for performance evaluation of PESA. Potential improvements are also discussed.

4.4.1 Experiment setup

Real-world charging records from users on the UCLA campus are utilized for our experiment setup. One day in March, 2015 is randomly selected as a test day. There are totally 21 charging sessions from multiple users on test day, associated with all Level II EVSEs. We set the time interval Δt for all data preprocessing and PESA to 15 minutes, which is long enough considering our problem size and performance requirement. The standard variance σ of ξ is set to *2* according to our observation and a is set to *0.4* in the wiener filter. Safety coefficient η is set *0.9*. CVX package [60] is used for solving the optimization problem in each step. As shown in Figure 4-4, real-world

data of building load for 70 days has been extracted from the database [83]. Note that, not all buildings on the campus are selected as test samples.

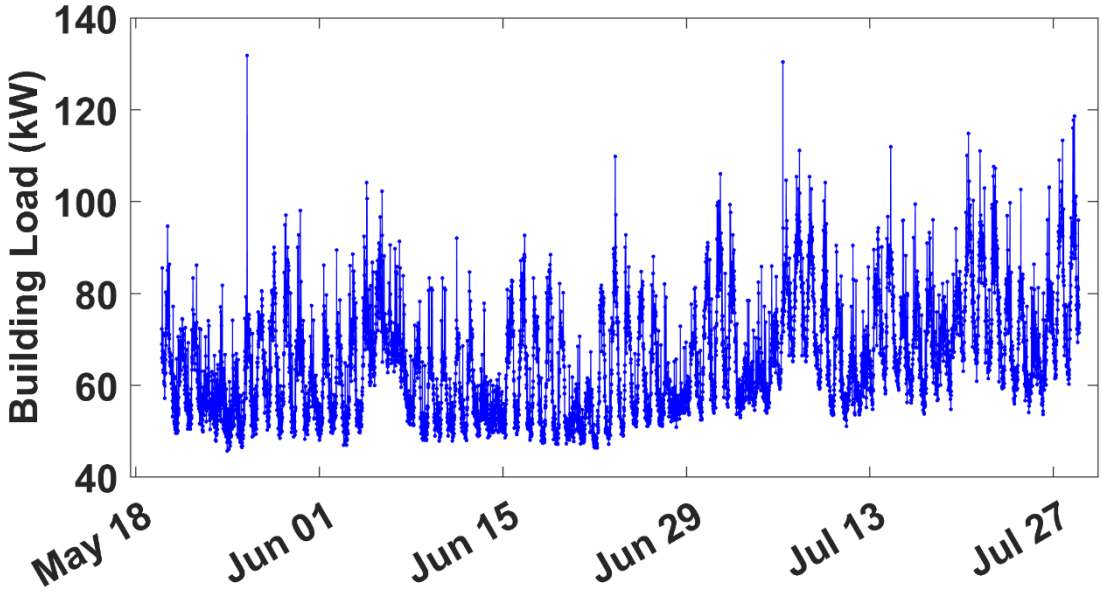

Figure 4-4 Building load data

Meanwhile, the corresponding solar generation data is displayed in Figure 4-5. According to the equation (4.10) – (4.13), the baseload is obtained by subtracting solar generation values from the build load, to represent the nominal power demand in microgrid, except EV charging load. Thus, the objective here becomes to utilize the EV charging load with uncertainties to flatten the baseload curve. Based on the historical records, the emulated baseload curved is generated and shown in Figure 4-6 (blue dotted curve). The read curve is the historical average of the baseload in each time interval of the day, denoted by $\overline{P_b(t)}$ in equation (4.11). The emulated blue dotted curved is latter used in optimization program, i.e. equation (4.18).

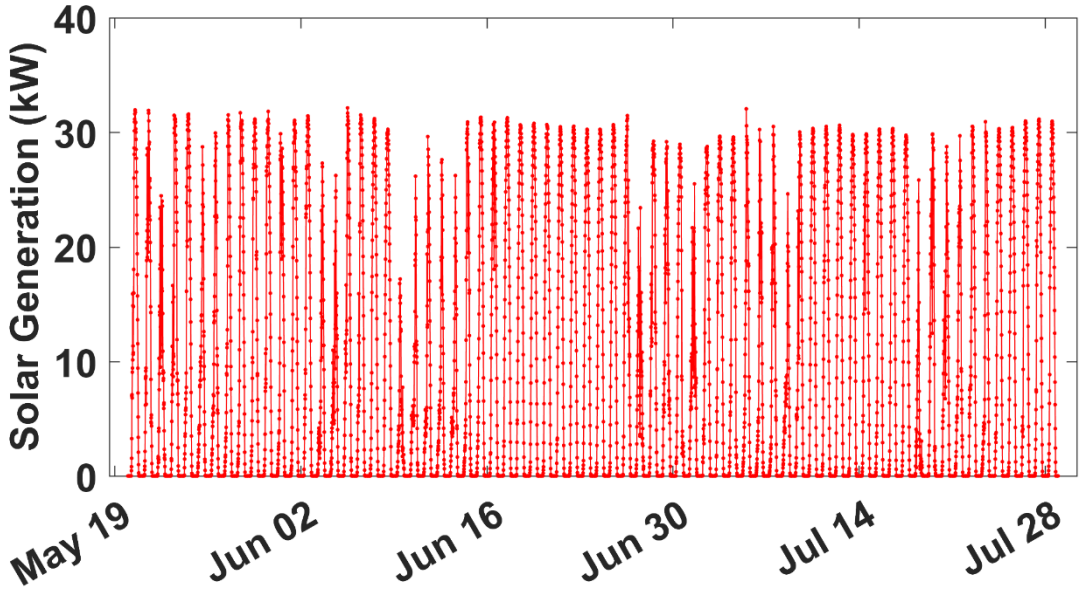

Figure 4-5 Solar data from UCLA solar integration project

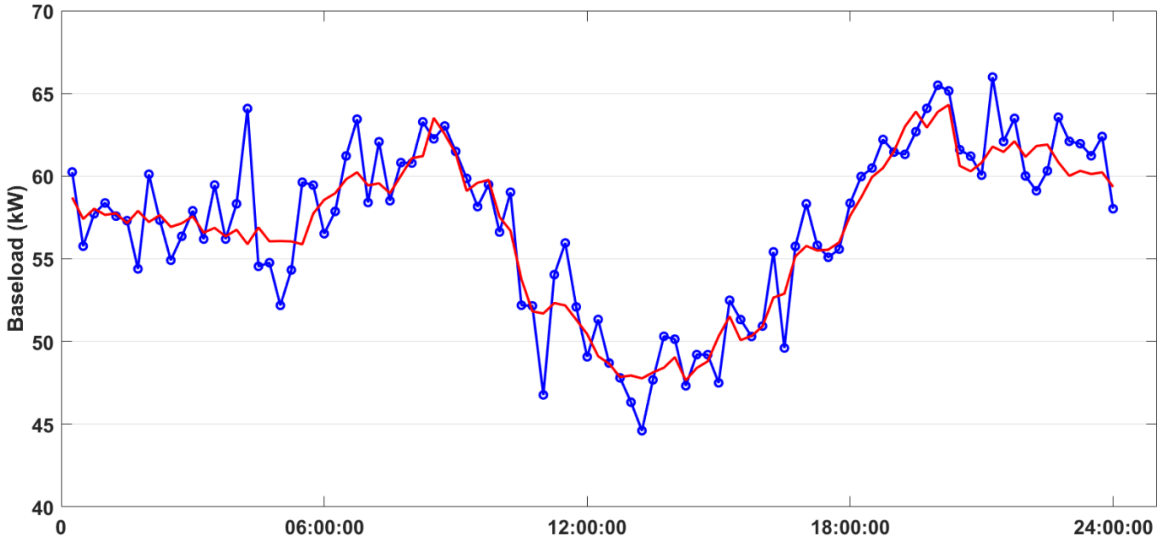

Figure 4-6 Baseload modeling

4.4.2 Scheduling Results and Future Improvements

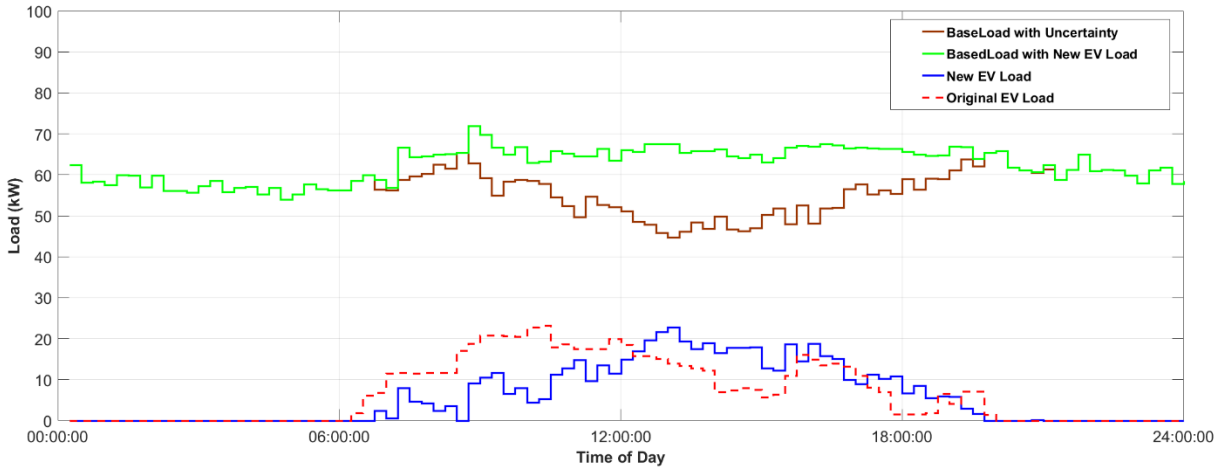

Figure 4-7 Predictive Scheduling Results

In Figure 4-7, the brown step curve is the baseload generated by (4.10) - (4.13) on the test day and the red dotted curve is the original EV load caused by the real-world charging behaviors. PESA is performed every 15 minutes and only the first schedule elements from the output is implemented. The blue curve is the new energy consuming schedules created by PESA. Visually, there is a portion of EV load is shifted from around 9:00 AM to 2:00 PM. Thus, the total load with EV, solar generation and building load is updated as the green curve in Figure 4-7. Thus, PESA's ability for valley filling is demonstrated.

Table 4-1 Comparison of load variation

	With PESA	**Without PESA**
Load Variation	40.1413	70.7471

Quantitatively, equation (4.18) can serve as a numerical metric for load variation. After applying the updated EV load, the variation values for system loads with and without PESA are compared in Table 4-1. Scheduled EV load with PESA can reduce the load variation drastically by more than 40%.

However, it should be noted that there is a slight difference between original total EV energy consumption and the new total EV consumption, which is reflected by the areas under the red-dotted curve and the blue curve, respectively. This deviation, caused by uncertainties of user behaviors, can be used as another criteria for performance evaluation. We define Average Schedule Error Rate (ASER) to represent this deviation:

$$ASER = \frac{1}{L} \cdot \sum_{n}^{L} \frac{e_n - e_{n,c}}{e_n} \cdot 100\% \tag{4.19}$$

where e_n is the original energy consumption for one charging session. $e_{n,c}$ is the energy consumption obtained from PESA. L denotes the number of charging sessions on a particular EVSE. Smaller ASER values denote less deviations and higher levels of satisfactions of energy demand from EV users. For each level II EVSE in experiment, single ASER is calculated as well as the overall value in Table 4-2.

Table 4-2 ASER values for different EVSEs

EVSE ID	**EVSE 1**	**EVSE 2**	**EVSE 3**	**EVSE 4**	**Overall**
ASER(%)	7.4061	24.6687	1.6531	19.6281	14.9745

After comparing different ASER values for different EVSEs, we find that, for EVSE 2 and EVSE 4, there are users, whose travel schedules and energy demands have quite large deviations from their historical routines, *i.e*, they leave unexpectedly at a much earlier time than before or demand much higher energy than usual. Even though the overall deviation level represented by ASER values are acceptable, users, whose daily charging behaviors are beyond estimations, will undermine the overall scheduling results. To solve this problem, the resemblance between current charging session and historical sessions should be estimated dynamically based on more information extracted from live system.

4.5 Summary

In this chapter, a predictive EV scheduling algorithm (PESA) is developed, taking into account the uncertainties of building load, renewable generation and EV load. Specifically, Wiener filter is utilized to model the intermittency of solar generation and building load, and virtual EV load is formulated based on the historical charging records. The simulation results indicate that PESA reduces the system load variation and maintains high level of satisfaction for energy demand from EV users.

Chapter 5 Price-based EV Charging Strategies

In this chapter, we propose and implement a smart Electric Vehicle (EV) charging algorithm to control the EV charging infrastructures according to users' price preferences. Charging boxes (EVSEs), equipped with bi-directional communication devices and smart meters, can be remotely monitored by the proposed charging algorithm applied to EV mobile app. On the server side, ARIMA model is utilized to fit historical charging load and perform day-ahead prediction. A pricing strategy with energy bidding policy is proposed and implemented to generate a charging price list to be broacast to EV users through mobile app. On the user side, EV drivers can submit their price preferences and daily travel schedules to negotiate with Control Center to consume the expected energy and minimize charging cost simultaneously. The proposed algorithm is tested and validated through the experimental implementations in UCLA parking lots.

5.1 Introduction

Electric Vehicle (EV) is considered as the innovative technology to gradually replace petroleum-driven vehicles that rely on diminishing reserves of crude oil [80], [87], [88]. Accordingly, many governments are now establishing clear deployment goals for EVs. The U.S. government, for instance, aims to achieve one million EVs on the road by the year 2015 [89], and up to 35% of total vehicles by 2020 [50]. Since the EV motors are powered by rechargeable battery sets, EVs need to be charged periodically. However, the increasing penetration of EVs will have a serious

impact on the power grid in uncontrolled charging scenarios, or named “dumb” charging. For example, the emerging fleet of EVs will introduce considerable amount of addition load, which potentially increases peak demand or generates new peak, and increase demand side uncertainties to local distribution power system. Even a small penetration of EVs might result in the unacceptable disturbance in power grid. Therefore, smart charging strategies become significantly important to schedule EV charging behaviors intelligently and effectively.

There are a number of EV smart charging studies have been addressed to date (see e.g. [33], [90]–[92]). The algorithm proposed in [33] introduced a method to maximize the electricity energy that is to be delivered to all the EVs in a fixed period of time. In [90], an operating framework for aggregators of EVs has been proposed, and a minimum-cost load scheduling algorithm is designed to determine the energy transaction strategy in the day-ahead market. The problem of optimizing EV charge strategy in order to reduce the energy cost and battery degradation is proposed in [91]. The intelligent EV scheduling method in [92] is based on the parking lot level to maximize the profit in grid power transactions. However, none of these studies considers charging behavior of EV users, and there is a lack of real-world implementations to support their algorithms through the testing EV infrastructures.

Many researches for “smart” algorithms to regulate EV charging behaviors have been proposed. Generally, they can be divided into three categories: centralized control [29], [32], [34], distributed control [35] and time of use (TOU) price based control [32], [93] on the side of utility and aggregator. However, these studies are non-practical, and they are conventionally based on static scenarios, where the model parameters (e.g. number of EVs, EV battery sizes, charging rates and schedule availabilities) are assumed to be known or fixed factors. On the other hand, vehicle arrival and departure are stochastic behaviors other than static assumptions. Additionally, lack of user

interaction mechanism with price and schedule preferences undermines the validity of the simulation results.

In this chapter, we model an aggregator to regulate all charging facilities in UCLA parking structures, which can perform bi-directional communication with a control center configured in the lab. Users are able to manage their charging sessions with price and schedule preferences through mobile App. This software system implementation is based on the charging hardware developed by UCLA Smart Grid Energy Research Center (SMERC) equipped with wireless communication modules, current multiplexing circuits and smart meters [54]. Thus real-time charging profile, such as charging rate and meter status, can be obtained by control center and user mobile App to perform charging controls. The algorithms on control center will be able to retrieve and pre-process the historical data into a proper format. ARIMA model is selected to model the real-world charging records in a fashion of time series. In the system model, we assume that Control Center is required to flatten the load curve based on day-ahead load prediction and generate corresponding price list for users to respond to. A simple price model is proposed to generate price according to the predicted load and the desired load curve. On user side, different price options (from highest to lowest) are available for selection, which indicates user's charging will start only the price value falls below the accepted one.

The objective of this chapter is to introduce, utilize and implement the proposed smart EV charging strategy considering user's price preferences to demonstrate a user-friendly and grid-friendly EV charging infrastructure. The contributions can be summarized as the following. First, we implement a flexible charging scheme with control algorithms on both server side and user side. Second, we deploy a pricing policy with simple bidding strategy, considering aggregator's

predicted charging load by ARIMA model and desired load profile. Third, the effectiveness of this algorithm to shift load from higher price period is validated by experiment data.

5.2 System Model

In the implementation of this smart charging system, generally there are three key components: server side control algorithms, user side mobile App and smart charging hardware, as shown in Figure 5-1.

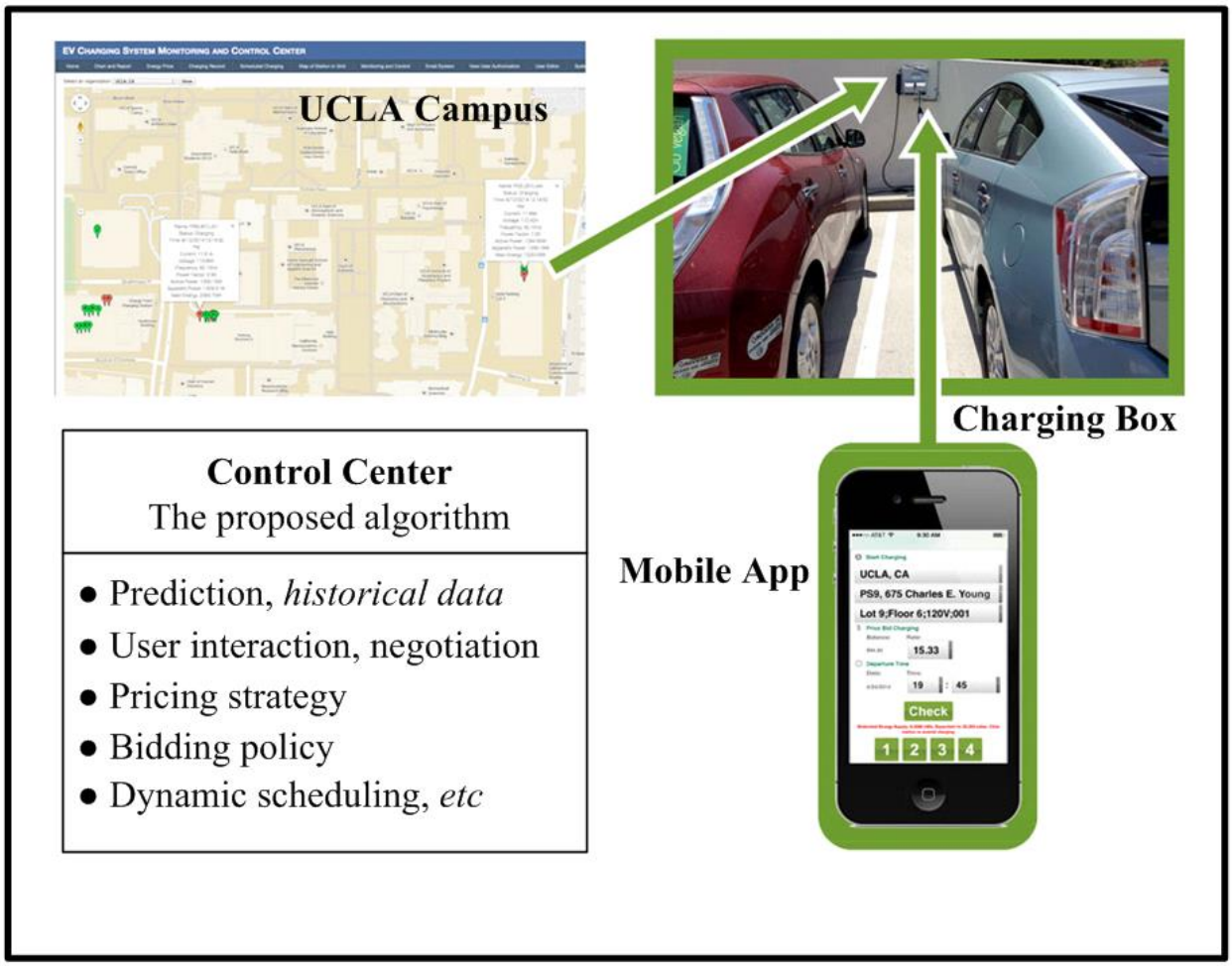

Figure 5-1 System overview

On server side, control center is able to monitor and regulate all charging behaviors. Historical charging records are fitted into ARIMA model for day-ahead load prediction. The predicted EV

load is then applied into a pricing model to generate EV price list, with the desired system EV load curve considered. The interval for price list is set to one hour in this implementation. Power information and meter status for all charging boxes are automatically collected. The other functional module on server side is the controlling algorithm to dynamically regulate charging behaviors by splitting current or time quantum according to users' varied schedule preferences and price preferences.

On user side, a mobile app is deployed to enable users to manage charging sessions interactively. EV users, whose daily travel schedules may vary, are able to select charging profile, when they arrive in parking structures in campus. Then, after user selects charging facility, he/she will be able to select charging parameters and schedule preferences, including price options (from higher to lower) and estimated departure time listed in mobile App. The selected price is maximum price this user accepts, which indicates the charging will start when price falls below the accepted one. After selection of charging profile, the server will respond to this charging request and calculate the predicted energy supply based on users' preferences and charging time range. If users do not agree with this arrangement, it is free for them to modify the charging preferences. This negotiation mechanism will help EV user avoid high prices intervals automatically.

5.3 EV Demand Prediction by ARMA

We average system-wide charging load on an hour basis for better prediction. As is shown in Figure 5-2 the system EV charging load indicates a periodicity property, i.e. the load has a similar pattern every other week and on each workday except Friday. However, the historical data is imperfect with data missing for certain time intervals and wrong value caused by hardware failure. Thus, data modification method is implemented to correct the data series.

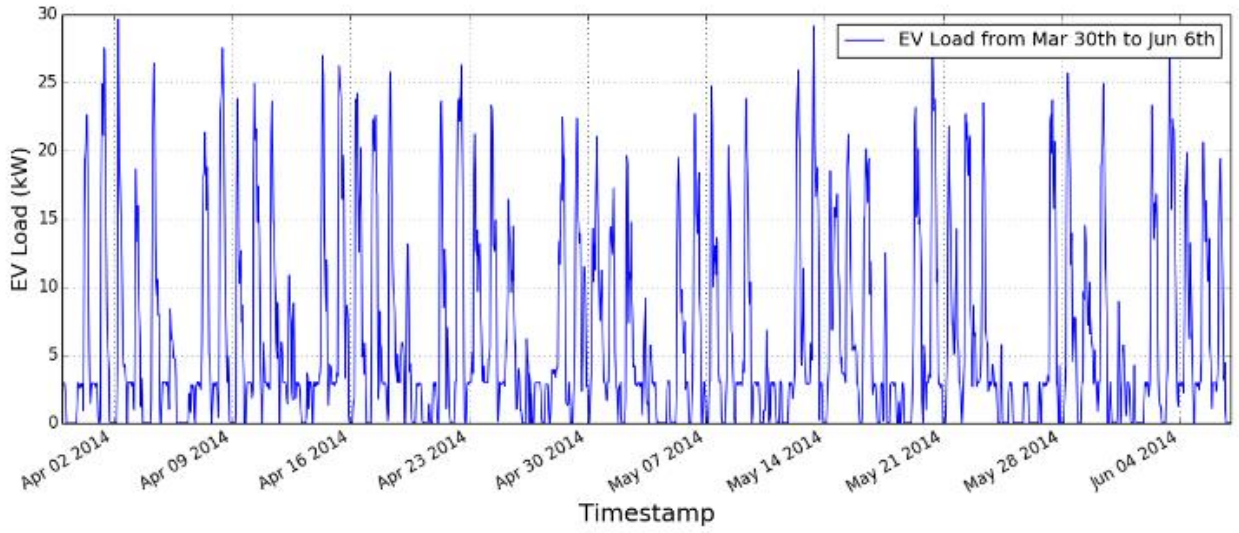

Figure 5-2 EV load from Mar. 30th to Jun. 6th

Autoregressive moving average (ARMA), as a stationary time series model, is chosen to model the data and perform prediction. There are two parts in ARMA model, i.e. autoregressive (AR) part with order p, and moving-average (MA) part with order q. The general expression is,

$$X_t - \phi_1 \cdot X_{t-1} - \cdots - \phi_p \cdot X_{p-1} = \epsilon_t - \theta_1 \cdot \epsilon_{t-1} - \cdots - \theta_q \cdot \epsilon_{t-q} \qquad (5.1)$$

And ϵ_t is a white noise with *0-mean* and variance equal to σ_ϵ^2. The procedures to handle historical charging load records are:

- Error correction and data pre-process;
- Determine orders for ARMA model, *i.e.* p and q;
- Model fit, *i.e.* calculate ϕ, θ values
- Model validation, *i.e.* error analysis

Since the raw data, even after modification, has non-stationarity property, differencing steps are necessary to transform into stationary time series. The seasonal factor is identified as 168 hours from plot, equivalent to one week, to remove data periodicity. Additionally, to make the model

stable without incremental and decremental trend, Y_t is first-order differentiated with adjacent values in time series.

$$Y_t = X_t - X_{t-1} \tag{5.2}$$

$$W_t = \nabla^1 Y_t = Y_t - Y_{t-1} \tag{5.3}$$

Akaike and Bayesian Information Criteria (AIC, BIC) is utilized to evaluate the selections of model orders. The prediction results are shown in Figure 5-3.

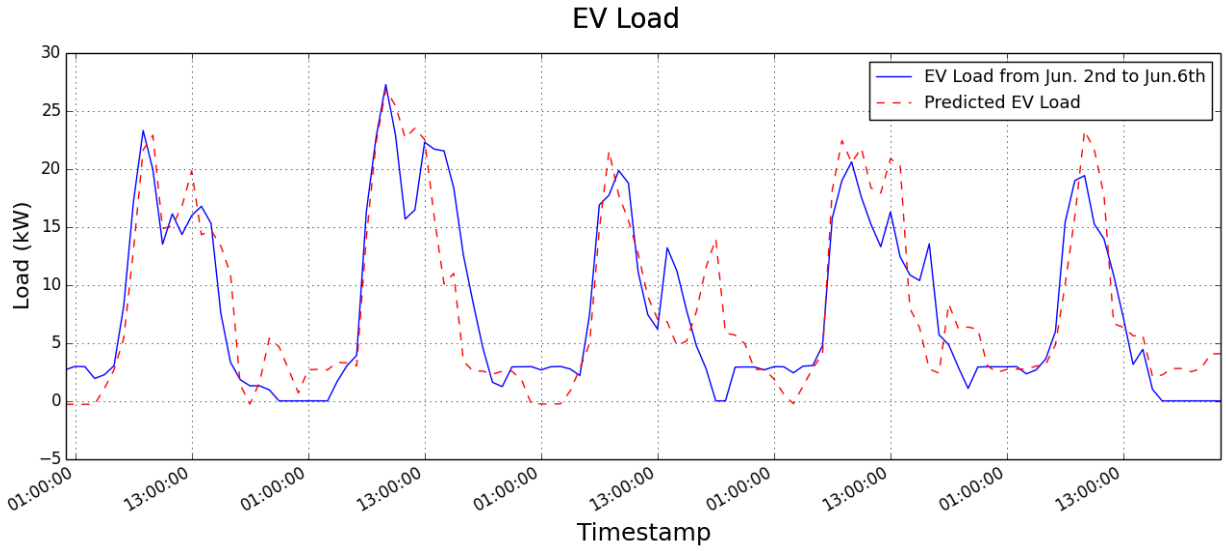

Figure 5-3 Actual load vs. virtual load on Jun. 3rd

5.4 Pricing and Bidding Strategy

5.4.1 Pricing Strategy

The purpose of designing an appropriate pricing strategy is to encourage EV users to shift their EV charging load to a preferable time range. Since charging facilities are installed in a university campus, charging behaviors are believed to have similar patterns in terms of arriving time, leaving time and energy required by faculty and students. It is assumed that varied persons may have

different reactions towards price options, e.g. for a certain day, 20% of all customers are willing to pay the highest prices to charge enough energy as soon as possible. Another assumption is that electricity price is linearly related to system-wide load/demand, i.e. price increases as predicted demand increases. Thus, 24 prices, one for each hour, are generated day ahead, by taking both EV predicted EV charging load and desired load into consideration. The price is defined by:

$$P_i = P_b + \alpha \cdot (L_i^p - L_i^d) \tag{5.4}$$

P_i denotes charging price in i_{th} hour of current day, P_b denotes the base price for the EVSE selected, L_{pi} is predicted load value for i_{th} hour, L_{di} denotes the desired load value for i_{th} hour. α is a coefficient defined to reflect the relationship between load and price. We offer users with 5 price options, from highest to lowest, as a charging threshold, i.e. accepted maximum price. As an example, if charging aggregator's purpose is to dis-encourage EV users to charge between 1:00 PM and 3:00 PM.

5.4.2 Bidding Strategy

For each level I EVSE, it has 4 outlets and only one input power source. Only one vehicle is allowed to charge due to the inner circuit design. Thus, the policy is to determine timing to switch from one vehicle to another according to users' preferences and priorities. An accepted price threshold is select before users submit charging, which is assumed to reflect how urgent he/she needs to charge. As a result, a charging session with higher price has higher priority and is able to consume more energy within every time quantum. The criteria for algorithm to switch charging session is

$$T_i = \left(P_i / \sum_{k=1}^{n} P_k \right) \cdot \Delta T = \gamma_i \cdot \Delta T \tag{5.5}$$

Where T_i is continuous charging time since turned on last time, P_i the price selected by i_{th} user, ΔT is the time quantum, denoting the timespan of EVSE control loop. γ_i is defined as priority coefficient according to bids provided by users for current EVSE.

The scenario for level II is different since level II EVSE has higher power supply with ability to multiplex current. The EVSE selected for implementation has single power source (240V, 30A). Multiple outlets (stations) can charge at the same time but current for each outlet should be between 5A (10% duty cycle) to 30A (50% duty cycle). Accordingly, the algorithm will determine the energy sharing policy in a current multiplexing manner. To determine each participating vehicle's charging duty cycle (DC), a two-step process is conducted. The first step calculation will rule out the vehicles whose duty cycle values are lower than 10%, and second step will calculate again to reallocate the source current.

$$DC_i = I_{max} \cdot \left(\frac{P_i}{\sum_{k=1}^{n} P_k} \right) = I_{max} \cdot \gamma_i \tag{5.6}$$

where priority coefficient γ_i is defined as $\gamma_i = \left(\frac{P_i}{\sum_{k=1}^{n} P_k} \right)$.

5.4.3 Billing Policy

The final cost for participating users consists of not only expense for purchasing electricity but the fee for occupying the charging service priority. Thus, the final cost for each user can be expressed in a simple model with electricity price for specific hour, P_i and current user's priority ratio, γ_i:

$$C = \sum_{k=k_0}^{k_l} \eta_k \cdot \Delta t \cdot P_k \cdot R_k = \sum_{k=k_0}^{k_l} (1 + \beta \cdot \gamma_k) \cdot \Delta t \cdot P_k \cdot R_k \qquad (5.7)$$

Where C denotes the final cost, η_k is the cost factor considering priority to occupy power source in k_{th} timeslot. For simplicity, we apply $\eta_k = 1 + \beta \cdot \gamma_k$ to include both the cost for purchasing electricity and priority service fee. η denotes priority price coefficient and is set to 0.1 tentatively in experiment. P_k is the price for k_{th} timeslot and R_k is the charging rate in i_{th} timeslot. In both level I and level II charging scenarios, priority coefficient γ_k can be obtained by calculating the ratio of current user's bid among all players in certain EVSE.

5.5 Algorithms for Implementation

Implemented algorithms on server side are capable of regulating charging sessions with dynamic arriving time, departure time and varied price preferences. For explanation, the simplified versions of implemented algorithms are illustrated Figure 5-4 and Figure 5-5.

For level I EVSE, after each control loop starts, algorithm will select active charging sessions for current EVSE from database, and sort them by their accepted prices and departure time. Only the charging sessions, whose prices agree with user price preferences, can be retrieved. It is assumed that EV drivers, with higher accepted prices and earlier departing time, are in more urgent need for energy and will be given higher priorities than others. To guarantee the energy assigned among users in each time quantum is proportional to their priorities, algorithm calculates priority coefficient γ_i and the continuous charging time T_i in each control loop. If current charging session has used up its portion of charging time in current time quantum, algorithm will switch from this charging to a lower one from charging session list. For level II EVSE, priority coefficients and corresponding duty cycle are calculated in a two-step manner. In the first step, charging session

will temporarily be disabled if the duty cycle calculated is lower than 10% or user accepted price is lower than current price. Then, after ruling out the unqualified charging sessions, algorithm will re-allocate the power source to each remaining session, proportionally to its priority coefficient. The charging sessions will be closed if current is lower than threshold or schedule deadline is reached.

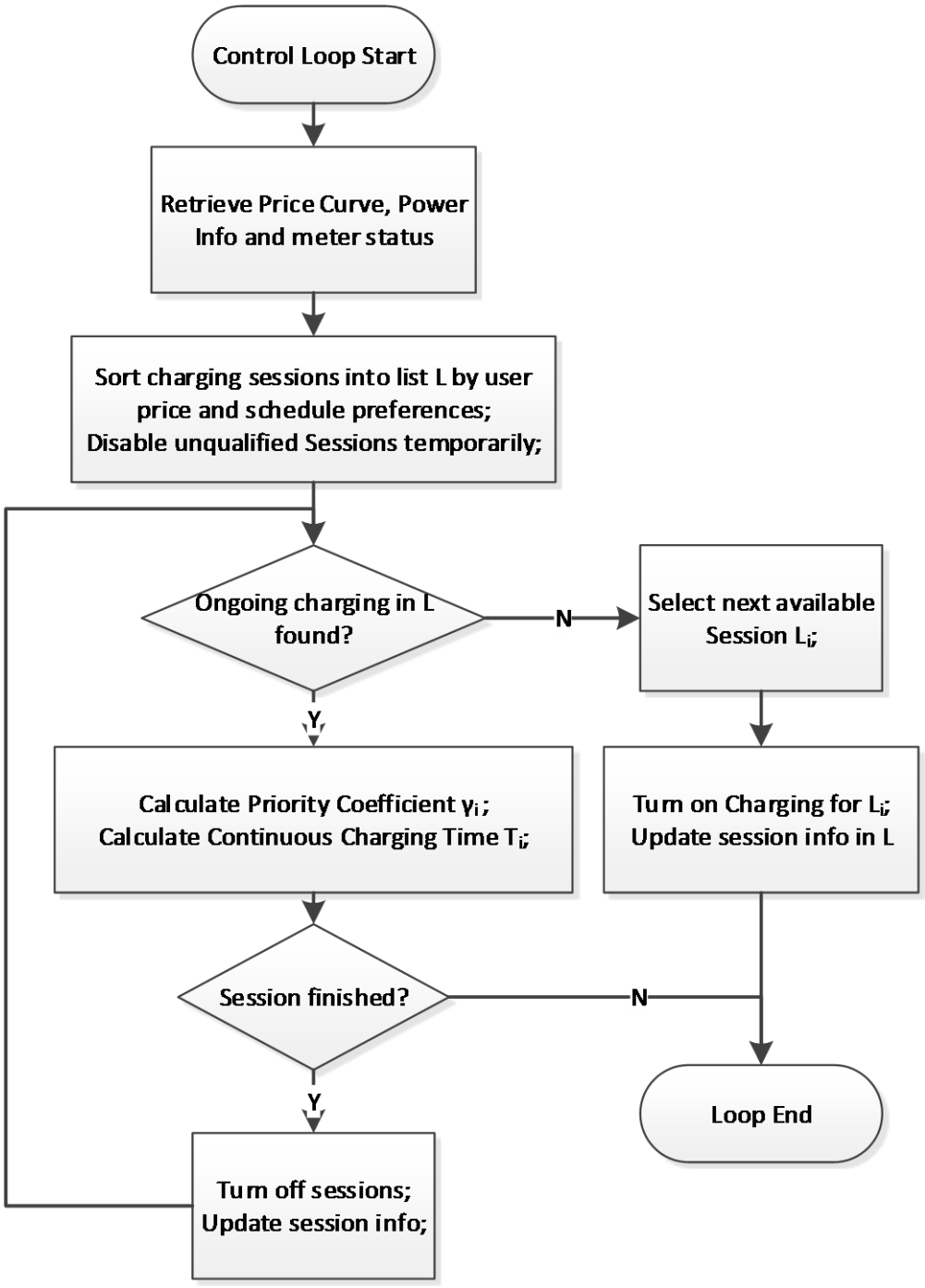

Figure 5-4 Level I scheduling strategy

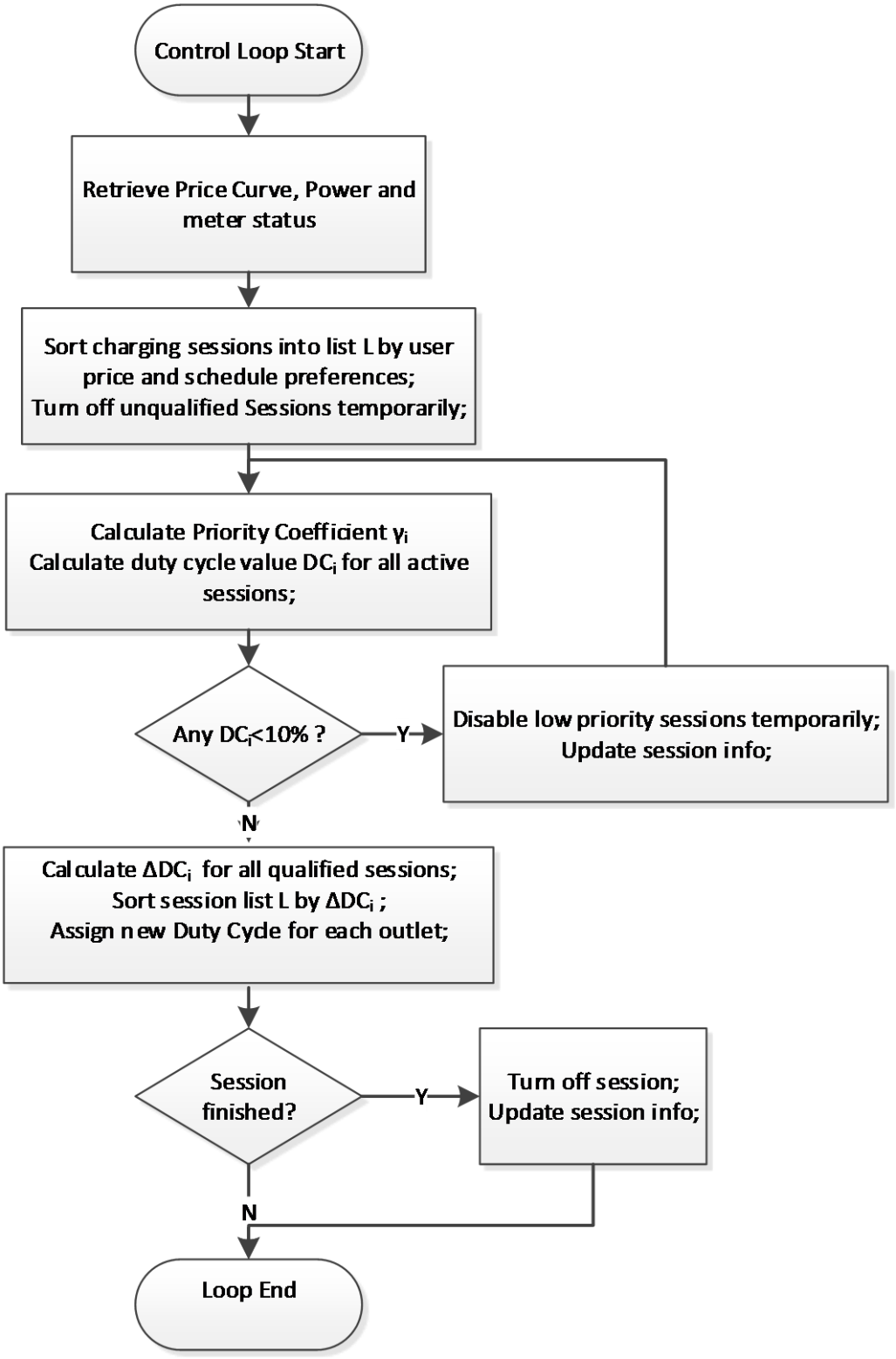

Figure 5-5 Level II scheduling strategy

5.6 Result Analysis

To explain the energy sharing and scheduling mechanism, charging records for typical days are retrieved from database for analysis. For level I EVSE, records for July 5th, 2014 are selected since there are 4 users submitted their charging sessions with different price preferences. The highest price is 15 cents/kWh, which happens around 13:30 PM.

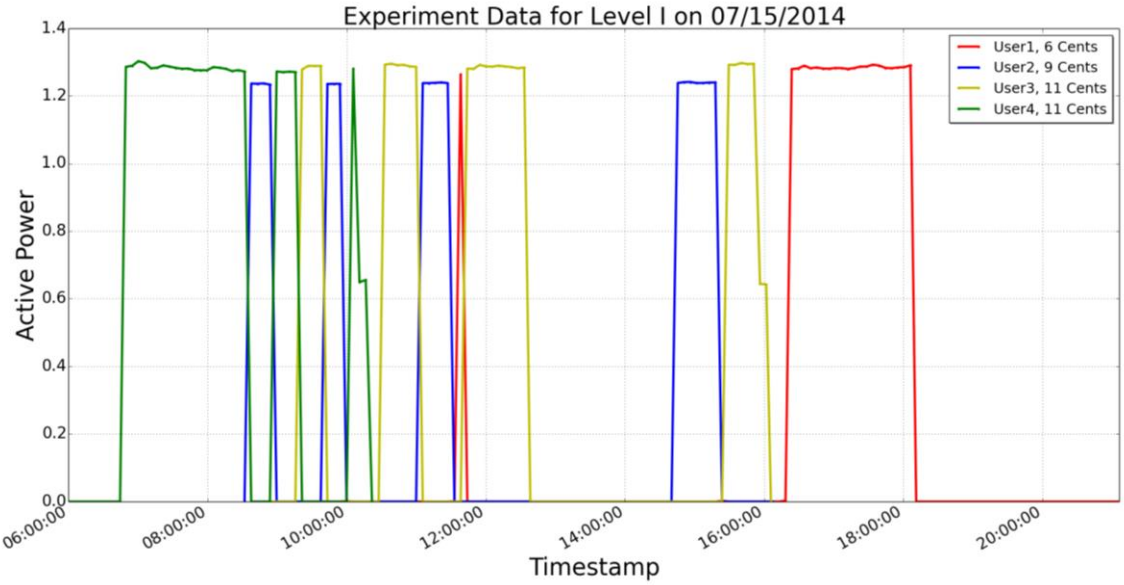

Figure 5-6 Level I experiment data

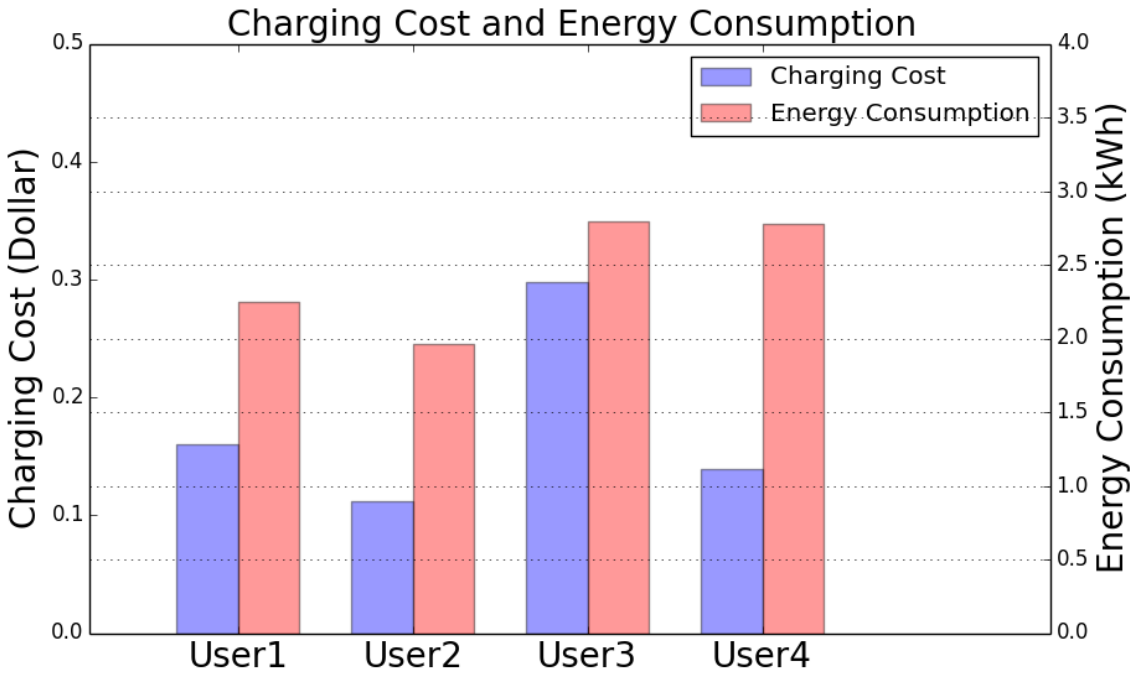

Figure 5-7 Level I cost vs. energy consumption

According to experiment data shown above, the first user (user4) started charging around 7:00 AM in the morning with 11 cents/kWh and finished charging around 10:30 AM. After a while, user2 and user3 joined the energy sharing program and occupied charging periods, which are proportional to their priority coefficients. The last user, user1, selected the lowest price of the day around noon. Thus, his/her charging was disabled soon after charging session initialization and re-activated after 16:00 PM when system price signal is lower than his/her accepted price. Since her/his duration of stay in campus is longer than other users, it is wise of her/him to wait until price is lower in latter hours and avoid higher price period. Charging cost plot implies that users may save charging cost by placing a proper price. Moreover, experiment results also suggest that users' schedules with price preferences is potentially grid-friendly because the charging load for higher price period, usually also higher system load period, can be shifted to time intervals with lower the system pressure.

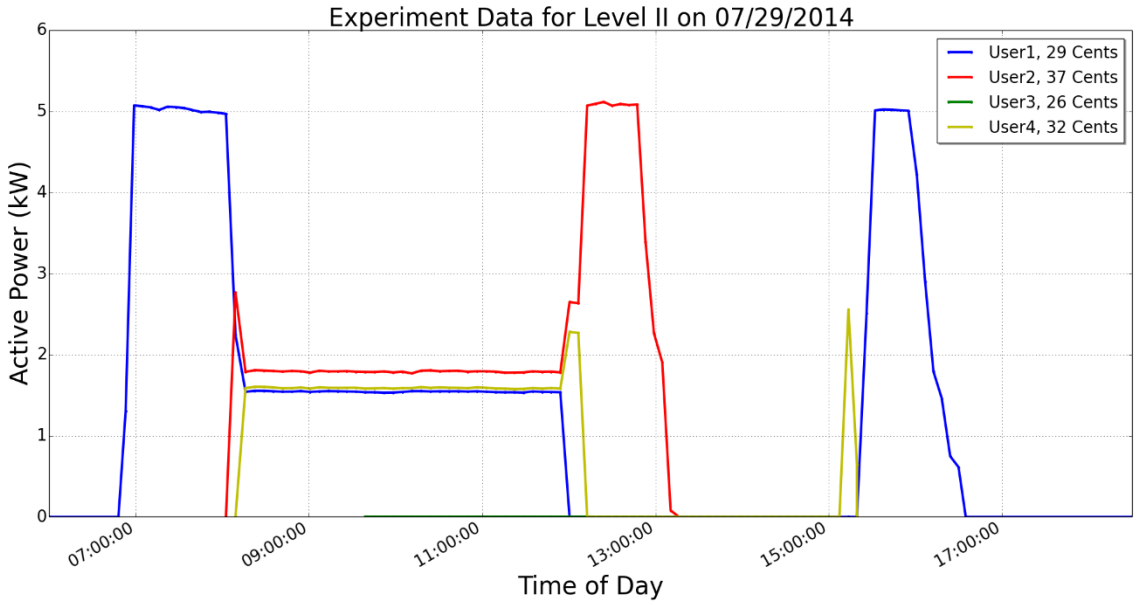

Figure 5-8 Level II experiment data

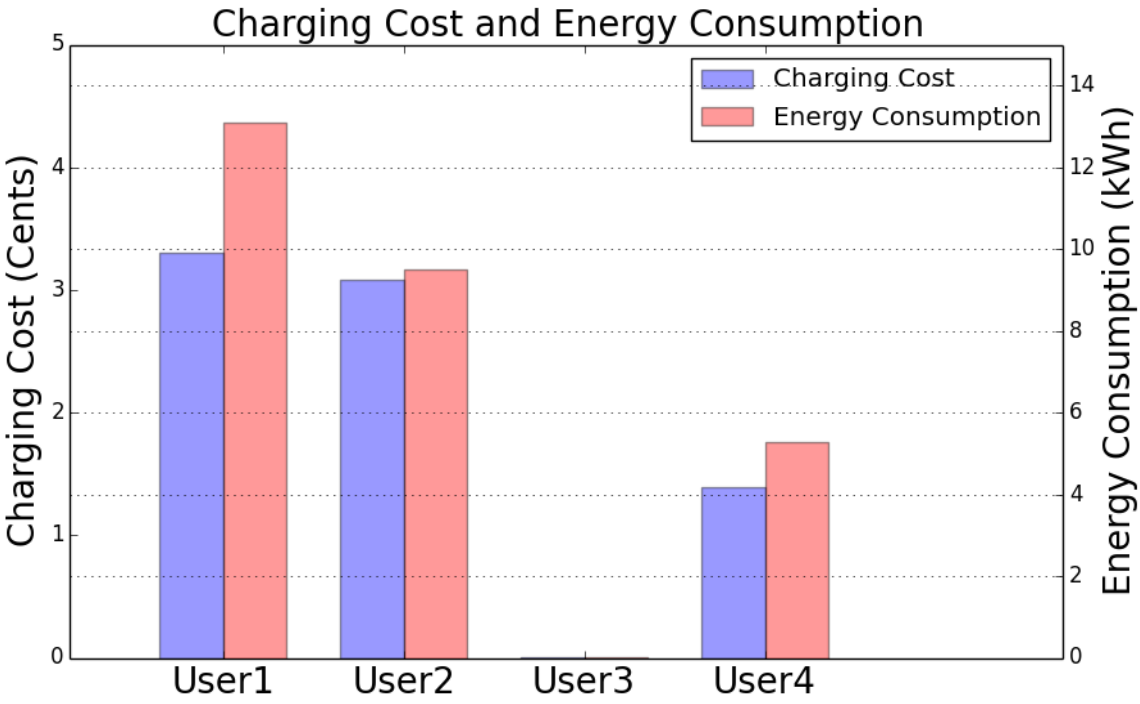

Figure 5-9 Level II cost vs. energy consumption

For level II EVSE, multiple vehicles can consume power from a single power source simultaneously. Charging records on July 29th, 2014, when the highest price is 37 cents/kWh, are

retrieved from database. As is shown in Figure 5-8, 4 active charging sessions are submitted by users. The first user (user1) selected a medium price (the third highest price) from the five price options offered by aggregator around 7:00 AM. When he is the only consumer for that EVSE, his priority coefficient γ_i is 1 and he was assigned with the maximum duty cycle. For circuit stability reason, maximum duty cycle for this EVSE is set to 45%. Around 8:15 AM, additional 2 users with higher prices submitted their charging sessions for that EVSE. Accordingly, the current is multiplexed for each user proportionally to γ_i. Around 12:00 PM, as the system price increases to a level which is higher than both user1 and user4's accepted prices, their charging sessions are disabled temporarily. Thus, user 2 with the highest price could consume all power supply until it finished charging. User1 and user4 halted their charging and waited for price to drop down. Finally user1 finished his charging around 17:00 PM. User 3 was unable to obtain any power supply, because the system price was never lower than her/his accepted price even she/he submitted charging schedule as from 9:00 AM to 12:00 PM. From the experiment results, charging sessions with higher price tend to charge at a higher rate and consume more energy than other users in the same period. Moreover, for users with longer time of stay in campus, a better price or bid strategy exists to charge enough energy, while save charging cost. The cost and energy consumption comparison is plotted in Figure 5-9.

5.7 Summary

In this chapter, we implemented a price-based smart charging algorithm in a university campus. ARIMA was applied to model the historical charging load and perform day-ahead prediction. We deployed a pricing strategy and a bidding policy, considering wholesale energy prices, predicted load and system desired load curve. The online scheduling algorithm has been implemented to

dynamically regulate charging sessions for a single EVSE according to price and schedule preferences. The experiment results indicate that the proposed strategy is beneficial for EV drivers in terms of cost saving and that it has potential to further optimize the EV energy allocations according to users' preferences.

Chapter 6 System Architecture and Implementation

6.1 Introduction

A multi-layer EV energy management system (EMS) has been implement to regulate EV charging behaviors with various scheduling strategies. There are three main components in the hierarchical 3-layer system architecture, i.e. smart Electric Vehicle Supply Equipment (EVSE), EV aggregated control center (EVCC), and the Integrated Super Control Center (iSCC). The major benefit of a centralized iSCC is to implement intelligent energy management strategies with a holistic consideration of the electricity market and resources within the entire microgrid, including Battery Energy Storage System (BESS), renewable generations, etc. In this chapter, we focus on the development and implementation of EVCC with components and interfaces to manage a number of charging devices and interact with the grid operation signals from upper layer. A communication network for all components in different layers is constructed to support the complex operations. EV energy scheduling algorithms within EVCC, with varied objectives and constraints, are developed to manage EV charging behaviors, considering the user energy price preferences, travel schedules, and the real-time grid signals from iSCC, utility companies or ISOs. For the entire energy management service, customized data models are constructed to support both the standardized and proprietary grid operations, e.g. demand response (DR), etc. The merits for this system can be summarized as follows:

- Multi-layer hierarchical architecture is developed to improve the system efficiency, reliability and interoperability, considering availability of other Distributed Energy Resources(DERs) in local distribution systems;
- Customized data models are developed among components in different layers to support more flexible grid operations, such as demand response, etc.;
- Adaptable application program interface (API) is developed with evolvable templates for energy scheduling algorithms and EVSEs. Based on that, the scheduling services are developed, incorporating the real-time DR signals;
- User-friendly mobile applications are developed for EV drivers with interfaces to initiate/terminate/monitor charging sessions, as well as submitting personal energy management preferences.

6.2 System Components and Integration

In the hierarchical system shown in Figure 6-1, the first layer is the integrated super control center (iSCC), the second layer is the EV aggregator and other distributed resources in local distribution grid, such as solar PV generation, Battery Energy Storage System (BESS), and the third layer is the physical devices, i.e. the Electric Vehicle Supply Equipment (EVSE) with current multiplexing capabilities. With communication devices inside the EVSE, EV drivers/users are able to monitor and control the charging sessions for their vehicles via mobile applications.

The iSCC performs management tasks considering both historical and real-time data for the components in the microgrid. Various algorithms can be implemented by iSCC to support microgrid regulation tasks, such as minimal EV power control, etc. In addition, iSCC has interfaces to communicate with each other component in microgrid with both standard and proprietary

protocols. For instance, OpenADR2.0a and a customized DR protocol are both supported between iSCC and the EV control center to aggregately control the EV energy consumption.

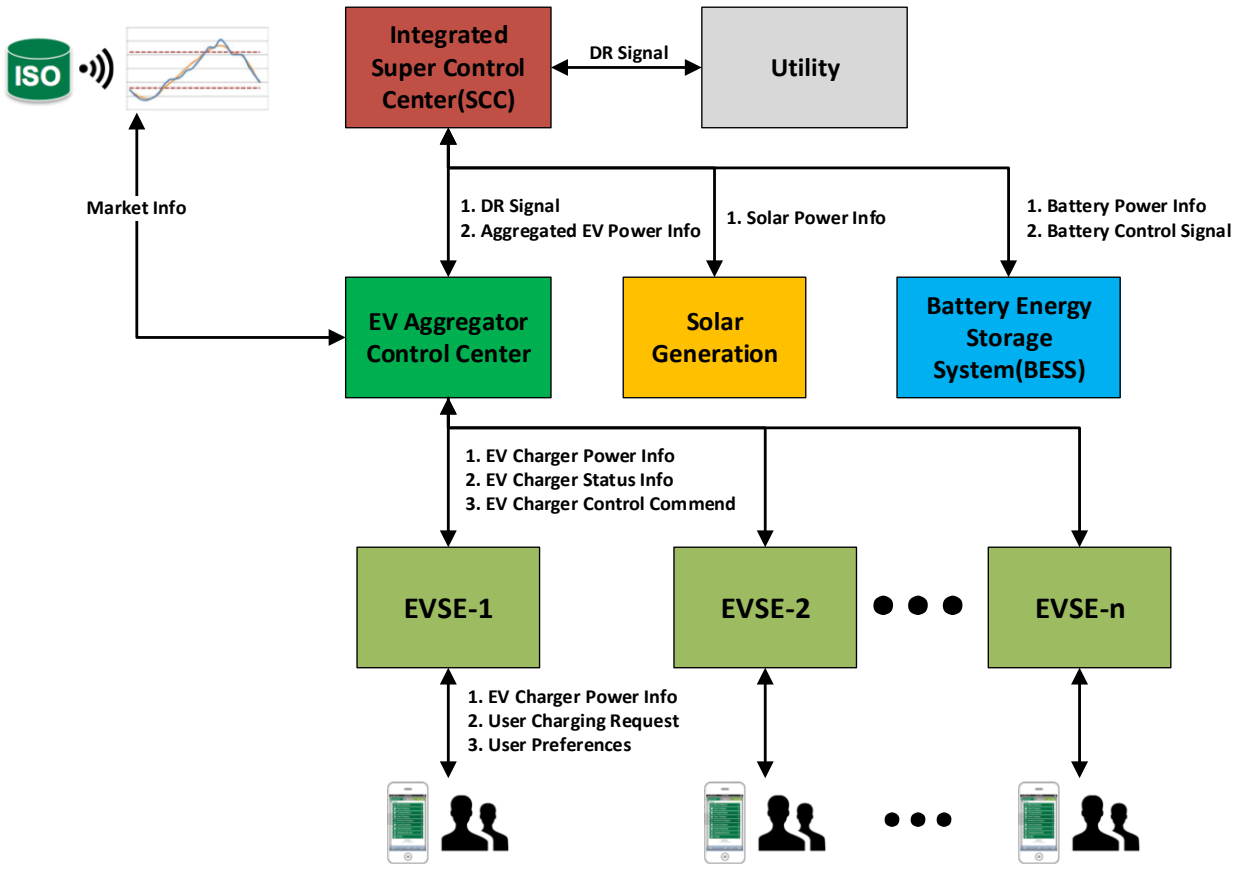

Figure 6-1. System architecture

EVCC manages both private EVs and public fleet EVs on the UCLA campus by real-time scheduling algorithms. It is capable of retrieving market information, including energy price signals from CAISO wholesale market, local utility or pricing services from third-party organization, and pulling real-time power/status information from a myriad of EVSEs on the UCLA campus. Based on the EV communication network, the scheduling algorithms that consider user preferences, energy prices, and DR signals from iSCC, are implemented to perform more efficient management of EV charging behaviors.

The EVSEs in the third layer of the implemented system have current multiplexing and power sharing capabilities, i.e. split the charging current to multiple connected vehicles from single power source, developed by UCLA SMERC. Network communication is also deployed in these devices to enable remote power monitoring and control functions.

6.3 Customized Data Model

To increase the system flexibility, multiple proprietary communication protocols and data models are developed. Data model for the communication between first layer and second layer is customized to include DR event parameters, exclusively for the parking structures and organizations. Similarly, the data model between second layer and third layer, is modified based on the combination of the real-time power information and charger status information. The details of their models are discussed as follows.

At each time interval, the raw data packets retrieved from EVSEs are first parsed by the data collector service on the EV control center. Subsequently, charger status information is retrieved and combined with the previous power information to be inserted into the database table with the data model shown in Figure 6-2. The advantage of the modified data model comes from 3 aspects: 1) completeness for power monitoring; 2) convenience to debug and troubleshooting, such as the [StatusErrorCode] field in the data model; 3) simplicity to process, i.e. each data tuple is labeled with a [Timestamp], which makes it easier to process large volume monitoring data.

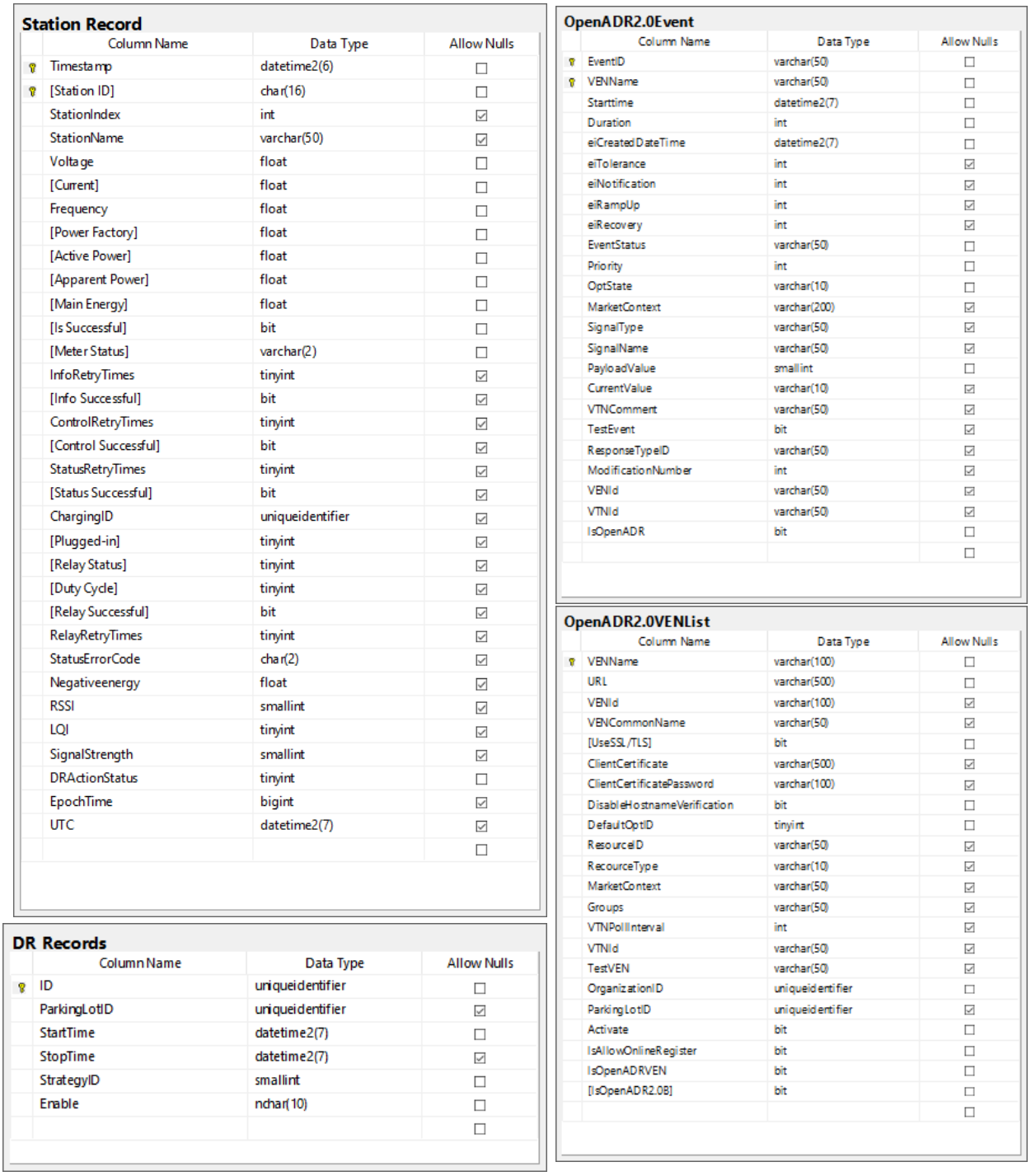

Station Record

Column Name	Data Type	Allow Nulls
Timestamp	datetime2(6)	☐
[Station ID]	char(16)	☐
StationIndex	int	☑
StationName	varchar(50)	☑
Voltage	float	☐
[Current]	float	☐
Frequency	float	☐
[Power Factory]	float	☐
[Active Power]	float	☐
[Apparent Power]	float	☐
[Main Energy]	float	☐
[Is Successful]	bit	☐
[Meter Status]	varchar(2)	☐
InfoRetryTimes	tinyint	☑
[Info Successful]	bit	☑
ControlRetryTimes	tinyint	☑
[Control Successful]	bit	☑
StatusRetryTimes	tinyint	☑
[Status Successful]	bit	☑
ChargingID	uniqueidentifier	☑
[Plugged-in]	tinyint	☑
[Relay Status]	tinyint	☑
[Duty Cycle]	tinyint	☑
[Relay Successful]	bit	☑
RelayRetryTimes	tinyint	☑
StatusErrorCode	char(2)	☑
Negativeenergy	float	☑
RSSI	smallint	☑
LQI	tinyint	☑
SignalStrength	smallint	☑
DRActionStatus	tinyint	☐
EpochTime	bigint	☑
UTC	datetime2(7)	☑
		☐

DR Records

Column Name	Data Type	Allow Nulls
ID	uniqueidentifier	☐
ParkingLotID	uniqueidentifier	☑
StartTime	datetime2(7)	☐
StopTime	datetime2(7)	☑
StrategyID	smallint	☐
Enable	nchar(10)	☐
		☐

OpenADR2.0Event

Column Name	Data Type	Allow Nulls
EventID	varchar(50)	☐
VENName	varchar(50)	☐
Starttime	datetime2(7)	☐
Duration	int	☐
eiCreatedDateTime	datetime2(7)	☐
eiTolerance	int	☑
eiNotification	int	☑
eiRampUp	int	☑
eiRecovery	int	☑
EventStatus	varchar(50)	☐
Priority	int	☐
OptState	varchar(10)	☐
MarketContext	varchar(200)	☑
SignalType	varchar(50)	☑
SignalName	varchar(50)	☑
PayloadValue	smallint	☐
CurrentValue	varchar(10)	☑
VTNComment	varchar(50)	☑
TestEvent	bit	☑
ResponseTypeID	varchar(50)	☑
ModificationNumber	int	☑
VENId	varchar(50)	☑
VTNId	varchar(50)	☑
IsOpenADR	bit	☐
		☐

OpenADR2.0VENList

Column Name	Data Type	Allow Nulls
VENName	varchar(100)	☐
URL	varchar(500)	☐
VENId	varchar(100)	☑
VENCommonName	varchar(50)	☑
[UseSSL/TLS]	bit	☐
ClientCertificate	varchar(500)	☑
ClientCertificatePassword	varchar(100)	☑
DisableHostnameVerification	bit	☐
DefaultOptID	tinyint	☐
ResourceID	varchar(50)	☑
RecourceType	varchar(10)	☑
MarketContext	varchar(50)	☑
Groups	varchar(50)	☑
VTNPollInterval	int	☑
VTNId	varchar(50)	☑
TestVEN	varchar(50)	☑
OrganizationID	uniqueidentifier	☐
ParkingLotID	uniqueidentifier	☑
Activate	bit	☐
IsAllowOnlineRegister	bit	☐
IsOpenADRVEN	bit	☐
[IsOpenADR2.0B]	bit	☐
		☐

Figure 6-2 Customized data models

For the EV charging system implemented on the UCLA campus and other organizations with different numbers of parking structures, there exist different needs to perform varied DR events in different parking lots. However, the original data model definition from OpenADR 2.0a and

OpenADR2.0b, does not distinguish the signals for parking lots and organizations, which makes the system deployment less efficient and reliable in cases where load curtailment should be applied to specific locations. For the implementations at UCLA, each parking lot is equipped with different communication network, which requires different computation process to handle the power management for the EVs in different parking lots. Thus, the original OpenADR data model, which is meant to specify the properties of a DR event, is extended to include the following parameters: 1) ParkingLotID, 2) OrganizationID, and 3) IsOpenADRVEN. Consequently, the scheduling service and database system at EV control center will be able to handles requests based on both standard OpenADR protocol and the proprietary ones, in which parking lot ID, event start time, event stop time and strategy ID, which specifies the different operation algorithm performed by EV control center, can be specified. With the additional flexibility, iSCC is able to issue more detailed DR signals to adapt to diverse local grid situations. Therefore, the modified data model improves the overall system flexibility and interoperability, especially in the case of implementations with multiple organizations.

6.4 Application Program Interface (API) and Scheduling Service

For monitoring and controlling the charging stations, we have developed the Application Program Interface (API) for EV charging system, which defines the patterns of communication and control signals to EV charging stations. Our design of API stems from the concept of OOP (Object Oriented Programming). We model the complex communications and control behaviors of charging stations as logically distinct classes. For instance, the EVSE class comprises the EVSEs and charging plugs of different levels, Chargingutility class provides functionality for web services

and web-based applications, and the Charging Algorithm class regulates the charging behaviors within control loops. This format provides a convenient scheme for developers to derive more EVSE and charging algorithm classes with different properties and methods. This format will also save time and energy for system administrators to maintain the EV charging system. In addition, we have also implemented other modules for use by utilities, such as a security module that ensures incoming function calls meet the system's security requirements.

Besides, physical and virtual devices are also modeled in this system API, involving all the possible status and values for the devices. Enumerations and structures are used to include all the parameters in a light-weight fashion. These data structures are available to be called by other functions or services that are built on top on the API. The architecture and main components of API is shown in Figure 6-3 and Figure 6-4.

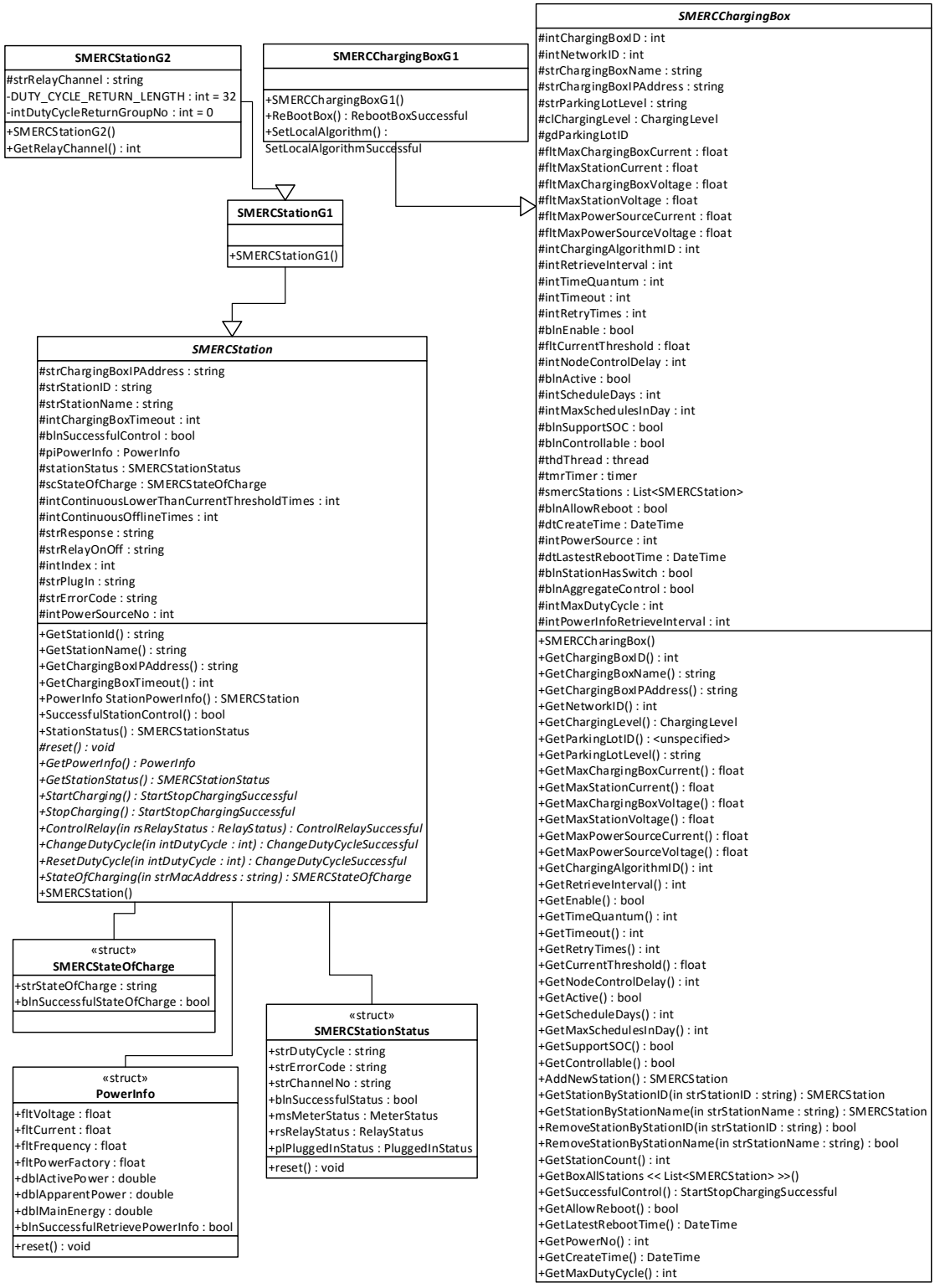

Figure 6-3 EVSE classes

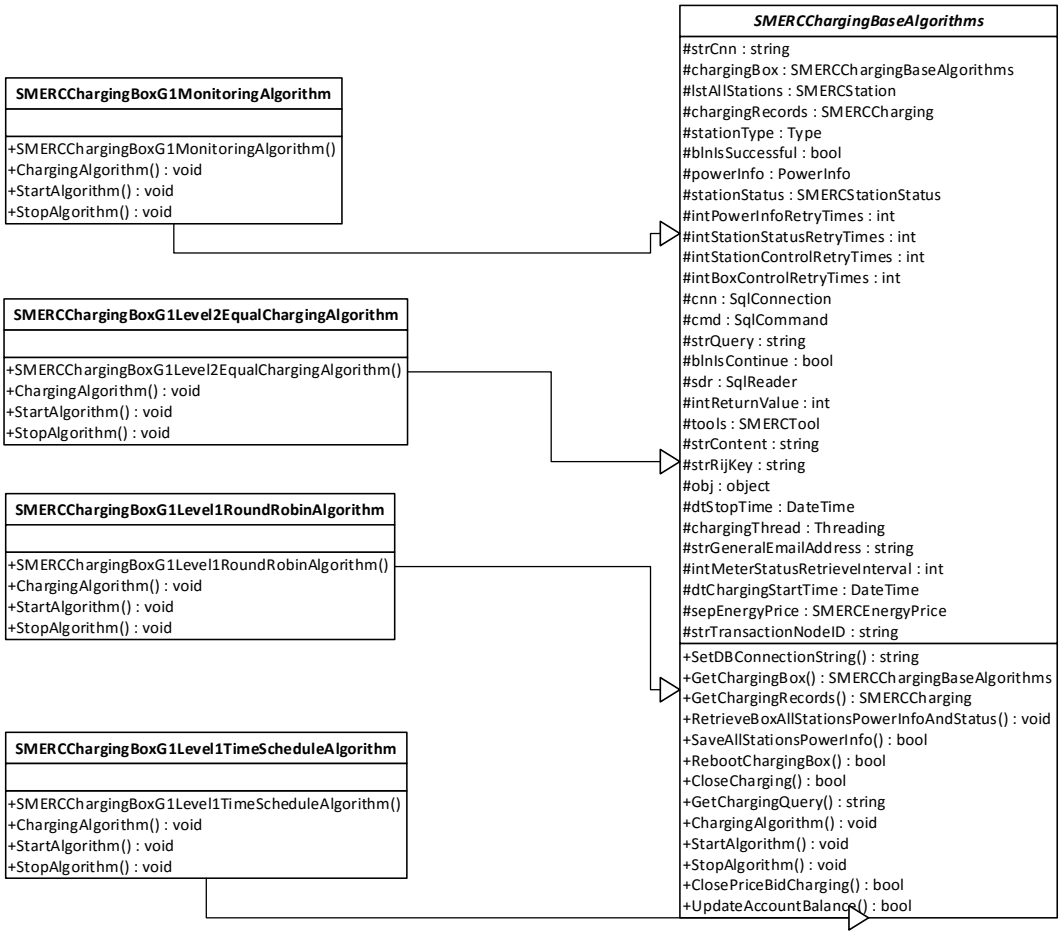

Figure 6-4 Architecture and data model for scheduling algorithms

6.5 EV Charging Monitoring & Control Center

In this section, system setup, configuration, network structure etc., are given with details. We have tested various communication networks and designed an optimal communication architecture based on the specific characteristics of the parking structures. Multiple communication protocols are involved in this network architecture, i.e. Wifi, 3G, Zigbee, etc. The EV charging network utilizes a centralized control system to monitor and regulate the network for real-time smart charging services. This smart charging infrastructure uses standard networking technologies to

create a network that facilitates charging services for the end users and monitors and controls tasks for maintainers/operators. Figure 6-5 shows the topology of the EV network's architecture.

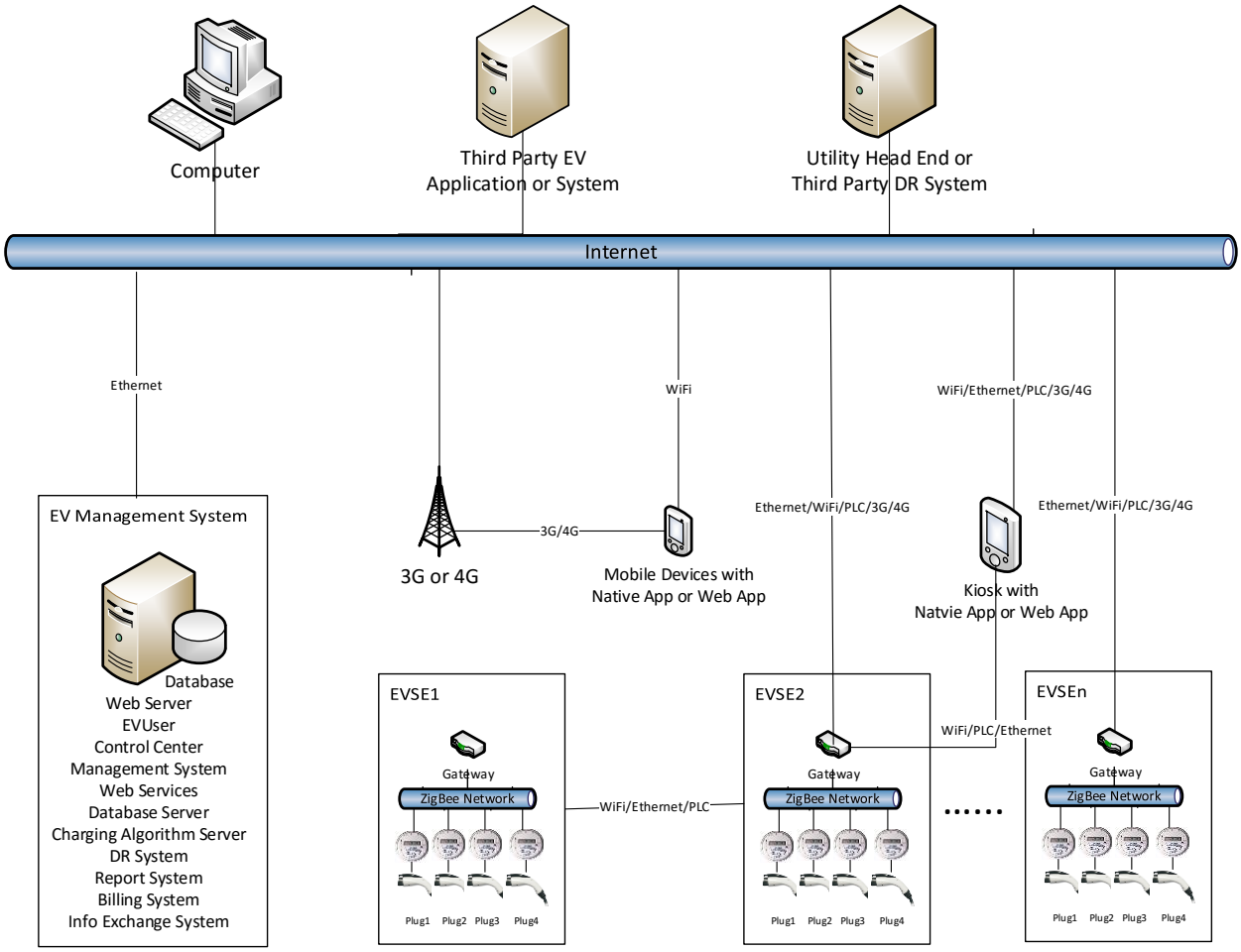

Figure 6-5. UCLA network architecture

As shown in Figure 6-5, built under UCLA campus network, the EV communication network utilizes campus Ethernet, PLC, WiFi or 3G/4G service to connect with ZigBee communication gateways which, in turns, connect with each individual EV charging stations through ZigBee communication protocol. The webserver and database server receive and send data through this hierarchical network connections. The mobile devices interact with the EV network through connection with 3G/4G or UCLA campus network.

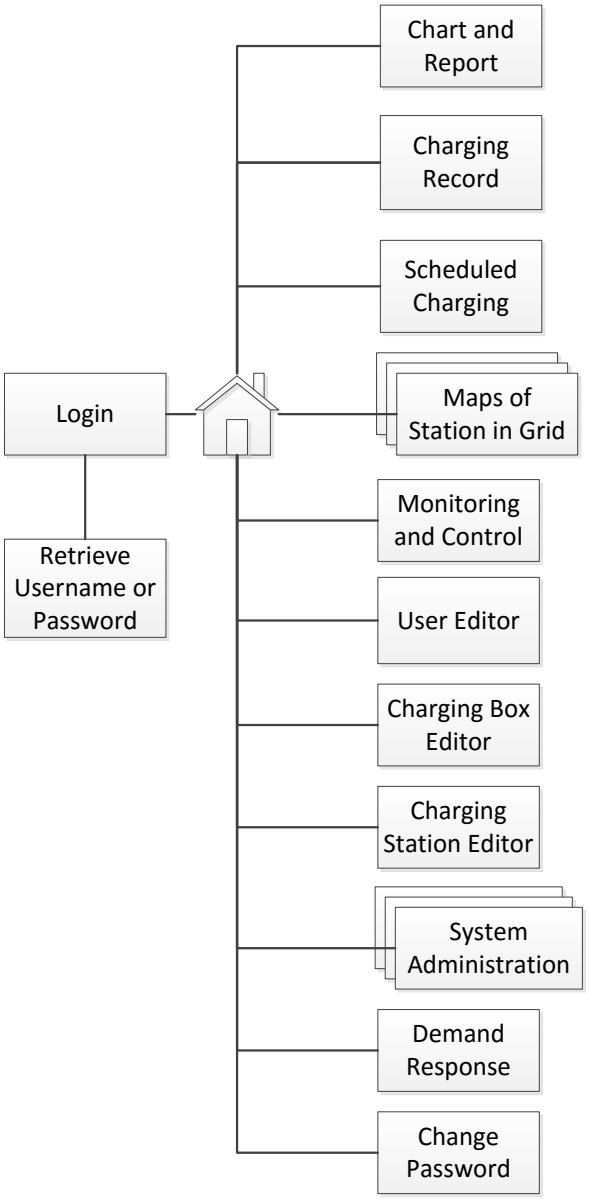

Figure 6-6. EV control center

The SMERC Monitoring and Control Center is a high performance server that allows administrators/operators to monitor and control all EV charging stations, registered to the network. The system defines control algorithms, provides real time and historical data for analysis, and allows the editing of information pertaining to charging boxes and EVs. The sitemap in Figure 6-6 shows the current features that are accessible after logging in.

Figure 6-7. Monitoring of EV user behaviors

In Figure 6-7, the monitoring page for the EV charging behaviors on the UCLA campus can be utilized for showing the real-time charging events. The EV info and the corresponding EVSE where this user's vehicle is in charging are shown. The user name are block in this figure for privacy concern. The available charging stations will be indicated as "Standby". Meanwhile, the real-time charging power, voltage, current and the accumulated energy consumed for the particular meter are recorded.

A more detailed visualization page for charging behaviors at the EVSE level have also been developed. As is shown in Figure 6-8, two charging sessions can be identified, including the time when the session initiated and the power consumption value while the vehicle is in charging.

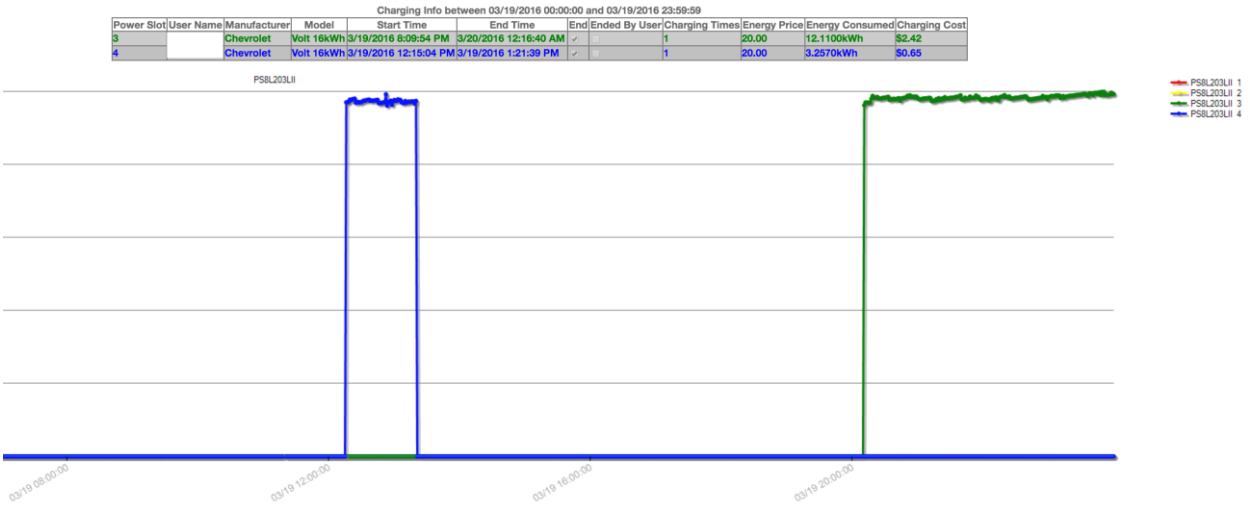

Figure 6-8. Monitoring of single EVSE

6.5.1 Data collection

In our previous implementation, the existing scheduling algorithm that serves the purpose to collect EV charging related data is a simple energy-sharing algorithm, *i.e.* Equal-Sharing Scheduling Algorithm (ESSA). It splits the total power supply from the power source equally by the number of connected vehicles in each scheduling loop. For simplicity, this ESSA does not require any input for user preferences but only a click on mobile application to initiate the charging session. However, significant session parameters for each user are preserved this way, such as charging start time, finish time, leave time and the energy consumption value for each session. Algorithm 4 indicates the details of ESSA when multiple vehicles are connected.

$maxDC$ denotes the maximum duty-cycle for each power source and η is a safety coefficient. In this algorithm, each vehicle will be assigned a percentage of circuit duty-cycle and continues

charging until current drops below a pre-defined threshold. Accordingly, the start time, finish time and energy consumption are collected. Another significant parameter indicating the vehicle leave time is the plug-in status, which is also returned by the firmware in EVSEs and hereby user's stay duration can be obtained by the difference between start time and leave time.

Algorithm 4: Equal Sharing Scheduling Algorithm (ESSA)

Each Loop:

Retrieve EVSE status;

V ← connected vehicles;

n ←number of active vehicles V;

Calculate average Duty-cycle: $DC \leftarrow \frac{maxDC}{n} \cdot \eta \cdot 100\%$;

For $i \in [1,2,\dots,n]$

If current value drops close to 0 or unplug

Close charging session;

Record session parameters in database;

Else if different DC value detected

Set duty-cycle to DC for i^{th} vehicle in V;

Wait for current to stabilize;

End

End

6.5.2 Inference for EV Charging Parameters

Decisions made by scheduling algorithms are based on the real-time data collected from EVSEs in time series. Unfortunately, there does not exist explicit signals from EVSEs, indicating termination of a charging session. Thus, proper inference is needed to determine some of the aforementioned parameters, such as leave time.

6.5.2.1 Determine when to close a charging session

Scheduling algorithm must adaptively check if power consumption rate falls below a threshold. However, at the end of charging sessions, power drawn by some types of EVs is not stable, which might be caused by different designs of internal Battery Management System (BMS). Therefore, we employ a method based on moving average to adaptively evaluate the power consumption rate.

Assume the real-time power data for each meter at time t is denoted by y_t. The action to close a charging session is determined by a parameter for the averaged power consumption level, denoted by c_t, which can be calculated by:

$$c_t = \frac{1}{H} \cdot \sum_{i=1}^{i=H} y_{t-i-1} \tag{6.1}$$

where H is the length of moving window, 10 in our case. When the average power consumption level c_t drops below a pre-defined threshold $\underline{c}$, 0.1 kW in our case, the close charging decision will be made. Figure 6-9 illustrates this inference process.

In addition, by evaluating the latest power data before closing the charging session, one can infer whether or not EV is fully charged. If the power value is still higher than the threshold, the plug is believed to be disconnected by the user when the charging is still in process.

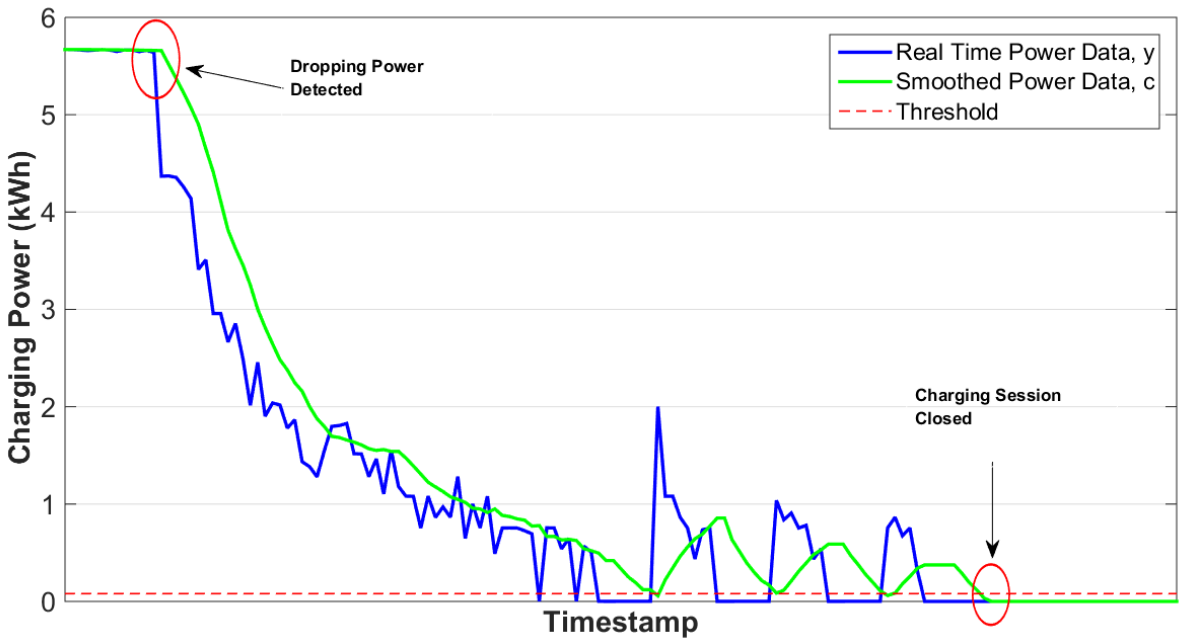

Figure 6-9 Inference Process to Close Charging Sessions

6.5.2.2 Determine leave time

Leave time can also be inferred from time series data by detecting the earliest time when plug-in status changes to negative. The inference is illustrated below:

$$t_l = \begin{cases} t_f, & c_{tf} > \underline{c} \\ min(t), & c_{tf} \leq \underline{c}, t > t_f \ where \ pl(t) = 0 \end{cases} \quad (6.2)$$

If the power consumption rate when charging session is being close, c_{tf} is larger than the threshold, $\underline{c}$, the time to close charging session is exactly the leave time because the vehicle is believed to be manually un-plugged. On the other hand, when power consumption is lower than threshold, the leave time can only be inferred from the time when plug-in status changes from 1 to 0. $pl(t)$ denotes the plug-in status at time t.

6.5.3 Scheduling Services

The scheduling service running on server can perform schedule optimization either periodically or triggered by pre-defined events. As shown in Figure 6-10, charging requests from users are submitted through the mobile application and are then stored in database as records before being directed to scheduling service, from which specific control commands are sent. Once the control action finishes, operation status is returned to users. Meanwhile, the scheduling service is able to host numerous threads, each of which can be a specific scheduling algorithm with varied optimization objective and constraints. The algorithm can be initiated periodically at the pre-set time interval, which is shown in the red box of Figure 6-10. Before any optimization is made in each loop, the first action is to retrieve the real-time data and status from EVSEs, which enables the algorithm to compute the optimal schedules based on the most up-to-date system states. Another interface to initiate the scheduling service is via pre-defined events through the interface between database and scheduling service. The events are detected by monitoring the real-time data from EVSEs. Once a charging session is terminated or any status updates are detected, notifications will be sent to users through mobile applications. Note that the data and status for EVSE come through mesh networks (from EVSE to control center) and thereby communication delay exists. In addition, if the commands lead to adjustments of power consumption, it will take longer time for the circuit to stabilize. Thus, delays of several seconds based on practical experiences are expected and too frequent control (*e.g.* more than 5 times per minute) is not recommended in this system.

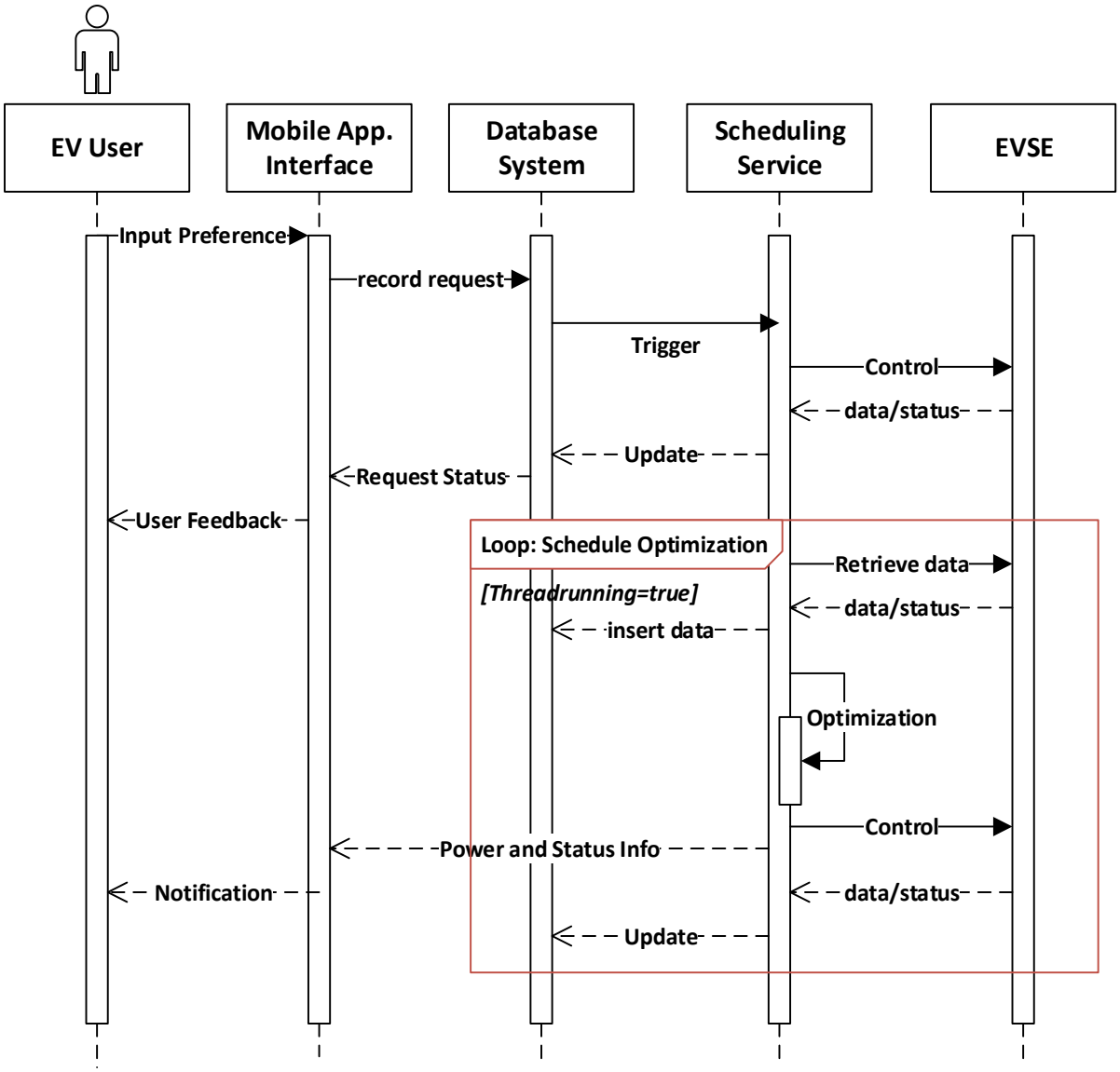

Figure 6-10 Sequence chart for scheduling service

6.6 EV Charging Mobile Application

Mobile applications are developed to satisfy the users by remotely and intelligently managing their charging sessions by their cell phone. Various functions are supported within mobile applications, such as specifying travel preferences, energy preferences, looking for EVSE availabilities, checking real-time status and power information, etc. When an EV is plugged into an EV charger, the user can activate a charging session through a smart phone or any Internet-connected device.

If a vehicle is equipped with the State of Charge (SOC) box, the SOC information is also obtained. These operations can be illustrated by the screen shots taken from the mobile app/interface in the Figure 6-11.

Other than the web-based mobile App for users to manage their charging sessions, we are also developing an iOS version, which is supposed to offer a better user experience, including responsive touch controls and more interactive actions. Based on the library of Swift languages provided by Apple, more functions, such as Navigation to charging stations, will be designed to provide more convenience for EV users. Similar to the web-based App, the control and display logic will guide the users to input their charging preferences step by step. After a user logs on through the App, the modified home view is presented in Figure 6-11 Navigation is a very significant function we have developed in the latest version, which will automatically provide links for each parking lot at UCLA with SMERC charging EVSEs and build connections with the Apple map navigation system. Thus, users are able to follow the highlighted routes on the map to initiate their charging sessions. Other functions remain similar to the web-based app, as shown in Figure 6-11.

The notification services will inform the users about the status change of their charging sessions. For example, the email with the charging information, including total energy consumed, charging cost and the charging location information, will be sent to users.

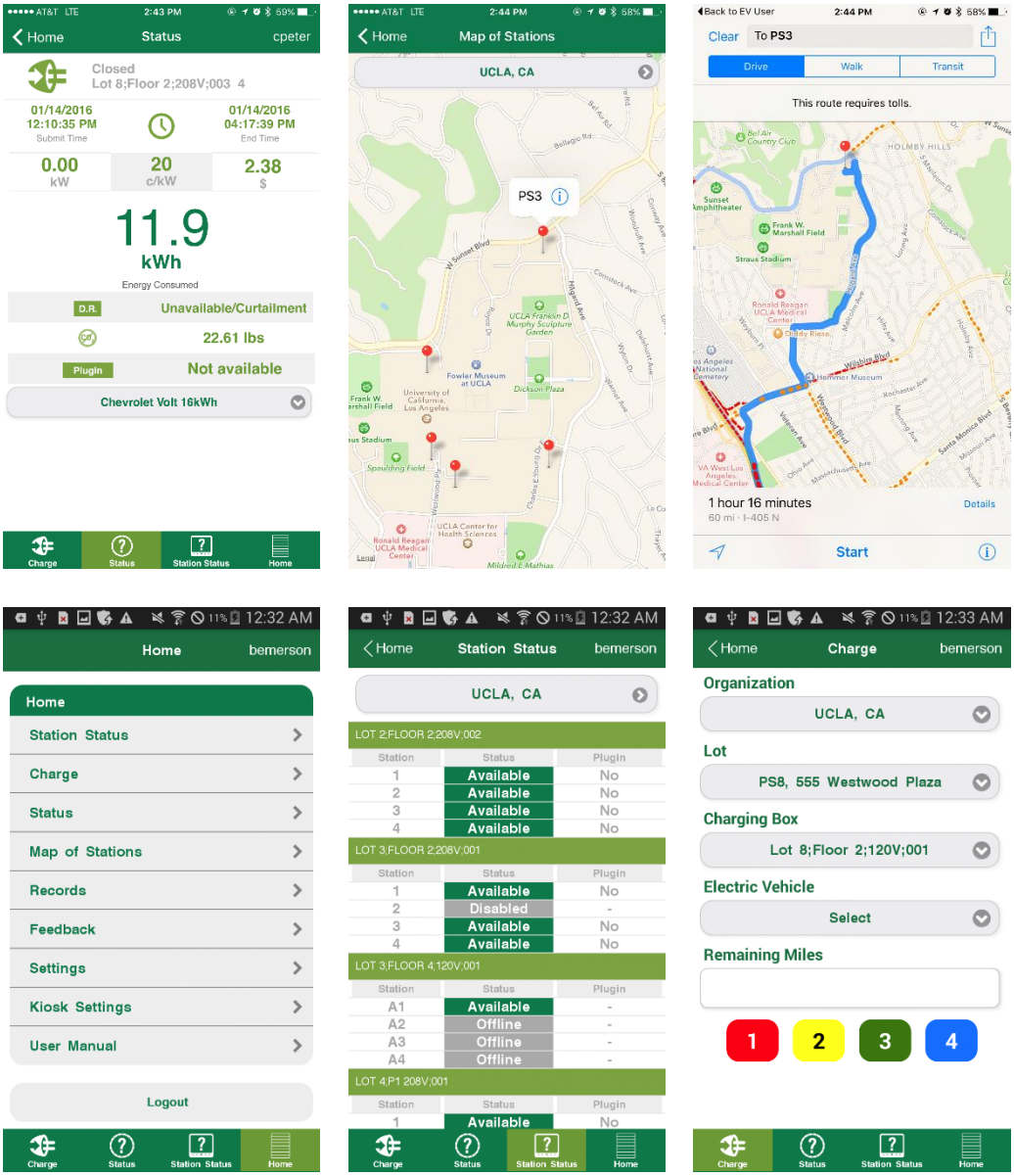

Figure 6-11 Interfaces of mobile application

The typical procedure to initiate a charging session is described as follows:

- Account log-in;
- Select available organization;
- Select available parking structure;
- Select/Input Charging preferences;

- Start charging session by selecting available charging outlet (station);
- Check the charging status;

Note that for the users, who have existing charging records in the system, selections of organization, parking structure, and even charging preferences, will be automatically performed.

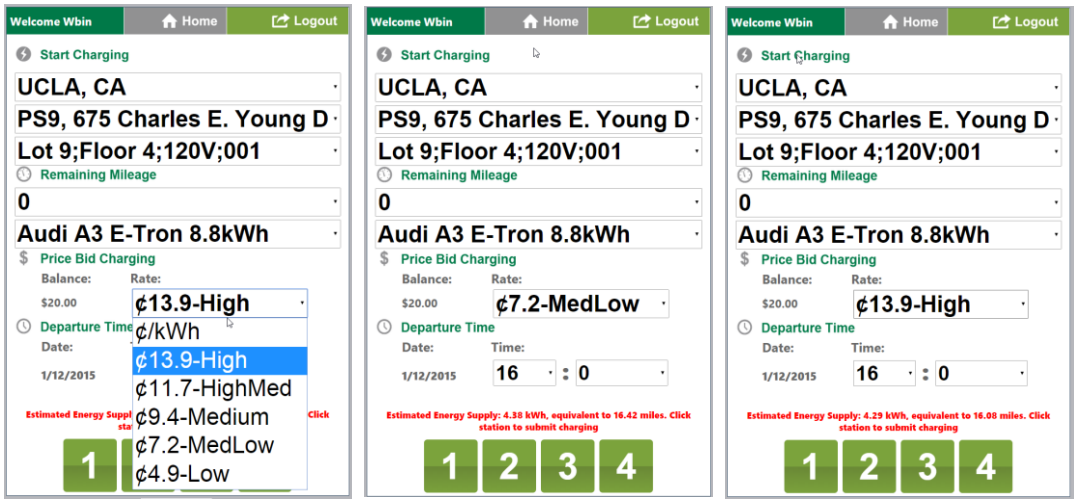

Figure 6-12 User-interface for price-based algorithms

In addition, user interfaces with the option to select price preferences and the personal travel schedules, are developed. As shown in Figure 6-12, 5 price levels are provided based on the regional price curve generated by (5.4), i.e. High, Medium-High, Medium, Medium-Low and Low. Priories are calculated for the connected vehicles on each EVSE, and accordingly the charging time ratio or duty-cycle values will be assigned by (5.5) and (5.6). Furthermore, a prediction service is provided as a feedback for users to make their charging decisions. Specifically, based on users' input schedules and the electricity price preferences, the estimated value of energy delivery is pushed back to users' mobile applications, so that the back-and-forth negotiation can be supported by this scheme. Finally, the charging behaviors are regulated in real-time by the price-based scheduling algorithms shown in Figure 5-4 and Figure 5-5.

6.7 DR Experiment

To support the integration of Demand Response signals from ISOs/Utility companies and even third-party organizations, OpenADR 2.0 standard has been integrated into the scheduling services on the EV control center. Each EVSE on campus is registered as a Virtual End Node (VEN) and the signal issuers are regarded as Virtual Top End (VTN). Based on the customized DR actions and data models, discussed in section 6.3, both one parking lot and or the whole campus can be modeled as the acting group to respond to the same DR signal. Besides, within the real-time EV scheduling algorithms, the steps to check the availability and status of DR signals are embedded, followed by the load curtailment steps. Through mobile applications, it is also viable for users to specify whether or not they are willing to engage in the DR program. The DR event monitoring page is shown in Figure 6-13. To test the functionalities of the EV energy management system with DR capabilities, real-world experiment results are displayed in Figure 6-14. Each curve represents the power consumption by EVs in each parking lot on campus. Once the DR signal is active, the power consumption is suppressed to the minimum to provide grid regulation services, while the signals are expired, the charging sessions will be resumed to previous states.

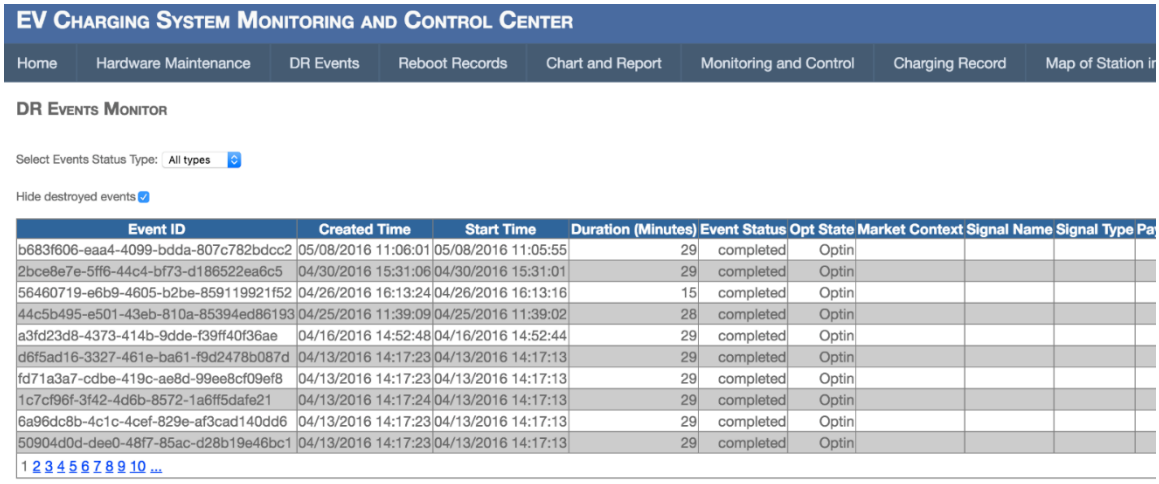

Figure 6-13 Demand response monitoring page

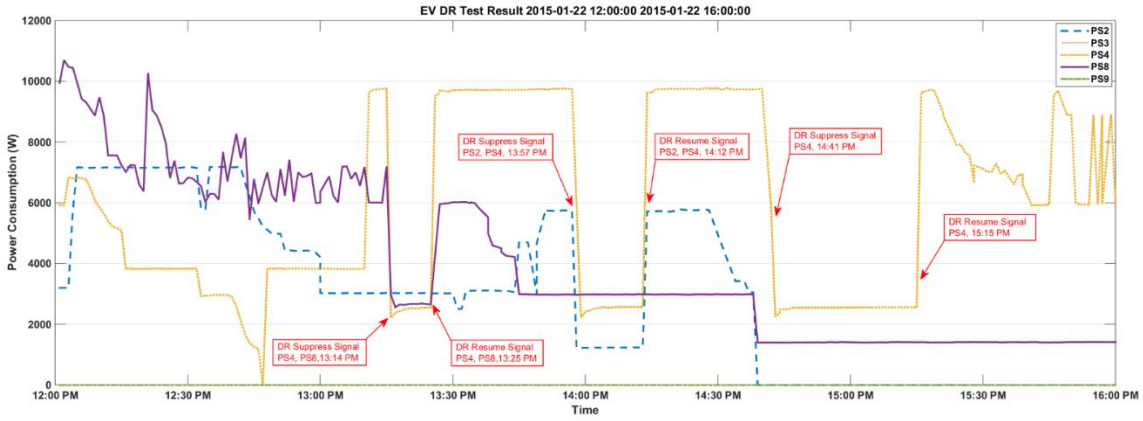

Figure 6-14 DR experiment results on campus parking lots

6.8 Summary

In this chapter, a real-world implementation of a smart EV energy management system is discussed with details of system architecture and the practical considerations. A multi-layer structure is constructed to support the interactions between EV system and the higher level energy management system via Demand Response signals. Customized data structures and communication protocols are developed among different system components to improved reliability, efficiency and interoperability. Finally, methods for data collection and parameter inferences are also discussed.

Chapter 7 Conclusion and Future Work

The integration of EVs under smart grid scenarios involves a variety of challenging tasks, which have not been completely solved by previous research. As the penetration of DERs grow larger, it becomes even more difficult to coordinate EV charging behaviors in real-time, considering the intermittency of renewable generation and stochastic user behaviors. Therefore, we develop an online predictive EV scheduling framework, which dynamically computes optimal EV energy scheduling. Meanwhile, this dissertation also solves practical issues by designing and implementing a scalable system architecture to capture the user preferences, enable multi-layer communication and control, and finally improve the system reliability and interoperability.

In Chapter 2, we develop a predictive scheduling framework which takes into account the uncertainties of EV user behaviors. Specifically, Gaussian kernel estimator is designed to dynamically estimate the charging session parameters with improved accuracies and receding horizon control strategies are implement to compute optimal EV energy schedules with virtual load constraint. The cost performance has been significantly improved while guaranteeing a high level of energy delivery rate. Based on the developed framework in Chapter 2, an event-based control strategy with the integration of IEC 61850 standard is developed in Chapter 3. Under event-based control paradigm, the data retrieval and computation are only initiated by the pre-defined events, which represent the critical change of the system states. The simulation results indicate that event-based strategies can effectively maintain a high level of energy delivery rate with low unit

energy cost while reducing the number of unnecessary computations. Chapter 4 extends this predictive framework to support load flatten/valley filling strategies, considering the uncertainties of building load and solar generation in a microgrid. The overall power fluctuation for the micro-grid is reduced up to 40% on the test days.

For the future work on the predictive energy management framework, more components in the microgrid scenario will be evaluated and formulated as controllable devices, to provide more grid service besides cost saving, and load flattening/valley filling, etc. Other data-driven methods for parameter estimation and behavior prediction, etc., will be studied.

In Chapter 5 and Chapter 6, a scalable architecture of system implementation is discussed. A price-based charging strategy, considering the EV users' price preferences and account priority, is developed to bridge end-user EV drivers with the wholesale energy markets. The online scheduling algorithm allocates energy to the connected vehicles dynamically through the scheduling services, which supports customized data models and communication protocols/standards with ISOs/utility companies, to implement more complex grid operations.

For the future work on this part, more research will be conducted to regulate the aggregated EVs to provide grid services in a more intelligent fashion. Methods based on statistical learning and distributed algorithms have the potential to provide further more reliable and efficient EV system implementations.

Bibliography

[1] M. Olken, "Smart Grid Technology: A Global Approach to Its Challenges [From the Editor]," *IEEE Power Energy Mag.*, vol. 10, no. 4, pp. 4–6, Jul. 2012.

[2] Y. Yan, Y. Qian, H. Sharif, and D. Tipper, "A Survey on Smart Grid Communication Infrastructures: Motivations, Requirements and Challenges," *IEEE Commun. Surv. Tutor.*, vol. 15, no. 1, pp. 5–20, First 2013.

[3] N. B. M. Isa, T. C. Wei, and A. H. M. Yatim, "Smart grid technology: Communications, power electronics and control system," in *2015 International Conference on Sustainable Energy Engineering and Application (ICSEEA)*, 2015, pp. 10–14.

[4] V. C. Gungor, D. Sahin, T. Kocak, S. Ergut, C. Buccella, C. Cecati, and G. P. Hancke, "Smart Grid Technologies: Communication Technologies and Standards," *IEEE Trans. Ind. Inform.*, vol. 7, no. 4, pp. 529–539, Nov. 2011.

[5] A. Molderink, V. Bakker, M. G. C. Bosman, J. L. Hurink, and G. J. M. Smit, "Management and Control of Domestic Smart Grid Technology," *IEEE Trans. Smart Grid*, vol. 1, no. 2, pp. 109–119, Sep. 2010.

[6] W. Shi, N. Li, X. Xie, C. C. Chu, and R. Gadh, "Optimal Residential Demand Response in Distribution Networks," *IEEE J. Sel. Areas Commun.*, vol. 32, no. 7, pp. 1441–1450, Jul. 2014.

[7] F. Rahimi and A. Ipakchi, "Demand Response as a Market Resource Under the Smart Grid Paradigm," *IEEE Trans. Smart Grid*, vol. 1, no. 1, pp. 82–88, Jun. 2010.

[8] P. Palensky and D. Dietrich, "Demand Side Management: Demand Response, Intelligent Energy Systems, and Smart Loads," *IEEE Trans. Ind. Inform.*, vol. 7, no. 3, pp. 381–388, Aug. 2011.

[9] R. H. Lasseter and P. Paigi, "Microgrid: a conceptual solution," in *Power Electronics Specialists Conference, 2004. PESC 04. 2004 IEEE 35th Annual*, 2004, vol. 6, p. 4285–4290 Vol.6.

[10] "Ackerkman Solar Rooftop Project 35kW." [Online]. Available: https://evsmartplug.net/smartgrid/ackerman_pv/. [Accessed: 03-Jan-2016].

[11] Y. Wang, B. Wang, C.-C. Chu, H. Pota, and R. Gadh, "Energy management for a commercial building microgrid with stationary and mobile battery storage," *Energy Build.*

[12] Y. Wang, B. Wang, R. Huang, C.-C. Chu, H. R. Pota, and R. Gadh, "Two-tier prediction of solar power generation with limited sensing resource," in *2016 IEEE/PES Transmission and Distribution Conference and Exposition (T D)*, 2016, pp. 1–5.

[13] H. Nazaripouya, B. Wang, Y. Wang, P. Chu, H. R. Pota, and R. Gadh, "Univariate time series prediction of solar power using a hybrid wavelet-ARMA-NARX prediction method," in *2016 IEEE/PES Transmission and Distribution Conference and Exposition (T D)*, 2016, pp. 1–5.

[14] B. Wang, R. Huang, Y. Wang, H. Nazaripouya, C. Qiu, C. C. Chu, and R. Gadh, "Predictive scheduling for Electric Vehicles considering uncertainty of load and user behaviors," in *2016 IEEE/PES Transmission and Distribution Conference and Exposition (T D)*, 2016, pp. 1–5.

[15] B. Wang, Y. Wang, C. Qiu, C. C. Chu, and R. Gadh, "Event-based electric vehicle scheduling considering random user behaviors," in *2015 IEEE International Conference on Smart Grid Communications (SmartGridComm)*, 2015, pp. 313–318.

[16] "FERC Reports on Demand Response & Advanced Metering." [Online]. Available: http://www.ferc.gov/industries/electric/indus-act/demand-response/dem-res-adv-metering.asp. [Accessed: 26-Aug-2016].

[17] M. Muratori and G. Rizzoni, "Residential Demand Response: Dynamic Energy Management and Time-Varying Electricity Pricing," *IEEE Trans. Power Syst.*, vol. 31, no. 2, pp. 1108–1117, Mar. 2016.

[18] C. Chen, J. Wang, and S. Kishore, "A Distributed Direct Load Control Approach for Large-Scale Residential Demand Response," *IEEE Trans. Power Syst.*, vol. 29, no. 5, pp. 2219–2228, Sep. 2014.

[19] S. Mohagheghi and N. Raji, "Dynamic Demand Response : A Solution for Improved Energy Efficiency for Industrial Customers," *IEEE Ind. Appl. Mag.*, vol. 21, no. 2, pp. 54–62, Mar. 2015.

[20] S. Mohagheghi and N. Raji, "Managing Industrial Energy Intelligently: Demand Response Scheme," *IEEE Ind. Appl. Mag.*, vol. 20, no. 2, pp. 53–62, Mar. 2014.

[21] U. Herberg, D. Mashima, J. G. Jetcheva, and S. Mirzazad-Barijough, "OpenADR 2.0 deployment architectures: Options and implications," in *2014 IEEE International Conference on Smart Grid Communications (SmartGridComm)*, 2014, pp. 782–787.

[22] E. Ebeid, S. Rotger-Griful, S. A. Mikkelsen, and R. H. Jacobsen, "A methodology to evaluate demand response communication protocols for the Smart Grid," in *2015 IEEE International Conference on Communication Workshop (ICCW)*, 2015, pp. 2012–2017.

[23] M. I. Ridwan, N. S. Miswan, M. S. M. Shokri, M. N. Noran, R. M. Lajim, and H. N. Awang, "Interoperability in Smart Grid using IEC 61850 standard: A power utility prospect," in *2014 IEEE Innovative Smart Grid Technologies - Asia (ISGT ASIA)*, 2014, pp. 261–266.

[24] "Monthly Plug-In Sales Scorecard." [Online]. Available: http://insideevs.com/monthly-plug-in-sales-scorecard. [Accessed: 19-Aug-2016].

[25] "Electric Vehicles Initiative (EVI) | Clean Energy Ministerial." [Online]. Available: http://cleanenergyministerial.org/Our-Work/Initiatives/Electric-Vehicles. [Accessed: 19-Aug-2016].

[26] B. Chen, K. S. Hardy, J. D. Harper, T. P. Bohn, and D. S. Dobrzynski, "Towards standardized Vehicle Grid Integration: Current status, challenges, and next steps," in *2015 IEEE Transportation Electrification Conference and Expo (ITEC)*, 2015, pp. 1–6.

[27] R.-C. Leou, C.-L. Su, and C.-N. Lu, "Stochastic Analyses of Electric Vehicle Charging Impacts on Distribution Network," *IEEE Trans. Power Syst.*, vol. 29, no. 3, pp. 1055–1063, May 2014.

[28] K. Clement-Nyns, E. Haesen, and J. Driesen, "The Impact of Charging Plug-In Hybrid Electric Vehicles on a Residential Distribution Grid," *IEEE Trans. Power Syst.*, vol. 25, no. 1, pp. 371–380, Feb. 2010.

[29] S. Bashash and H. K. Fathy, "Cost-Optimal Charging of Plug-In Hybrid Electric Vehicles Under Time-Varying Electricity Price Signals," *IEEE Trans. Intell. Transp. Syst.*, vol. 15, no. 5, pp. 1958–1968, Oct. 2014.

[30] Y. Wang, H. Nazaripouya, C.-C. Chu, R. Gadh, and H. R. Pota, "Vehicle-to-grid automatic load sharing with driver preference in micro-grids," in *Innovative Smart Grid Technologies Conference Europe (ISGT-Europe), 2014 IEEE PES*, 2014, pp. 1–6.

[31] Y. Wang, O. Sheikh, B. Hu, C.-C. Chu, and R. Gadh, "Integration of V2H/V2G hybrid system for demand response in distribution network," in *2014 IEEE International Conference on Smart Grid Communications (SmartGridComm)*, 2014, pp. 812–817.

[32] S. Han, S. Han, and K. Sezaki, "Development of an Optimal Vehicle-to-Grid Aggregator for Frequency Regulation," *IEEE Trans. Smart Grid*, vol. 1, no. 1, pp. 65–72, Jun. 2010.

[33] P. Richardson, D. Flynn, and A. Keane, "Optimal Charging of Electric Vehicles in Low-Voltage Distribution Systems," *IEEE Trans. Power Syst.*, vol. 27, no. 1, pp. 268–279, Feb. 2012.

[34] C. Chen and S. Duan, "Optimal Integration of Plug-In Hybrid Electric Vehicles in Microgrids," *IEEE Trans. Ind. Inform.*, vol. 10, no. 3, pp. 1917–1926, Aug. 2014.

[35] L. Gan, U. Topcu, and S. H. Low, "Optimal decentralized protocol for electric vehicle charging," *IEEE Trans. Power Syst.*, vol. 28, no. 2, pp. 940–951, May 2013.

[36] L. Gan, A. Wierman, U. Topcu, N. Chen, and S. H. Low, "Real-time deferrable load control: handling the uncertainties of renewable generation," in *Proceedings of the fourth international conference on Future energy systems*, 2013, pp. 113–124.

[37] N. Chen, L. Gan, S. H. Low, and A. Wierman, "Distributional analysis for model predictive deferrable load control," in *2014 IEEE 53rd Annual Conference on Decision and Control (CDC)*, 2014, pp. 6433–6438.

[38] L. Chen, N. Li, L. Jiang, and S. H. Low, "Optimal Demand Response: Problem Formulation and Deterministic Case," in *Control and Optimization Methods for Electric Smart Grids*, A. Chakrabortty and M. D. Ilić, Eds. Springer New York, 2012, pp. 63–85.

[39] N. G. Paterakis, O. Erdinc, A. G. Bakirtzis, and J. P. S. Catalao, "Optimal Household Appliances Scheduling Under Day-Ahead Pricing and Load-Shaping Demand Response Strategies," *IEEE Trans. Ind. Inform.*, vol. 11, no. 6, pp. 1509–1519, Dec. 2015.

[40] X. Xi and R. Sioshansi, "Using Price-Based Signals to Control Plug-in Electric Vehicle Fleet Charging," *IEEE Trans. Smart Grid*, vol. 5, no. 3, pp. 1451–1464, May 2014.

[41] Y. Cao, S. Tang, C. Li, P. Zhang, Y. Tan, Z. Zhang, and J. Li, "An Optimized EV Charging Model Considering TOU Price and SOC Curve," *IEEE Trans. Smart Grid*, vol. 3, no. 1, pp. 388–393, Mar. 2012.

[42] A. Dubey, S. Santoso, M. P. Cloud, and M. Waclawiak, "Determining Time-of-Use Schedules for Electric Vehicle Loads: A Practical Perspective," *IEEE Power Energy Technol. Syst. J.*, vol. 2, no. 1, pp. 12–20, Mar. 2015.

[43] C. Jin, J. Tang, and P. Ghosh, "Optimizing Electric Vehicle Charging: A Customer's Perspective," *IEEE Trans. Veh. Technol.*, vol. 62, no. 7, pp. 2919–2927, Sep. 2013.

[44] B. Wang, B. Hu, C. Qiu, P. Chu, and R. Gadh, "EV charging algorithm implementation with user price preference," in *Innovative Smart Grid Technologies Conference (ISGT), 2015 IEEE Power Energy Society*, 2015, pp. 1–5.

[45] T. Zhang, W. Chen, Z. Han, and Z. Cao, "Charging Scheduling of Electric Vehicles With Local Renewable Energy Under Uncertain Electric Vehicle Arrival and Grid Power Price," *IEEE Trans. Veh. Technol.*, vol. 63, no. 6, pp. 2600–2612, Jul. 2014.

[46] P. Grahn, K. Alvehag, and L. Soder, "PHEV Utilization Model Considering Type-of-Trip and Recharging Flexibility," *IEEE Trans. Smart Grid*, vol. 5, no. 1, pp. 139–148, Jan. 2014.

[47] M. Majidpour, C. Qiu, P. Chu, R. Gadh, and H. R. Pota, "Fast Prediction for Sparse Time Series: Demand Forecast of EV Charging Stations for Cell Phone Applications," *IEEE Trans. Ind. Inform.*, vol. 11, no. 1, pp. 242–250, Feb. 2015.

[48] M. Alizadeh, A. Scaglione, J. Davies, and K. S. Kurani, "A scalable stochastic model for the electricity demand of electric and plug-in hybrid vehicles," *Smart Grid IEEE Trans. On*, vol. 5, no. 2, pp. 848–860, 2014.

[49] B. Wang, Y. Wang, H. Nazaripouya, C. Qiu, C. C. Chu, and R. Gadh, "Predictive Scheduling Framework for Electric Vehicles with Uncertainties of User Behaviors," *IEEE Internet Things J.*, Jan. 2016.

[50] "California Statewide Plug-In Electric Vehicle Infrastructure Assessment - CEC-600-2014-003.pdf." [Online]. Available: http://www.energy.ca.gov/2014publications/CEC-600-2014-003/CEC-600-2014-003.pdf. [Accessed: 03-Jan-2016].

[51] J. Pan, R. Jain, S. Paul, T. Vu, A. Saifullah, and M. Sha, "An Internet of Things Framework for Smart Energy in Buildings: Designs, Prototype, and Experiments," *IEEE Internet Things J.*, vol. 2, no. 6, pp. 527–537, Dec. 2015.

[52] B. Wang, Y. Wang, C. Qiu, C.-C. Chu, and R. Gadh, "Event-based Electric Vehicle Scheduling Considering Random User Behaviors."

[53] C.-Y. Chung, J. Chynoweth, C.-C. Chu, R. Gadh, C.-Y. Chung, J. Chynoweth, C.-C. Chu, and R. Gadh, "Master-Slave Control Scheme in Electric Vehicle Smart Charging Infrastructure, Master-Slave Control Scheme in Electric Vehicle Smart Charging Infrastructure," *Sci. World J. Sci. World J.*, vol. 2014, 2014, p. e462312, May 2014.

[54] J. Chynoweth, C.-Y. Chung, C. Qiu, P. Chu, and R. Gadh, “Smart electric vehicle charging infrastructure overview,” in *Innovative Smart Grid Technologies Conference (ISGT), 2014 IEEE PES*, 2014, pp. 1–5.

[55] J. Shawe-Taylor and N. Cristianini, *Kernel Methods for Pattern Analysis*. Cambridge University Press, 2004.

[56] “C21 Model predictive control.” [Online]. Available: http://www.eng.ox.ac.uk/~conmrc/mpc/. [Accessed: 29-Aug-2016].

[57] G. James, D. Witten, T. Hastie, and R. Tibshirani, *An Introduction to Statistical Learning*, vol. 103. New York, NY: Springer New York, 2013.

[58] “Locational Marginal Prices.” [Online]. Available: http://oasis.caiso.com. [Accessed: 03-Jan-2016].

[59] Y. Wang, B. Wang, R. Huang, C.-C. Chu, H. R. Pota, and R. Gadh, “Two-Tier Prediction of Solar Power Generation with Limited Sensing Resource,” *ArXiv150802669 Stat*, Aug. 2015.

[60] “CVX: Matlab Software for Disciplined Convex Programming | CVX Research, Inc.” [Online]. Available: http://cvxr.com/cvx/. [Accessed: 11-Jan-2016].

[61] “U.S. Photovoltaic Prices and Cost Breakdowns: Q1 2015 Benchmarks for Residential, Commercial, and Utility-Scale Systems - 64746.pdf.” [Online]. Available: http://www.nrel.gov/docs/fy15osti/64746.pdf. [Accessed: 18-Jul-2016].

[62] Z. Tan, P. Yang, and A. Nehorai, “An Optimal and Distributed Demand Response Strategy With Electric Vehicles in the Smart Grid,” *IEEE Trans. Smart Grid*, vol. 5, no. 2, pp. 861–869, Mar. 2014.

[63] I. J. Fernández, C. F. Calvillo, A. Sánchez-Miralles, and J. Boal, “Capacity fade and aging models for electric batteries and optimal charging strategy for electric vehicles,” *Energy*, vol. 60, pp. 35–43, Oct. 2013.

[64] T. Zhang, W. Chen, Z. Han, and Z. Cao, “Charging Scheduling of Electric Vehicles With Local Renewable Energy Under Uncertain Electric Vehicle Arrival and Grid Power Price,” *IEEE Trans. Veh. Technol.*, vol. 63, no. 6, pp. 2600–2612, Jul. 2014.

[65] J. Schmutzler, C. Wietfeld, and C. A. Andersen, “Distributed energy resource management for electric vehicles using IEC 61850 and ISO/IEC 15118,” in *2012 IEEE Vehicle Power and Propulsion Conference*, 2012, pp. 1457–1462.

[66] O. Sundstrom and C. Binding, “Flexible Charging Optimization for Electric Vehicles Considering Distribution Grid Constraints,” *IEEE Trans. Smart Grid*, vol. 3, no. 1, pp. 26–37, Mar. 2012.

[67] F. Lu and M. Song, “Event-based control technology for the optimization of subway train #x2019;s operation,” in *7th World Congress on Intelligent Control and Automation, 2008. WCICA 2008*, 2008, pp. 1810–1813.

[68] X. Lagorce, C. Meyer, S. H. Ieng, D. Filliat, and R. Benosman, "Asynchronous Event-Based Multikernel Algorithm for High-Speed Visual Features Tracking," *IEEE Trans. Neural Netw. Learn. Syst.*, vol. 26, no. 8, pp. 1710–1720, Aug. 2015.

[69] R. Meier and V. Cahill, "On Event-Based Middleware for Location-Aware Mobile Applications," *IEEE Trans. Softw. Eng.*, vol. 36, no. 3, pp. 409–430, May 2010.

[70] X. Hu, C. Jiang, W. Zhang, J. Zhang, R. Yu, and C. Lv, "An Event Based GUI Programming Toolkit for Embedded System," in *Services Computing Conference (APSCC), 2010 IEEE Asia-Pacific*, 2010, pp. 625–631.

[71] F. Borrelli, P. Falcone, and C. D. Vecchio, "Event-Based Receding Horizon Control for Two-Stages Multi-Product Production Plants," in *2006 American Control Conference*, 2006, pp. 562–567.

[72] N. Xi, T.-J. Tarn, and A. K. Bejczy, "Intelligent planning and control for multirobot coordination: An event-based approach," *IEEE Trans. Robot. Autom.*, vol. 12, no. 3, pp. 439–452, Jun. 1996.

[73] C.-Y. Chung, J. Chynoweth, C. Qiu, C.-C. Chu, and R. Gadh, "Design of fast response smart electric vehicle charging infrastructure," *ArXiv Prepr. ArXiv13116009*, 2013.

[74] C.-Y. Chung, A. Shepelev, C. Qiu, C.-C. Chu, and R. Gadh, "Design of RFID mesh network for electric vehicle smart charging infrastructure," in *RFID-Technologies and Applications (RFID-TA), 2013 IEEE International Conference on*, 2013, pp. 1–6.

[75] C.-Y. Chung, C.-C. Chu, and R. Gadh, "Master-Slave Control Scheme in Electric Vehicle Smart Charging Infrastructure, Master-Slave Control Scheme in Electric Vehicle Smart Charging Infrastructure," *Sci. World J.*, vol. 2014, p. e462312, May 2014.

[76] A. Elgargouri, M. M. Elfituri, and M. Elmusrati, "IEC 61850 and smart grids," in *2013 3rd International Conference on Electric Power and Energy Conversion Systems (EPECS)*, 2013, pp. 1–6.

[77] R. E. Mackiewicz, "Overview of IEC 61850 and Benefits," in *2006 IEEE PES Power Systems Conference and Exposition*, 2006, pp. 623–630.

[78] R. Huang, "Integration of Renewable Distributed Energy Resources into Microgrids," 2015.

[79] "California Statewide Plug-in Electric Vehicle Infrustructure Assessment." [Online]. Available: http://www.energy.ca.gov/2014publications/CEC-600-2014-003/CEC-600-2014-003.pdf. [Accessed: 20-Aug-2016].

[80] S. M. M. Agah and A. Abbasi, "The impact of charging plug-in hybrid electric vehicles on residential distribution transformers," in *2012 2nd Iranian Conference on Smart Grids (ICSG)*, 2012, pp. 1–5.

[81] B. Wang, B. Hu, C. Qiu, P. Chu, and R. Gadh, "EV charging algorithm implementation with user price preference," in *Innovative Smart Grid Technologies Conference (ISGT), 2015 IEEE Power Energy Society*, 2015, pp. 1–5.

[82] Y. Wang, O. Sheikh, B. Hu, C. C. Chu, and R. Gadh, "Integration of V2H/V2G hybrid system for demand response in distribution network," in *2014 IEEE International Conference on Smart Grid Communications (SmartGridComm)*, 2014, pp. 812–817.

[83] "Real Time Building Utility Use Data." [Online]. Available: http://portal.emcs.cornell.edu/. [Accessed: 20-Aug-2016].

[84] "Ackerkman Solar Rooftop Project 35kW." [Online]. Available: https://evsmartplug.net/smartgrid/ackerman_pv/. [Accessed: 20-Aug-2016].

[85] IEC Standards, "IEC 61850-Communication networks and systems for power utility automation." Edition 2.0, 2011.

[86] R. Huang, E. K. Lee, C. C. Chu, and R. Gadh, "Integration of IEC 61850 into a Distributed Energy Resources system in a smart green building," in *2014 IEEE PES General Meeting | Conference Exposition*, 2014, pp. 1–5.

[87] Y. Assolami and W. G. Morsi, "Mitigating the impact of Charging second generation plug-in battery electric vehicles on distribution transformer's insulation life using TOU prices," in *2015 IEEE Electrical Power and Energy Conference (EPEC)*, 2015, pp. 32–35.

[88] S. G. Wirasingha and A. Emadi, "Pihef: Plug-In Hybrid Electric Factor," *IEEE Trans. Veh. Technol.*, vol. 60, no. 3, pp. 1279–1284, Mar. 2011.

[89] J. Lassila, J. Haakana, V. Tikka, and J. Partanen, "Methodology to Analyze the Economic Effects of Electric Cars as Energy Storages," *IEEE Trans. Smart Grid*, vol. 3, no. 1, pp. 506–516, Mar. 2012.

[90] D. Wu, D. C. Aliprantis, and L. Ying, "Load Scheduling and Dispatch for Aggregators of Plug-In Electric Vehicles," *IEEE Trans. Smart Grid*, vol. 3, no. 1, pp. 368–376, Mar. 2012.

[91] H.-J. Kim, J. Lee, G.-L. Park, M.-J. Kang, and M. Kang, "An efficient scheduling scheme on charging stations for smart transportation," in *Security-Enriched Urban Computing and Smart Grid*, Springer, 2010, pp. 274–278.

[92] C. Hutson, G. K. Venayagamoorthy, and K. A. Corzine, "Intelligent Scheduling of Hybrid and Electric Vehicle Storage Capacity in a Parking Lot for Profit Maximization in Grid Power Transactions," in *IEEE Energy 2030 Conference, 2008. ENERGY 2008*, 2008, pp. 1–8.

[93] S. Shao, T. Zhang, M. Pipattanasomporn, and S. Rahman, "Impact of TOU rates on distribution load shapes in a smart grid with PHEV penetration," in *IEEE PES T D 2010*, 2010, pp. 1–6.